OPTIMAL APPROACH TO ENERGY MANAGEMENT AND GAS DELIVERY OF A COMPRESSED NATURAL GAS STATION

by

Charles Muiruri Kagiri

Submitted in partial fulfillment of the requirements for the degree
Philosophiae Doctor (Electrical)

in the

Department of Electrical, Electronic and Computer Engineering
Faculty of Engineering, Built Environment and Information Technology

UNIVERSITY OF PRETORIA

August 2019

SUMMARY

OPTIMAL APPROACH TO ENERGY MANAGEMENT AND GAS DELIVERY OF A COMPRESSED NATURAL GAS STATION

by

Charles Muiruri Kagiri

Promotor:	Prof. Xiaohua Xia
Co-promotor:	Prof. Lijun Zhang
Department:	Electrical, Electronic and Computer Engineering
University:	University of Pretoria
Degree:	Philosophiae Doctor (Electrical)
Keywords:	Compressed natural gas, Fast-fill compressed natural gas station, Demand side management, Demand response, Optimal control, Model predictive control, Hierarchical control, Alternative fuels, Natural gas vehicle, time-of-use tariff, Optimization.

The global growth in demand for transportation has been phenomenal, owing to an exponential increase in population, industrialization and urbanization. This has led to a corresponding increase in the number of motor vehicles on the roads globally which has made the transport industry one of the main contributors to environmental pollution and energy insecurity. The profile of alternative fuels has been rising as an important component of the solutions to the challenge of energy sustainability. Compressed natural gas is one of the most successful alternative fuels for motor vehicle applications because of its compatibility with the internal combustion engine, reduced engine maintenance costs, reduced criteria air pollutants, low cost, abundance and the existence of renewable sourced natural gas from biomass. The infrastructure for the delivery of compressed natural gas forms part of the primary energy supply network, which has a significant interdependence with the electricity supply network. The compressed natural gas fuelling station is one of the vital nodes of the gas delivery network, that

is also reliant on the electricity supply due to the energy intensive compressors that are required to achieve the right pressure conditions for gas transfer to vehicle tanks.

At the same time, the increase in human population, industrialization, urbanization and market volatility have threatened the reliability and stability of electricity supply networks. Traditional reliance on supply upgrading to meet rising demand has proven to be unsustainable due to prohibitively high costs and associated environmental impact. As a result, demand side management solutions, where better use of the existing capacity is emphasized have received increasing attention. Demand side management requires that electricity consumers also play a role in the efficient operation of the electricity grid by minimizing their electricity usage as well as shifting their flexible loads away from peak electricity demand periods, so that grid stability is sustained.

In order to participate in demand side management initiatives, operators of compressed natural gas stations need technically and economically sound strategies for the operation of station compressors and system components so that energy costs are minimized and gas transfer performance is enhanced. The compressed natural gas fast-fill station, being the most used configuration for commercial fuelling service is the focus of the work carried out in this thesis, with a description of solutions to minimize energy consumption, minimize energy costs and improve gas transfer performance through reduction of filling time.

For this purpose, firstly, an optimal control strategy that minimizes energy cost by shifting the compressor load optimally away from the peak electricity pricing period under a time-of-use electricity tariff, while meeting the gas demand is modelled and evaluated. The controller further minimizes the switching frequency of the compressor thereby avoiding an increase in wear and tear which would lead to higher maintenance costs. The results show the effectiveness of the optimal operation model to achieve a huge reduction in electricity cost for the compressed natural gas station, when compressor-on time is shifted to offpeak and standard electricity pricing times. Further strategies for the minimization of switching frequency are compared and the superior approach identified.

Secondly, a hierarchical operation optimization model is designed and evaluated. The strategy achieves minimized electricity cost and optimal vehicle filling time by optimally controlling the gas dispenser and priority panel valve function under an optimised schedule of compressor operation. The results show that the proposed approach is effective in achieving a minimum electricity costs in the upper

layer optimisation while meeting vehicle gas demand over the control horizon. Further, a reduction in filling time is achieved through a lower layer model predictive control of the pressure-ratio-dependent fuelling process.

Thirdly, an evaluation of compressor optimal sizing is carried out to minimize energy consumption and cascade the benefits of optimal operation of the compressed natural gas compressor under the time-of-use tariff. A comparison of the implication of using a variable speed drive or a fixed speed drive which are optimally sized is carried out. Results show that indeed further reduction in electricity costs for the compressed natural gas station is realized when optimally sized compressor drives are used in combination with optimal operation strategies. Additionally, the four line priority panel is evaluated for gas transfer performance and found to further increase the efficiency of vehicle fuelling which is a performance indicator for consumer convenience.

The outcomes of this work demonstrate the effectiveness of the approaches proposed as necessary to integrate compressed natural gas stations, which are vital nodes of the gas delivery network, with the demand side management of the electricity grid while at the same time enhancing the gas transfer performance. This increases the economic efficiency of the compressed natural gas as an alternative fuel and also advances the goals of demand side management in electricity grid reliability and stability.

DEDICATION

This thesis is dedicated to my brave and wonderful son Ryan Kagiri. I hope that this life is long enough for both of us, to make up for missed moments spent pursuing this noble goal. And I hope this achievement inspires you to stay determined when meeting life's challenges. I love you. To my beautiful wife Kate Njeri, your love kept me warm, your words soothed me, you suffered when I suffered and you celebrated when I celebrated. You are the glue that held things together through the tough times. This is your achievement.

I also dedicate this thesis to my parents Mr Bernard Kagiri and Mrs Jane Kagiri because this milestone is built on the foundation of your sacrifices and unconditional love. And to my siblings Irene, Jacob and Lydia who always believe in me.

ACKNOWLEDGEMENT

This work has been made possible because of the financial support of the National Hub for Energy Efficiency and Demand Side management (EEDSM) and the University of Pretoria, Centre of New Energy Systems (CNES). This invaluable support is hereby acknowledged. I also acknowledge Dedan Kimathi University of Technology for allowing me a favourable study leave to undertake this research.

I have been privileged beyond measure to have been guided through my doctoral studies by Prof. Xiaohua Xia, who is a veteran of great ideas, a master of instruction and a global expert in the energy field. I am heavily indebted to you for your kindness and support that have kept me motivated to do better and I will be influenced by your example for years to come. My second supervisor Prof. Lijun Zhang, I am forever grateful for the valuable time you spent helping me scrutinize my ideas. It has been a challenging journey made easier by yours and Prof Xia's constant presence to provide advice and guidance. Thank you.

My colleagues at the research hub, Dr. E. Wanjiru, Dr. S. Sichilalu, Mr. F. Wamalwa, Ms A. Ikuzwe, Dr. J. Mei, Dr. X. Ye, Mr. T. Nyamayoka, Mr. J. Tshikaya, Mr. D. Bajany, Mr. T. Kunatsa, Mr. D. Mulongoti, Ms. S. Taghizadeh and Mr A. Njepu, I am grateful for having you as company in this noble pursuit of knowledge.

My son Ryan Kagiri, my wife Catherine Njeri, my parents Mr. and Mrs. Kagiri and my inlaws Mr. and Mrs. Mwema. Thank you for being the sources of encouragement and emotional support throughout this journey.

LIST OF ABBREVIATIONS

ACO	Ant colony optimization
AVF	Alternative fuel vehicle
CNG	Compressed natural gas
CPP	Critical peak pricing
DPV	Discounted present value
DR	Demand response
DSM	Demand side management
EDP	Extreme day pricing
EEDSM	Energy efficiency and demand side management
FSD	Fixed speed drive
GHG	Green house gases
HVAC	Heating, ventilation and air conditioning
HSGT	High speed ground transport
IBP	Incentive based programs
LCC	Life cycle cost
MIDACO	Mixed integer distributed ant colony optimization
MINLP	Mixed integer non-linear programming
MPC	Model predictive control
NG	Natural gas
NMOG	Non-methane organic gases
NOX	Nitrogen oxides
PBP	Price based programs
POET	Performance, operation, equipment and technology
ROI	Return on investment
RTP	Real time pricing
SCIP	Solving constraint integer programs
TOU	Time-of-use
VSD	Variable speed drive

LIST OF FIGURES

LIST OF TABLES

TABLE OF CONTENTS

CHAPTER 1 INTRODUCTION

1.1 CHAPTER OVERVIEW

In this chapter, Section 1.2, provides the background information that necessitates the optimization of energy efficiency, economic efficiency and performance of the compressed natural gas station. Section 1.3 describes the concept of electricity demand management and its relevance to the study of the compressed natural gas station. Section 1.4 provides the research objectives and contributions, while Section 1.5 enumerates the research outputs reported from this study. Section 1.6 gives a description of the thesis layout.

1.2 BACKGROUND

Minimizing green house gas emissions and environmental pollution has become an urgent global endeavour as the effects of human activity on the habitability of the earth become more and more apparent. By far, the transportation sector is now the biggest contributor to air pollution through the exhaust gases emitted by millions of motor vehicles that run on the internal combustion engine [1, 2]. Motorized transportation has however become an indispensable part of the human experience, because it allows for the movement of people beyond the natural abilities. It is also a crucial component of the global economy, facilitating the movement of goods and the delivery of services. Consequently, industry stake holders and policy makers have had to consider interventions aimed at minimizing the associated environmental costs of transportation. The efforts to intervene are evident in all areas of the transportation sector including road, rail and high-speed ground transport (HSGT), sea and air transportation, where a combination of policy responses and technology evolution have caused an ongoing dynamic shift to a lower pollution state of the art [3]. The ideal outcome of a zero-emission transportation sector is still far from being achieved because of practical, technological and

economic constraints [4]. These constraints have resulted in a slow uptake of alternatives to the internal combustion engine for powering automobiles in road transportation, such as electric and fuel cell technologies [5]. Besides the strategies that involve a complete replacement of the internal combustion engine with alternative technologies, alternative fuels have shown promising potential in acting as less polluting substitutes to petrol and diesel fuels for the internal combustion engine.

Compressed natural gas (CNG) is among the fuels that have been successfully adopted for this application. CNG is not only compatible with the internal combustion engine, but is also associated with reduced criteria air pollutants [6] and the use of CNG correlates with the lowest emissions of particulate matter, non-methane organic gases (NMOG), nitrogen oxides (NO_x), carbon monoxide (CO) and other air toxics, among hydrocarbon fuels [7]. Just like other transportation infrastructure for different technologies such as petrol/diesel fuelling stations and electric vehicle charging stations, the infrastructure to deliver CNG to vehicular customers is an important component in the success of CNG as an alternative fuel for the transportation sector because of customer consideration for fuelling convenience [8].

Elsewhere, energy insecurity as relates to reliable access to electricity for consumers is one of the other great challenges facing societies globally. The increase in human population, increase in urbanization, grid expansion, market volatility, environmental pollution and the effects of climate change have resulted in a scenario where the stability and reliability of electricity grid is at risk [9]. Investment in new capacity on the supply side to match all demand has proven to be an unsustainable approach owing to the steep capital costs as well as negative environmental impacts [10]. Consequently, there has been a ratcheting up of efforts to encourage efficient use of the electricity by maximizing the use of demand side management (DSM) [11].

The supply of CNG to consumers intersects in consequential ways with the use of electricity because gas delivery infrastructure is heavily reliant on electricity supply for the energy intensive compressors that make up crucial nodes of the gas supply network. As electricity consumers, operators of CNG delivery infrastructure can enhance the benefits that the alternative fuel offers through management of electricity demand at the electricity consumption nodes within the network. The CNG station is one of the crucial nodes in the gas supply network, being the final point of gas delivery to vehicular consumers.

1.3 ELECTRICITY DEMAND MANAGEMENT

In the early days of the electrical grid, electricity producers had a singular task of satisfying the demand of their customers; they did not attempt to change the usage patterns of electricity by those customers. Over the years, producers maintained a dedicated focus on providing a reliable supply and held a stoic view of fluctuation in demand, whether hourly, daily, monthly or seasonal, as an unchangeable fact of life. In order to meet this fluctuating demand, installed generation capacity has to not only meet the maximum possible demand (peak demand), but also have enough excess capacity to deal with uncertainty in generation availability and unpredictable increases in demand [12]. With a standard capacity margin at 10%, and given the average demand, the outcome is an average utilisation capacity of below 77% which is an inefficient utilisation of generation capacity resulting in inefficiency of the generation investment [13].

Changing conditions in the electricity market, and the explosion of demand have however challenged this approach in the recent past. It is no longer sustainable to depend only on supply side adaptation to reliably and economically cater to all of the additional demand as well as react to peak to peak demand variation. In 2008, South Africa experienced an electrical power crisis that led to the implementation of a disastrous power rationing program in the form of load shedding, where some customers were cut off from accessing electricity from the national grid for certain hours of the day when demand spiked and the supply could not cope [14]. The crisis had far reaching negative effects on the country's economy and brought the policy makers together to decide on the most appropriate intervention to ensure a more secure energy future for the country. A study by Olasoji *et al*. [15] estimated that a loss of 2GW on the South African power grid plunges the South African power utility provider, ESKOM into stage 2 load shedding, and costs the national economy R2 billion per day. Stakeholders agreed on the need to implement energy efficiency and demand side management (EEDSM) measures, which are not just economical, but also easily scalable [16]. Further, because South Africa ranked as the 7^{th} largest emitter of green house gases (GHG), the country's power utility firm ESKOM set targets for a new energy mix profile in the country, where coal power would be displaced from it's main power source status in country's energy mix profile, with renewable energy generated power, which would come in as new generation investment. Thus a combined strategy of investment in new renewable generation capacity and implementation of DSM interventions was adopted to tackle the electrical power crisis. The targets for the DSM programs were to permanently reduce electricity demand by 3000MW by the year 2012 and a further 5000MW by 2025 occurring in both residential

and industrial sectors [17]. The DSM strategies envisioned included building retrofitting for lighting technology and heating, ventilation, and air conditioning (HVAC) technologies and the use of industrial energy efficiency measures such as load shifting, encouraged through time differentiated electricity tariffs.

The success of DSM interventions is reliant not only on electricity consumers being sufficiently incentivized to alter their use behaviours, but also on the customers having the access to the technical means to implement such strategies. These means consist of access to the energy efficient equipment as well as the existence of competent strategies required to adequately participate in DSM programs. There have been various milestones in the development of technologies and strategies that advance the achievement of energy efficiency. The necessary integration of these technologies in various sectors is a major motivation for the work carried out in this thesis, which is to provide optimal, economical and comprehensive solutions to efficient energy use in a crucial node of the gas delivery infrastructure; the CNG refuelling station.

1.4 RESEARCH OBJECTIVES AND CONTRIBUTIONS

Responsible use of energy is beneficial to both the supply side and demand side participants in the energy ecosystem. These benefits also spill out to positively affect the interaction of an energy system with the society through environmental conservation and the economic efficiency. Broadly, the generation of electricity is within a few renewable and non renewable technologies and the approach to improvement of electricity generation efficiency can be shared by many operators of generation infrastructure. In contrast, on the demand side, users of electricity are diverse, with differentiated need profiles and varying levels of flexibility of use habit. Different electricity users may have unique and consequential characteristics of the systems that they operate such that similarly unique approaches are required to pursue the energy efficiency in each case. CNG stations serve customers who have chosen compressed natural gas powered vehicles as an alternative to diesel and petrol based ones. Compared to diesel and petrol stations, CNG station have very high electricity consumption, owing to the presence of compressors that keep the gas delivery system in the right pressure conditions for transfer to motor vehicles. The interaction between the CNG station compressors and electricity grid requires energy management strategies to minimise a significant component of the operating costs of the station. Because of the growing number of CNG stations, the development of strategies that

make CNG stations responsible users of electricity is a timely intervention that ensures that this growth occurs sustainably from an electricity grid perspective.

This thesis presents an integrated approach to energy efficiency in the operation of a CNG station incorporating strategies to lower energy cost, participate in DSM programs that result in desirable load profile for a stable and reliable grid, lower energy consumption and optimize the gas transfer from the CNG station cascade storage to the vehicle tanks. The work demonstrates the methodologies necessary to overcome technical and operational challenges of achieving the desirable interaction of the CNG station and the electricity grid, as well as the desirable performance of the filling process in combination with energy efficiency interventions. To reach these outcomes, following objectives were achieved;

1. To design and evaluate an optimal controller that minimizes the cost of electricity incurred at the CNG station from compressor operation. The controller minimizes the cost of electricity incurred by optimally shifting compressor operation from expensive peak electricity pricing periods to less expensive standard and off-peak electricity pricing periods under a time of use tariff, while meeting the gas demand. The controller simultaneously contains the maintenance costs by minimizing the switching frequency through two compared strategies.
2. To design and evaluate a hierarchical optimal control strategy that achieves a reduction in electricity costs in the upper layer through optimal load shifting of the compressor operation, while optimizing the gas transfer of CNG from the cascade storage to vehicle tanks in the lower layer. The solution of the open loop upper layer controller serves as an input to the lower layer MPC controller that determines the optimal operation of priority panel and dispenser valves.
3. To optimally size and compare performance of variable speed drive (VSD) and fixed speed drive (FSD) driven compressors to ensure closer matching to demand which minimizes energy consumption. The VSD and FSD drives are operated under a natural gas (NG) generator and grid dual powered system. Further, to compare the performance of the optimally sized drives on the filling process efficiency for a four line priority panel.

1.5 RESEARCH OUTPUTS

1. C. Kagiri, E. M. Wanjiru, L. Zhang, X. Xia. "Optimized response to electricity time-of-use tariff of a compressed natural gas fuelling station," *Applied Energy* 222 (2018): 244-256.

2. C. Kagiri, L. Zhang, X. Xia. "A Hierarchical Optimisation of a Compressed Natural Gas Station for Energy and Fuelling Efficiency under a Demand Response Program," *Energies* 12, no. 11 (2019): 2165.

3. C. Kagiri, L. Zhang, X. Xia. "Performance, equipment and operation optimization of a compressed natural gas station, powered by grid and natural gas generator," Journal of cleaner productions (submitted, August 2019)

4. C. Kagiri, L. Zhang, X. Xia. "Optimal control of a hybrid battery/supercapacitor storage for neighborhood electric vehicles," *8th International Conference on Applied Energy*, October 8-11, 2016, Beijing, China.

5. C. Kagiri, L. Zhang, X. Xia. "Optimization of a compressed natural gas station operation to minimize energy cost," *9th International Conference on Applied Energy*, August 21-24, 2017, Cardiff, United Kingdom.

6. C. Kagiri, L. Zhang, X. Xia. "Optimal energy cost management of a CNG fuelling station," *Control Conference Africa*, December 7-8, 2017, Johannesburg, South Africa.

7. C. Kagiri, L. Zhang, X. Xia. "Optimal energy cost management of a CNG fuelling station," *11th Asian Control Conference (ASCC)*, December 17-20, 2017, Gold Coast, Australia.

8. C. Kagiri, L. Zhang, X. Xia. "Model predictive control strategy of energy cost management for a compressed natural gas fuelling station," *10th Advanced Control of Chemical Processes*

(ADCHEM), July 25-27, 2018, Shenyang, Liaoning, China.

9. C. Kagiri, L. Zhang, X. Xia. "Receding Horizon Operation Control of a Compressed Natural Gas Station," *10th International Conference on Applied Energy*, August 22-25, 2018, Hong Kong, China.

10. C. Kagiri, L. Zhang, X. Xia. "Optimal control of a variable speed drive compressor for energy efficiency of a compressed natural gas station," *1st International Conference on Industrial Artificial Intelligence*, July 23-25, 2019, Shenyang, Liaoning, China.

11. C. Kagiri, L. Zhang, X. Xia. "Optimal dispatch of grid and natural gas generator power in a scheduled compressed natural gas fuelling station," *38th Chinese Control Conference*, July 27-30, 2019, Guangzhou, China.

1.6 THESIS LAYOUT

The structure of this thesis is as follows:

Chapter 1 presents an introduction of this research work. The chapter presents the relevant background information and describes the problem and the corresponding research gap. Additionally, the motivation, objectives and contributions of the research are described.

Chapter 2 is a comprehensive literature review of the CNG station modelling and operation optimization. The chapter describes existing work relating to CNG station energy consumption. Further the chapter describes the importance of optimal energy consumption management for the CNG station.

Chapter 3 describes the approach to energy cost reduction through an optimal response to the time-of-use tariff for a CNG station, while meeting demand experienced by each level of the cascade storage. The optimal operation of the priority panel valves to replenish the three levels of the cascade storage under the scheduled operation of the compressor is also described.

Chapter 4 is a description of a hierarchical optimisation of the CNG station for energy and fuelling efficiency. The method involves an upper layer feed-forward optimal control of compressor

switching combined with a lower layer MPC control of the gas transfer process. The upper layer provides the compressor switching control solution while the lower layer provides the priority panel and dispenser valve optimal control solution.

Chapter 5 involves a comparison of the performance of optimally sized VSD and FSD driven compressors for the CNG station. Additionally, the optimal gas transfer performance for the four line priority panel configuration of the CNG station is analysed and discussed.

Chapter 6 includes a summary of the methods and outcomes described in the previous chapters. Consequently, an outline of the recommendations and necessary further research is offered.

CHAPTER 2 LITERATURE STUDY

2.1 CHAPTER OVERVIEW

Energy consumption by CNG delivery infrastructure is an industrial energy efficiency problem. This growing sector includes nodes with significant energy consumption in the form of compressors, the majority of which are in CNG vehicle filling stations. In order to achieve desirable energy consumption and gas transfer profiles, and thus encourage more migration of customers from petrol and diesel fuels, an evaluation of the CNG station structure and operation is necessary as well as a description of DSM interventions available for CNG stations.

In this chapter, Section 2.2 describes the configuration of the CNG fast-fill station, while Section 2.3 presents the gas flow studies undertaken with respect to the CNG fast-fill station. Section 2.4 includes the studies related to CNG infrastructure and Section 2.5 contains existing literature on the interaction of CNG infrastructure and the grid. Section 2.6 describes the POET philosophy of energy efficiency interventions, while demand response programs are discussed in Section 2.7. Section 2.8 presents a conclusion of the literature review chapter.

2.2 CNG FAST-FILL STATION

The use of CNG for motor vehicles begun to gain momentum in the 1990s. One of the unique challenges the gaseous fuels face is the customer convenience with regards to fuelling time [18]. For vehicles filling in groups, the filling process involves batch filling where a number of vehicles are filled one after the other in one session [19]. Vehicles are filled directly from the compressor with a buffer tank to prevent the compressor switching off between vehicles. This type of filling is known as the time-filling or buffer-filling process and is suitable for scenarios where vehicles are filled in

immediate succession of each other [20]. However, for commercial road-side fuelling stations, this type of operation is not feasible because it is designed for slow filling [19]. Also, vehicles in the roadside scenario fuelling arrive independent of each other and gaps in the time between fuelling successive vehicles mean that the operation of the compressor would involve too many on/off switching instances which would result in a high rate of wear and tear.

The fast-fill station configuration has helped overcome the fuelling time challenge and has achieved average filling time of below five minutes per vehicle, which is comparable to petrol and diesel fuelling time [21]. In fast fill stations, CNG powered vehicles are filled from reservoirs that form the cascade storage bank of the CNG fuelling station, in which gas is stored at high pressure. The cascade storage bank of the fast-fill fuelling station is divided into low pressure, medium pressure and high pressure levels [22]. The dispenser of the fast-fill station contains three electronic sequencing valves under the control of a microprocessor algorithm, paired with sensors for measuring mass flow of gas from each of the reservoir levels of the cascade storage to the vehicle on-board tank [23]. When a vehicle arrives at the dispenser with low pressure in its on-board tank, the filling is started by opening the dispenser valve connecting the vehicle tank to the low pressure reservoir of the cascade storage. The differential pressure induces a flow of gas into the vehicle tank and the pressure in this target vehicle tank gradually rises. The rising pressure in the target tank reduces the differential pressure with the source cascade reservoir and the mass flow rate of gas falls to a limit. The dispenser algorithm then switches the filling of the target vehicle tank to the medium pressure reservoir for a higher mass flow rate [24]. As the filling of the vehicle tank continues from the medium pressure reservoir, the mass flow rate once again falls until the limit is reached and the dispenser algorithm switches the dispenser valves from the medium pressure reservoir to the high pressure reservoir. Vehicle tank filling is then completed by the high pressure reservoir of the cascade storage [25]. In some scenarios, the vehicle arrives with some gas in the on-board tank hence a higher tank pressure. In these cases, if the differential pressure does not allow for filling to start from the low pressure reservoir, the vehicle starts filling from the medium or high pressure reservoirs, depending on how high the starting pressure of the vehicle tank is. The dispenser algorithm reads the initial vehicle tank pressure from the dispenser sensors and determines which reservoir to start with [26]. It is also the case that some customers may require quantities of gas that do not result in complete filling of the vehicle tank and therefore can be filled from the low pressure reservoir only, or the low pressure reservoir and the medium pressure reservoir. Demand for gas in each of the reservoirs may therefore be unsynchronized in some instances. The CNG station dispenser algorithm compensates for temperature effects on pressure, to ensure that correct mass of

gas requested by consumers are dispensed during the filling process. This means that the target vehicle tank is isolated from fluctuations in temperature and pressure that may result from unsynchronized gas demand in the cascade reservoirs, operation control or ambient condition changes [27, 28].

The priority panel is made up of three valves leading to each of the reservoirs of the three level cascade storage bank [29]. An algorithm to control the gas flow from the reciprocating compressor into the reservoirs of the cascade storage runs on a programmable logic controller, such that each reservoir level is filled independently in a sequence [30]. The compressor is the main electrical load of the CNG station contributing the highest proportion of electricity costs as well as maintenance costs from wear and tear [31]. The expected inlet flow rate from the municipal supply line and the anticipated level of gas demand to be dispensed by the CNG station, form the initial basis for the compressor size [32].

2.3 CNG GAS FLOW

Kountz *et al*. [23] undertook the first study modelling gas flow in the fast-fill CNG station scenario. A mathematical model was developed for the flow of gas from one of the cascade storage tanks into the target vehicle tank which formed the basis for subsequent studies of gas flow dynamics for gaseous fuel transfer from reservoirs to target vehicle tanks [33]. Kountz [34] further developed an approach to the design of dispenser algorithm, to ensure accuracy in the quantities of gas dispensed into the target vehicle tank with compensation for temperature effect. The approach was an improvement to existing metering methods with an aim to increase accurate dispensing of desired quantities of gas under varying environmental conditions [35]. The modelling of the CNG station gas flow has been further extended by other researchers to evaluate the effects of other components of the CNG station on gas flow such as the hoses [36] and dispensers [37]. These studies have aided in the development of a basis for the standardisation of different components of the gas flow equipment and best practises for the use of the corresponding component. Farzaneh *et al*. [38] developed a numerical method of analysing thermodynamic characteristics of gas flow in the reservoir filling process, which is important in expanding knowledge on determining ideal operating conditions for the cascade storage reservoir with regards to the ambient environment. The ratio of target vehicle tank pressure to the pressure of the cascade storage tanks is a major determinant of instantaneous gas flow rate into the vehicle tank. This ratio provides a pressure gradient that causes gas to flow from storage tank to target tank and it

evolves as the vehicle tank gets filled up with gas and thus the filling time is influenced primarily by the state of this ratio, which was the demonstrated in a study by Deymi-Dashtebayaz *et al.* [39].

2.4 CNG INFRASTRUCTURE

In most countries where adoption of CNG is established or increasing, transportation of CNG to consumer access points is by pipeline. Natural gas pipelines have been in existence in many cities and countries for domestic and other non-transportation applications [40]. Research related to the establishment of CNG fuelling stations has been carried out by several researchers. In order to determine the optimal location of CNG stations in a network that also includes petrol and diesel fuelling stations, Frick *et al.* [41] carried out a cost-benefit analysis for the possible location of new fuelling stations, intended as additions to the existing CNG fuelling stations in the Swiss natural gas industry. The optimization framework considered the co-placement of CNG stations among the existing liquid fuelling stations and established a scoring criteria to determine most suitable distribution of 350 new CNG stations among 3470 existing petrol and diesel stations. Kuby [42] took a deeper look at evaluating the location problem for stations serving alternative fuel vehicles (AFVs) by reviewing the state of relevant research work and the factors that slow down the market diffusion process of alternative fuels. The study described the existence of the chicken-and-egg dilemma of the growth of alternative fuel adoption where lack of fuelling stations discourages automakers, which results in less AVFs being produced which inturn discourages fuel companies from building more stations [43]. Reviewed solutions for breaking this chicken-and-egg loop included fleet-first approach of incentives and mandates, which establish seed fleets and fuelling stations that will serve as starters around which a growth cycle can occur [44]. Further, market diffusion of AVFs and their associated infrastructure was found to need some form of government support in order to achieve competitiveness in the market dominated by conventional petrol and diesel fuels [45]. Kuby *et al* [46] further underscored the importance of optimal placement of the starter AVF fuelling stations, as it could be an existential determinant of growth, stagnation or collapse of AVF penetration in the market. The study concluded that drivers of AFVs exhibit deliberate behaviour in choosing where to refuel within sparse refuelling networks, with convenience weighing more significantly than price.

Other studies have examined the overall performance of natural gas fuelling infrastructure, with regard to emissions on a well-to-wheel assessment. Hagos *et al.* [47] determined that, inclusive of infrastructure, the use of CNG in vehicular transportation resulted in a 15-27% reduction in green

house gas emissions per kilometre of travel when compared to petrol and diesel fuels. This effect has the potential of being greatly improved if CNG infrastructure could undertake energy efficiency interventions, such as participation in DSM programs, because these reduce the green house gas emissions related to supplying electricity to the CNG infrastructure [48]. Similar studies such as Tong *et al.* [49, 50] also found that inclusive of the infrastructure, the use of CNG for vehicles resulted in less energy use in transportation as well as lower emissions when a well-to-wheel assessment of impact was carried out [51, 52].

2.5 CNG DELIVERY INFRASTRUCTURE AND THE ELECTRIC GRID

The interdependence between primary energy supply networks, such as natural gas, and electricity networks has received some attentions in literature because of the increasing need to maximize efficiency in the performance of each of these systems. Martinez *et al.* [53], undertook a study that proposed an integrated energy flow analysis of natural gas and electric power networks, regarding energy consumption in gas networks and the effect on gas based electricity generation in the wider electricity network, using a unified framework that is based on the Newton-Rhapson formulation. Numerous other studies have developed methods for the analysis of the combined natural gas and electricity power flow, with a view to optimizing gas flow in pipeline networks and minimize energy consumption, as well as provide solutions that maximize social welfare considering both gas and electricity networks [54, 55, 56]. An ant colony optimization (ACO) algorithm was used in [57] for operation optimization of a steady flow gas pipeline. The purpose of the study was to use ACO methods to develop a decision aid tool for operators of compression stations within a gas pipeline network to determine operation of turbocompressors that boost gas pressure inside the gas pipeline network. Woldeyohannes *et al.* [58] studied the gas pipeline network and developed a model for the analysis of flow parameters and nodal pressures in the gas pipelines with an aim of developing optimal operation of nodal compressors to minimize energy consumption.

When gas is transmitted through the gas pipeline, it is transmitted at high pressure (5-7 MPa) in order to overcome pressure loses and reach the intended distances which are often many kilometres long [59]. This high pressure is reduced at pressure reduction stations before it reaches the final consumption points on the last miles [60]. There have been efforts at energy recovery through electricity generation at these pressure reduction stations, by taking advantage of the pressure drop as a way of increasing the energy efficiency of the natural gas delivery network [61]. Often, this valuable pressure exergy held by

the high pressure natural gas in the pipeline is lost to the environment through the use of expansion valves. Farzaneh-Gord *et al*. [61] carried out a study to evaluate the potential quantities of electricity that could be generated through at the pressure reduction stations in a natural gas pipeline network in the Khorasan province of Iran. An extrapolation of the results to the whole of Iran showed that 762MW of electricity could be generated in the gas pipeline network through the utilization of this wasted exergy alone, which would be a gigantic boost to the electrical energy efficiency of the gas network. A similar study in Egypt reached an estimate of 110MW of potential electricity generation from the pressure reduction stations in the Egyptian natural gas pipeline network [62].

It is necessary to extend the study of the interaction between gas delivery infrastructure interaction and the electricity grid from the compressor nodes within the pipeline, to the CNG fuelling stations in the periphery, in order to determine and exploit the energy efficiency and energy saving opportunities at these terminal nodes. The effects of such an intervention would mean that lower costs of gas delivery are achieved and CNG fuelling stations become more responsible users of electricity, which enhances the pursuit of energy efficiency in both the gas delivery network and electricity grid. Bang *et al*. [33] described how users who had chosen CNG as a fuel for their vehicles improvised by having domestic fuelling devices where there was a scarcity of fuelling station in the US, since piped natural gas is widely available in American homes. The study modelled the CNG residential refuelling system, and demonstrated the potential effects of an increase in the number of such systems on the electricity grid, given the energy intensive compressors that are the main component of such systems. These effects become aggregated at the CNG fuelling stations when they are established and customers migrate from domestic refuelling to fuelling at the commercial stations. With the potential increase in the number of CNG fuelling stations globally, the additional electrical load that these stations introduce to the power infrastructure will be significant. This makes the CNG fuelling station a centralized location for electricity DSM interventions for fuelling operations. Saadat *et al*. [30] developed a thermodynamic analysis to quantify the energy consumption of the reciprocating compressor per unit of gas dispensed. This study described the dominating significance of the CNG station compressor as the biggest consumer of electrical energy at the station. The energy consumption and energy efficiency DSM interventions for the CNG station must therefore focus on the station compressor and the optimization of gas delivery. This thesis is a contribution to the technical, economic and operation considerations that lead to better electricity demand management at the CNG station while also ensuring the DSM interventions are coupled with optimization of gas transfer to motor vehicles.

2.6 POET APPROACH

One of the most comprehensive ways that initiatives towards energy efficiency of energy converting systems on the demand side have been classified is the unifying POET framework [63]. The POET framework describes these initiatives as belonging to these layers: performance efficiency (P), operation efficiency (O), equipment efficiency (E) and technology efficiency (T). Contemplating the structure of the POET framework provides a systematic way of determining the existing energy saving opportunities for electricity consumers such as CNG fuelling stations as carried out in this thesis. Subsequently, the quantified benefits of the evaluated approaches provide an information basis for decision makers to prioritize the identified interventions. Figure 2.1 shows a graphic description of the POET framework [63].

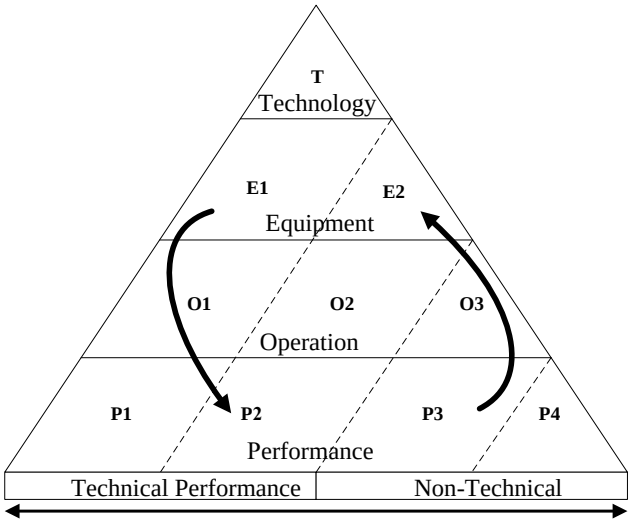

Figure 2.1. POET framework of energy efficiency.

2.6.1 Technology efficiency

According to the POET philosophy by Xia and Zhang [63], technology efficiency is the measure of energy conversion efficiency, processing efficiency, transmission efficiency and usage efficiency, with the limits being those emanating from natural laws. The indicators for technology efficiency include: life cycle cost (LCC), return on investment (ROI), feasibility and the coefficients of the conversion, processing, transmission and usage efficiencies [64]. Disruptive novel technologies always challenge old technologies in the same space and capture the market quickly while pushing optimality to the

extremes of scientific limits. Technology efficiency has a deterministic relationship with equipment efficiency, operation efficiency and performance efficiency. The decomposition of the POET layers into the components of deterministic relationships is shown in Figure 2.1. The use of variable speed drives in place of fixed speed drives for pumps, compressors, fans and other rotary equipment has been shown to lead to significant energy savings and productivity improvement [65]. This type of intervention would constitute a technology efficiency intervention and their payback period indicators have been shown to fall between 1-3.5 years, when used to replace fixed speed drives [66].

2.6.2 Equipment efficiency

Equipment efficiency measures the output energy of an isolated energy equipment with respected to the design specifications of the technology involved. The indicators for equipment efficiency include: specifications and standards, capacity, constraints and maintenance. The main aim for equipment efficiency initiatives is to make sure that the actual equipment parameters stay as close as possible to the design specifications. Part E1 of equipment efficiency represents the deviation of output energy from the specifications while E2 represents efforts that keep the equipment close to specification such as maintenance. Technology efficiency affects the deviation from specifications in E1 but does not affect the initiatives in E2. When the technology to replace energy inefficient components of a system has been identified and tested, relevant equipment must be purchased and installed, that matches the system requirements as closely as possible [66]. The matching of the specifications of the equipment to the system requirement such as determining the variable speed drive specifications for an application constitute an equipment efficiency endeavour [66].

2.6.3 Operation efficiency

Operation efficiency is concerned with the measurement of the level of system-wide coordination of different system components. The relevant indicators for operation efficiency include: sizing, time control, matching and operator skill level. This is because system-wide coordination includes physical components, time consideration and human operator coordination. Part O1 of operation efficiency is determined by technology efficiency and also affected by equipment efficiency, while part O2 is determined by E2 and deals with such things as time-dependent operational strategies for efficiency improvement and component coordination considerations during equipment maintenance. Part O3

includes indicators and initiatives not affected by factors in the technology and equipment efficiency layers. Determining the optimal operating point of a variable speed drive for different time instances of a process constitutes an operation efficiency undertaking [67]. As the output requirements of a system change with time, controlling the operating speed of the variable speed drive to track an optimal operating point will improve productivity and save energy. Similarly, training manpower to operate equipment efficiently in a system also falls under this category [68].

2.6.4 Performance efficiency

Performance efficiency measures aspects of energy efficiency determined by factors that are external to the system but are still deterministic indicators like cost of production, environmental impact and others. There are four parts to this layer. P4 involves energy losses that are not affected by the OET layers such as thefts and leakages. P3 is determined by factors in O3 such as output as a result of operator skill level. P2 is conditioned by equipment efficiency E2 and operation efficiency O2 and is often expressed by indicators such as the time performance of the system. Part P1 involves the energy performance of the system determined by operation part O1 and hence by equipment part E1 and Technology efficiencies. Measures that guarantee energy security such as preventive maintenance scheduling belong in the performance efficiency category of POET initiatives [66]. Strategies such as providing adequate back-up power sources that guarantee minimum energy requirements are met at all times are additional relevant examples of the performance efficiency class of energy efficiency strategies [69].

2.7 DEMAND RESPONSE PROGRAMS

One of the main incentives for electricity users to adopt any of the POET initiatives is the cost benefits available from demand response (DR) programs. DR programs are implemented by power utility operators so as to nudge electricity users into a desirable electricity use profile, which aids the operator in better matching supply to demand. In order to reliably operate the grid, power utility providers must perfectly balance between demand and supply. This balance is continuously threatened by the possibility of changes in the demand or supply side and power utility operators have demand side response as one of the cheaper resources that are available for achieving the desired balance, given that the supply side is extremely capital intensive [9, 70].

DR programs involve a change in electricity prices with time so that peak electricity demand periods are priced significantly higher than lower electricity demand periods [11]. Similarly, this can be viewed as incentive payments by the utility provider, intended to lower the use of electricity at times when the system reliability is compromised or the wholesale prices of electricity are high [9]. DR programs cause end-use customers to implement intentional modifications of electricity consumption patterns by altering the timing, demand level and total electricity consumption [71, 72, 73].

Demand response programs can be classified into two broad categories; incentive-based programs (IBPs) and price-based programs (PBPs) [74]. IBPs involve system-led initiatives where customers are paid an amount for participating in the programs to cut their electricity loads when the grid stability is jeopardized. In IBPs the system operators get into agreements with customers where the system operator pays for some level of customer load control [9]. In PBPs, dynamic electricity pricing rates are used as market-led tools for influencing customer behaviour. The goal of PBPs is to level the demand curve, by having higher prices of electricity in peak demand periods and lower electricity prices in off-peak demand periods [75]. PBPs are implemented as: real time pricing (RTP), where electricity price changes in real time in response to wholesale market price, extreme day pricing (EDP), where a high electricity price is charged for a few extreme days in a year when electricity demand is highest or wholesale prices are highest, critical peak pricing (CPP), which is similar to EDP but can be implemented for varying time frames in a year from a few hours to several days, and the time-of-use (TOU) tariff, which uses a fixed rate to approximate average electricity cost during different time blocks in a day [74, 76].

DR programs cause customers to carry out three classes of actions to lower their cost of electricity [11]. Firstly, customers could lower their electricity consumption during peak periods and either leave consumption during other times as it was before or lower [77, 78]. This would involve energy saving measures that result in lower energy consumption in total, which if adopted by many customers would also lead to slowing down the growth of energy demand in the power supply system. This type of response might involve investment in better technology that consumes less energy to produce the same results, or adoption of better operation techniques that result in lower energy consumption for the energy consuming system, or even the optimization of system performance requirements that achieve the intended functions while demanding less energy. Secondly, customers could shift some system operations from the peak times of electricity demand to offpeak periods of electricity demand [79, 80, 81]. In this case no costs are incurred by the customer and no loss in system output is expected.

Thirdly, customers could use on-site generation solutions, such as on-site generators and back-up sources such as renewable energy sources etc [82, 83]. In this case, the customer has determined that using on-site generation costs less than using electricity from the grid at peak electricity pricing. The operations of the energy consuming system remain as before but the view from the grid is that a reduction in electricity demand has occurred.

To support customer decision making in responding to the conditions of the DR programs, it is necessary to develop strategies that suit the energy consuming system under consideration. The development of such strategies results in the optimal performance of the customer system, where they save costs for their operations, and participate in achieving the grid stability and reliability sought by the power system operators. This thesis describes strategies for CNG station operators to participate in DR programs, through optimal system design and operation that results in lower energy consumption, lower operation costs and better product performance.

2.8 CONCLUSION

Review of literature on energy use in the natural gas delivery network shows that there exists significant scientific literacy on energy efficiency concerning the CNG delivery infrastructure. However, most of the contributions in the improvement of energy efficiency in gas has been concentrated within the pipeline network, precisely on the compressor stations (pressure boosting) and pressure reduction stations. In so doing, an integral part of gas delivery to vehicular consumers of CNG has remained unaddressed when it comes to energy consumption and energy efficiency. The achievement of maximum energy efficiency in gas delivery would be incomplete when only internal nodes of the network are considered, while peripheral nodes are ignored. The CNG fast-fill station is not only an energy intensive node in the gas delivery network, but with the expected growth in number of such stations, it is likely to be a major contributor to the electricity consumption profile of the entire network. As such, addressing energy consumption at the CNG fuelling station will contribute to the improvement of interactions between a primary energy delivery network and the electricity grid.

As a first for the contribution intended at achieving energy efficiency at a major node in the peripherals of the gas delivery infrastructure, the next chapters of this document present proposals for the optimal design and operation of the CNG fuelling station for minimum energy consumption as well as optimal electricity consumption profiles, in line with DSM goals.

CHAPTER 3 OPTIMAL RESPONSE OF A COMPRESSED NATURAL GAS FUELLING STATION TO ELECTRICITY TIME-OF-USE TARIFF

3.1 CHAPTER OVERVIEW

This chapter presents the application of an optimal compressor operation strategy for the CNG fuelling stations, so as to benefit from participation in a demand response (DR) program which is implemented by power utility operator in the form of a time-of-use tariff. The intention is to lower the costs incurred through power consumption. The approach involves shifting of the operation of the main CNG station load away from peak electricity demand periods. An evaluation and comparison of strategies proposed to achieve minimum compressor switching frequency and therefore mitigate the associated wear and tear is also carried out. This chapter describes the implementation of an optimal operation response to the TOU tariff, when it is the DR program under which the CNG station operates, while meeting gas demand. The operation profile of the compressor is optimally altered, with respect to operation times with the aim of achieving reduced electricity costs, thereby lowering operating costs of the station. Lower operation costs of CNG fuelling stations are desirable in that they improve the appeal of CNG as an alternative fuel, since savings in the cost of gas delivery can be passed on by the station operators directly to the customer. A breakthrough is achieved through the proposed method in the form of an optimal scheduling of the on/off switching of the compressor, considering CNG gas demand, the electricity TOU tariff and the mitigation of potential damage to the compressor as a result of wear and tear from frequent cycling. These methods present a framework for optimal use of electricity in the delivery of alternative fuels.

The rest of this chapter is organized as follows: Section 3.2 provides the description of the optimal operation modelling. Section 3.3 contains the case data considered and Section 3.4 presents the results and a discussion of the optimization outcomes. Section 3.5 presents the conclusion of this chapter.

3.2 OPERATION MODELLING AND FORMULATION

Figure 3.1 shows the schematic diagram of a fast-fill CNG station based on a three level cascade reservoir bank. The CNG station compressor fills up the cascade storage from the municipal gas line whenever switch u is on. This switch is activated when the quantity of gas in the three levels of the cascade storage drops to the lower limits that also correspond to the lower operating pressure limits [84]. The gas enters the storage tanks through the valves of the priority panel which are controlled to switch the flow of the incoming gas between the three levels of the cascade storage. The valves are activated such that u_{hp} connects to the high pressure reservoir, u_{mp} connects to the medium pressure reservoir and u_{lp} connects to the low pressure reservoir. At any time, only one of the valves is open hence only one reservoir level is being replenished. Switch u is turned off when the upper limits of the quantity of gas that can be held in the cascade reservoir bank is reached. Gas held at high pressure in the cascade storage tanks is transferred to vehicle tank via a dispenser, which is controlled by a dispensing algorithm that also compensates for temperature effects on pressure ensuring that correct quantities are dispensed to the vehicle tanks [85]. Depending on the initial pressure in the vehicle tank, the dispenser sequences the gas transfer to the target vehicle tank between the three cascade storage reservoirs sustaining the gas flow rate above a set minimum. m_{ohp}, m_{omp} and m_{olp} are the metered gas demand values for the high pressure, medium pressure and low pressure cascade storage reservoirs respectively. The proposed optimal control strategy seeks to schedule the on and off status of the reciprocating compressor through switch u, and the priority panel valves u_{hp}, u_{mp} and u_{lp} such that minimum cost of power is incurred from the operation of the compressor under a TOU tariff of electricity purchase. The control variables for the current problem are, the binary status of the compressor switch $u\{0,1\}$, as well as the binary status of priority panel valves $u_{hp}\{0,1\}$, $u_{mp}\{0,1\}$ and $u_{lp}\{0,1\}$, where 0 represents the off status and 1 represents the on status.

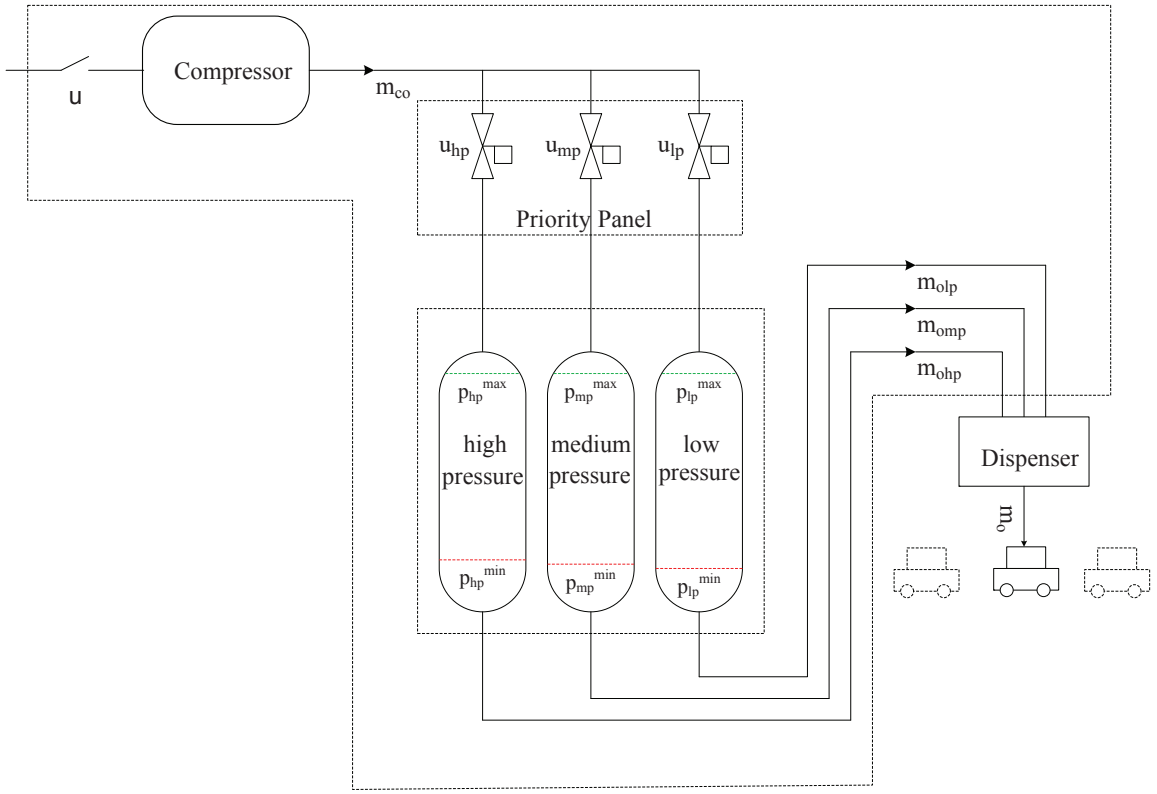

Figure 3.1. Schematic of a CNG fuelling station with a cascade storage system

3.2.1 Objective function

The objective of this strategy is to minimize the cost of power incurred by the CNG station compressor considering the limits of the cascade storage bank over the length of a control horizon [86]. The objective function can therefore be written as

$$J = \sum_{t=1}^{N} p_{co} p_e(t) u(t) t_s, \tag{3.1}$$

where t is the sampling instance, p_{co} is the power rating of the station compressor's electric motor in kW, $p_e(t)$ is the TOU price of electricity per kWh in a sampling instant, N is the total number of sampling instants in the control horizon and t_s is the sampling time.

3.2.2 Constraints

The problem described by this model is subject to the following constraints.

3.2.2.1 Cascade reservoir capacity

For the tth sampling instant, the mass of gas held in the high pressure, medium pressure and low pressure reservoirs are respectively expressed as

$$m_{hp}(t) = m_{hp}(0) + \sum_{i=1}^{t-1} t_s \dot{m}_{cmp} u_{hp}(i) - \sum_{i=1}^{t-1} m_{ohp}(i), \tag{3.2}$$

$$m_{mp}(t) = m_{mp}(0) + \sum_{i=1}^{t-1} t_s \dot{m}_{cmp} u_{mp}(i) - \sum_{i=1}^{t-1} m_{omp}(i), \tag{3.3}$$

$$m_{lp}(t) = m_{lp}(0) + \sum_{i=1}^{t-1} t_s \dot{m}_{cmp} u_{lp}(i) - \sum_{i=1}^{t-1} m_{olp}(i), \tag{3.4}$$

where $m_{ohp}(i)$, $m_{omp}(i)$ and $m_{olp}(i)$ are masses of gas demand dispensed in the ith sampling instant from the high pressure, medium pressure and low pressure reservoirs of the cascade storage bank respectively in kg. The rated mass flow rate of CNG from the compressor $\dot{m}_{cmp}$ in kg/h is obtained through (3.5) [30]

$$\dot{m}_{cmp} = \rho_{std} \times Q_{std} = (\frac{Mw_g}{Mw_a}) \times \rho_{a,std} \times Q_{std}, \tag{3.5}$$

where Mw_g is the molecular weight of CNG, Mw_a is the molecular weight of air, ρ_{std} is the density of CNG, which is the gas being compressed in kg/m^3, $\rho_{a,std}$ is the density of air in kg/m^3 and Q_{std} is the rated capacity of the compressor in m^3/h. The values of ρ_{std}, $\rho_{a,std}$ and Q_{std} are under standard conditions (0^oC temperature and $10^5 pascals$ pressure) [87].

The mass of gas held in the cascade reservoirs as described by (3.2),(3.3) and (3.4) should remain within the the maximum and minimum operating limits, which correspond to maximum and minimum pressure limits for the three cascade reservoir levels respectively, such that

$$m_{hp}^{min} \leq m_{hp}(0) + \sum_{i=1}^{t-1} t_s \dot{m}_{cmp} u_{hp}(i) - \sum_{i=1}^{t-1} m_{ohp}(i) \leq m_{hp}^{max}, \tag{3.6}$$

$$m_{mp}^{min} \leq m_{mp}(0) + \sum_{i=1}^{t-1} t_s \dot{m}_{cmp} u_{mp}(i) - \sum_{i=1}^{t-1} m_{omp}(i) \leq m_{mp}^{max}, \tag{3.7}$$

$$m_{lp}^{min} \leq m_{lp}(0) + \sum_{i=1}^{t-1} t_s \dot{m}_{cmp} u_{lp}(i) - \sum_{i=1}^{t-1} m_{olp}(i) \leq m_{lp}^{max}, \tag{3.8}$$

where m_{hp}^{min}, m_{mp}^{min} and m_{mp}^{min} are the values of lower limits of the quantity of gas for the high pressure, medium pressure and low pressure reservoirs respectively, while m_{hp}^{max}, m_{mp}^{max} and m_{lp}^{max} are the values of the upper limits for quantity of gas for the high pressure, medium pressure and low pressure reservoirs respectively. These quantity limits are obtained from the relationship between the system rated pressure limits and the properties of the CNG gas in the equation of state

$$pV = znRT, \tag{3.9}$$

where p is the pressure value in *bars*, V is the volume of the gas container in L, T is the absolute temperature, R is the universal gas constant, z is the compressibility factor and n is the gas quantity in *moles* [88, 89].

$$n = \frac{m}{M} = \frac{pV}{zRT}, \tag{3.10}$$

where m is the mass of the gas and M is the molar mass of the gas. Equation (3.10) is thus used to calculate the upper and lower operating limits of the mass of gas to be held in the reservoir tanks of the cascade storage bank in the CNG refuelling station. An assumption that the temperature of the cascade storage bank normalizes to the ambient temperature is made in this work, which is consistent with previously modelled operating conditions of the cascade storage [29]. The day's highest and lowest temperatures are used as the maximum and minimum temperatures for the control horizon respectively. Because pressure will rise in the cascade storage reservoirs when the ambient temperature rises, it is possible for the upper operating pressure limit to be breached if the upper mass limit is not calculated at the highest temperature of the day. The upper limit of mass that can be held in the cascade storage is therefore calculated and set using the upper operating pressure limit and the highest temperature over the control horizon. Similarly, the lower mass limit for the cascade reservoirs is calculated and set using the low operating pressure limit and the lowest temperature over the control horizon so as to prevent the pressure of gas held in storage from falling below the lower operating pressure limit when ambient temperature falls, causing a pressure drop. The relationship between the mass and pressure limits with consideration for temperature conditions is thus expressed as

$$m_{hp}^{max} = \frac{MV p_{hp}^{max}}{zRT_{max}} \qquad m_{hp}^{min} = \frac{MV p_{hp}^{mim}}{zRT_{min}}, \tag{3.11}$$

$$m_{mp}^{max} = \frac{MV\,p_{mp}^{max}}{zRT_{max}} \qquad m_{mp}^{min} = \frac{MV\,p_{mp}^{min}}{zRT_{min}}, \tag{3.12}$$

$$m_{lp}^{max} = \frac{MV\,p_{lp}^{max}}{zRT_{max}} \qquad m_{lp}^{min} = \frac{MV\,p_{lp}^{min}}{zRT_{min}}, \tag{3.13}$$

where p_{hp}^{max}, p_{mp}^{max} and p_{lp}^{max} are the maximum pressure limits for the respective reservoirs, p_{hp}^{min}, p_{mp}^{min} and p_{lp}^{min} are the minimum pressure limits for the respective reservoirs and T_{max} and T_{min} are the maximum and minimum ambient temperatures in the control horizon respectively.

3.2.2.2 Switching combinations

During operation, when the compressor switch u is on and gas is flowing to the cascade storage through the priority panel, only one of the valves u_{hp}, u_{mp} and u_{lp} can be on and all the valves must be off whenever the compressor is off such that

$$u_{hp} + u_{mp} + u_{lp} - u = 0. \tag{3.14}$$

3.2.3 Compressor switching frequency

A high rate of compressor start/stop actions increase the mechanical stresses induced in the components of the compressor. This causes a corresponding increase in wear and tear of those components [90] and therefore increases costs incurred to maintain or replace them, while also reducing the compressor lifetime [91]. It has been demonstrated that the transient states of start-up and shut-down induce the highest stresses in different components of the compressor [92]. Additionally, torsional oscillations cause vibrations due to loading changes through the length of the compressor shaft, as well as within the coupled mechanisms and the seals as the motor accelerates the load towards stability, which causes further wear and tear [93]. Therefore, it is desirable that the compressor operates in wide bands of on and off states, staying in each state as long as possible before transitioning to the opposite state [94]. This is the main consideration that motivated the inclusion of switching frequency minimization in this model. Although it would be more precise to directly quantify and minimize the actual wear and tear caused by the transient states in the model instead of minimizing the number of on/off transient instances, there are no accurate models that have accurately described the relationship between the

number of switching actions and the rate of wear and tear. The most widely accepted approach by researchers is to introduce a penalty for each occurrence of a transient state in the solution, when dealing with optimization of operations involving rotary machine systems such as compressors [86, 90, 95]. This approach is justified because the increase in wear and tear as the frequency of transient states increases is a known prior.

In this chapter, the goal is to achieve the lowest number of transient instances without raising the cost electricity above the cost incurred when optimization is implemented without a penalty for the switching frequency. Two methods are proposed to achieve the minimum number of switching instances for the CNG compressor and evaluated. Firstly, the Pretoria method from Mathaba *et al* [96], which has also been used by other researchers in subsequent optimization problems that involved the performance of water pumping systems, is used [97, 98]. The Pretoria method uses an auxiliary variable $s(t)$ [96], which takes a value of 1 when an on state of the compressor occurs. This auxiliary variable is then added to the objective function (3.1) for minimization of its summation over the control horizon such that

$$J = \xi \sum_{t=1}^{N} p_{co} p_e(t) u(t) t_s + (1-\xi) \sum_{t=1}^{N} s(t), \tag{3.15}$$

where ξ is a weighting factor. Additional constraints arise when the Pretoria method is used for the compressor switching minimization. These constraints that are specifically related to the use of the auxiliary variable are

$$u(1) - s(1) \leq 0, \tag{3.16}$$

$$u(t) - u(t-i) - s(t) \leq 0. \tag{3.17}$$

In the inequality (3.16), the status of the auxiliary variable is initialized to take up the initial status of switch u, while in the inequality (3.17) control actions that favour a lower value of the auxiliary variable are preferred [99]. In a comparison study carried out in [97], the Pretoria method was demonstrated to be superior to a different method that used a fixed value constraint that restricted the number of switching instances. This fixed value constraint method was determined to have a high risk of infeasibility under most control conditions. Currently in this chapter, a quadratic objective function method is proposed and described in Section 3.2.6

3.2.4 Boundaries

The states of the compressor switch u and the priority panel valves u_{hp}, u_{mp} and u_{lp} as well as the state of the auxiliary variable s are binary such that

$$u(t), u_{hp}(t), u_{mp}(t), u_{lp}(t), s(t) \in \{0,1\} \quad (1 \leq t \leq N). \tag{3.18}$$

3.2.5 Algorithm

The optimization problem in the generalized form for the present study is to minimize $f^T X$ subject to equality constraints ($A_{eq}X = b_{eq}$), inequality constraints ($AX \leq b$) and the upper and lower boundaries of the control variables ($L_B \leq X \leq U_B$) [100]. The control variables $u(t), u_{hp}(t), u_{mp}(t), u_{lp}(t)$ and $s(j)$ are contained in vector X, while A and A_{eq} are matrices. b, L_B and U_B are vectors represented as

$$\boldsymbol{X} = [u(1)\cdots u(N) \quad u_{hp}(1)\cdots u_{hp}(N) \quad u_{mp}(1)\cdots u_{mp}(N) \quad u_{lp}(1)\cdots u_{lp}(N) \quad s(1)\cdots s(N)]^T_{5N\times 1}, \tag{3.19}$$

and the objective function as

$$\boldsymbol{f^T} = [\xi p_{co} t_s p_e(1)\cdots \xi p_{co} t_s p_e(N) \quad 0\cdots 0 \quad 0\cdots 0 \quad 0\cdots 0 \quad (1-\xi)\cdots(1-\xi)]_{1\times 5N}, \tag{3.20}$$

from the inequality constraints (3.6),(3.7),(3.8), (3.16) and (3.17), if we denote

$$\boldsymbol{A_c} = \begin{bmatrix} -t_s\dot{m}_{cmp} & 0 & \cdots & 0 \\ -t_s\dot{m}_{cmp} & -t_s\dot{m}_{cmp} & \cdots & 0 \\ \vdots & \vdots & \ddots & \vdots \\ -t_s\dot{m}_{cmp} & -t_s\dot{m}_{cmp} & \cdots & -t_s\dot{m}_{cmp} \end{bmatrix}_{N\times N}, \tag{3.21}$$

$$\boldsymbol{A_u} = \begin{bmatrix} 1 & 0 & 0 & \cdots & 0 \\ -1 & 1 & 0 & \cdots & 0 \\ 0 & -1 & 1 & \cdots & 0 \\ \vdots & \vdots & \vdots & \ddots & \vdots \\ 0 & 0 & \cdots & -1 & 1 \end{bmatrix}_{N\times N}, \tag{3.22}$$

then

$$\boldsymbol{A_1} = \begin{bmatrix} \mathbf{0} & \boldsymbol{A_c} & \mathbf{0} & \mathbf{0} & \mathbf{0} \end{bmatrix}_{N\times 5N}, \tag{3.23}$$

$$\boldsymbol{A_2} = \begin{bmatrix} \mathbf{0} & \mathbf{0} & \boldsymbol{A_c} & \mathbf{0} & \mathbf{0} \end{bmatrix}_{N\times 5N}, \tag{3.24}$$

$$\boldsymbol{A_3} = \begin{bmatrix} \mathbf{0} & \mathbf{0} & \mathbf{0} & \boldsymbol{A_c} & \mathbf{0} \end{bmatrix}_{N\times 5N}, \tag{3.25}$$

$$\boldsymbol{A_4} = \begin{bmatrix} \boldsymbol{A_u} & \mathbf{0} & \mathbf{0} & \mathbf{0} & -\boldsymbol{I} \end{bmatrix}_{N\times 5N}, \tag{3.26}$$

$$\boldsymbol{b_1} = \begin{bmatrix} m_{hp}(0) - m_{hp}^{min} - m_{ohp}(1) \\ m_{hp}(0) - m_{hp}^{min} - \Big(m_{ohp}(1) + m_{ohp}(2)\Big) \\ \vdots \\ m_{hp}(0) - m_{hp}^{min} - \Big(m_{ohp}(1) + m_{ohp}(2) + \cdots + m_{ohp}(N)\Big) \end{bmatrix}_{N\times 1}, \tag{3.27}$$

$$\boldsymbol{b_2} = \begin{bmatrix} m_{hp}^{max} - m_{hp}(0) + m_{ohp}(1) \\ m_{hp}^{max} - m_{hp}(0) + \Big(m_{ohp}(1) + m_{ohp}(2)\Big) \\ \vdots \\ m_{hp}^{max} - m_{hp}(0) + \Big(m_{ohp}(1) + m_{ohp}(2) + \cdots + m_{ohp}(N)\Big) \end{bmatrix}_{N\times 1}, \tag{3.28}$$

$$\boldsymbol{b_3} = \begin{bmatrix} m_{mp}(0) - m_{mp}^{min} - m_{omp}(1) \\ m_{mp}(0) - m_{mp}^{min} - \Big(m_{omp}(1) + m_{omp}(2)\Big) \\ \vdots \\ m_{mp}(0) - m_{mp}^{min} - \Big(m_{omp}(1) + m_{omp}(2) + \cdots + m_{omp}(N)\Big) \end{bmatrix}_{N\times 1}, \tag{3.29}$$

$$\boldsymbol{b_4} = \begin{bmatrix} m_{mp}^{max} - m_{mp}(0) + m_{omp}(1) \\ m_{mp}^{max} - m_{mp}(0) + \Big(m_{omp}(1) + m_{omp}(2)\Big) \\ \vdots \\ m_{mp}^{max} - m_{mp}(0) + \Big(m_{omp}(1) + m_{omp}(2) + \cdots + m_{omp}(N)\Big) \end{bmatrix}_{N\times 1}, \tag{3.30}$$

$$\boldsymbol{b_5} = \begin{bmatrix} m_{lp}(0) - m_{lp}^{min} - m_{olp}(1) \\ m_{lp}(0) - m_{lp}^{min} - \Big(m_{olp}(1) + m_{olp}(2)\Big) \\ \vdots \\ m_{lp}(0) - m_{lp}^{min} - \Big(m_{olp}(1) + m_{olp}(2) + \cdots + m_{olp}(N)\Big) \end{bmatrix}_{N\times 1}, \tag{3.31}$$

$$\boldsymbol{b_6} = \begin{bmatrix} m_{lp}^{max} - m_{lp}(0) + m_{olp}(1) \\ m_{lp}^{max} - m_{lp}(0) + \Big(m_{olp}(1) + m_{olp}(2)\Big) \\ \vdots \\ m_{lp}^{max} - m_{lp}(0) + \Big(m_{olp}(1) + m_{olp}(2) + \cdots + m_{olp}(N)\Big) \end{bmatrix}_{N\times 1}, \tag{3.32}$$

$$\boldsymbol{b_7} = [0]_{N\times 1}, \tag{3.33}$$

then the linear inequality constraints become

$$\boldsymbol{A} = \begin{bmatrix} \boldsymbol{A_1} \\ -\boldsymbol{A_1} \\ \boldsymbol{A_2} \\ -\boldsymbol{A_2} \\ \boldsymbol{A_3} \\ -\boldsymbol{A_3} \\ \boldsymbol{A_4} \end{bmatrix}_{7N\times 5N} \quad \boldsymbol{b} = \begin{bmatrix} \boldsymbol{b_1} \\ \boldsymbol{b_2} \\ \boldsymbol{b_3} \\ \boldsymbol{b_4} \\ \boldsymbol{b_5} \\ \boldsymbol{b_6} \\ \boldsymbol{b_7} \end{bmatrix}_{7N\times 1}, \tag{3.34}$$

for the equality constraint (3.14) we denote

$$\boldsymbol{A}_{eq} = \begin{bmatrix} -\boldsymbol{I} & \boldsymbol{I} & \boldsymbol{I} & \boldsymbol{I} & \mathbf{0} \end{bmatrix}_{N\times 5N} \quad \boldsymbol{b}_{eq} = \begin{bmatrix} \mathbf{0} \end{bmatrix}_{N\times 1}, \tag{3.35}$$

The MATLAB Solving Constraint Integer Programs (SCIP) solver in the OPTI toolbox interface is used for the solution of this optimization problem [101].

3.2.6 The quadratic objective function to minimize compressor switching instances

In this method, a quadratic element $\sum \Big(u(t+1)-u(t)\Big)^2$ is introduced in the objective function. The quadratic element minimizes the switching frequency of the compressor switch status over the control horizon, so that longer operating bands of on and off states are preferred in the solution. The control variables are u, u_{hp}, u_{mp} and u_{lp} and the objective function (3.1) using this method becomes

$$J = \psi \sum_{t=1}^{N} p_{co} p_e(t) u(t) t_s + (1-\psi) \sum_{t=1}^{N-1} \Big(u(t+1)-u(t)\Big)^2, \tag{3.36}$$

where ψ is the weighting factor. The constraints under this method are the same as those in Sections 3.2.2.1 and 3.2.2.2. The optimization problem can be written in the standard form

$$x = [u(1)\cdots u(N) \quad u_{hp}(1)\cdots u_{hp}(N) \quad u_{mp}(1)\cdots u_{mp}(N) \quad u_{lp}(1)\cdots u_{lp}(N)]^T_{4N\times 1}, \tag{3.37}$$

and in the general algorithm for the OPTI toolbox solver [101], the objective function is formulated as

$$min_x\ f^T x\ subject\ to = \begin{cases} A \cdot x \leq b \\ A_{eq} \cdot x \leq b_{eq} \\ l_b \leq x \leq U_b \\ x \in \{0,1\} \end{cases}, \tag{3.38}$$

from the linear inequality constraints (3.6),(3.7),(3.8), we denote

$$\boldsymbol{A_1'} = \begin{bmatrix} \mathbf{0} & \boldsymbol{A_c} & \mathbf{0} & \mathbf{0} \end{bmatrix}_{N \times 5N}, \tag{3.39}$$

$$\boldsymbol{A_2'} = \begin{bmatrix} \mathbf{0} & \mathbf{0} & \boldsymbol{A_c} & \mathbf{0} \end{bmatrix}_{N \times 5N}, \tag{3.40}$$

$$\boldsymbol{A_3'} = \begin{bmatrix} \mathbf{0} & \mathbf{0} & \mathbf{0} & \boldsymbol{A_c} \end{bmatrix}_{N \times 5N}, \tag{3.41}$$

then the linear inequality constraints become

$$\boldsymbol{A'} = \begin{bmatrix} \boldsymbol{A_1'} \\ -\boldsymbol{A_1'} \\ \boldsymbol{A_2'} \\ -\boldsymbol{A_2'} \\ \boldsymbol{A_3'} \\ -\boldsymbol{A_3'} \end{bmatrix}_{6N \times 4N} \quad \boldsymbol{b'} = \begin{bmatrix} \boldsymbol{b_1} \\ \boldsymbol{b_2} \\ \boldsymbol{b_3} \\ \boldsymbol{b_4} \\ \boldsymbol{b_5} \\ \boldsymbol{b_6} \end{bmatrix}_{6N \times 1}, \tag{3.42}$$

for the equality constraint (3.14) we can denote

$$\boldsymbol{A'_{eq}} = \begin{bmatrix} -\boldsymbol{I}; -\boldsymbol{I}; -\boldsymbol{I}; -\boldsymbol{I} \end{bmatrix}_{N \times 4N} \quad \boldsymbol{b'_{eq}} = \begin{bmatrix} \mathbf{0} \end{bmatrix}_{N \times 1}, \tag{3.43}$$

The MatLab SCIP solver in the OPTI toolbox interface is similarly used for this quadratic optimization problem.

3.2.7 Consideration for terminal constraints

At the end of the control horizon, it is desirable that the quantity of gas in the cascade storage match the initial quantities of gas held in the reservoirs of the cascade storage which ensures that initial condition values are repeated for the succeeding control period, because for open loop strategies, proper operation is not guaranteed in the subsequent control periods if initial conditions are not the same [98, 102]. From (3.2), (3.3) and (3.4), at the last instant of the control horizon, the mass of gas held in the three levels of the cascade storage are therefore expressed as;

$$m_{hp}(N) = m_{hp}(0) = m_{hp}(0) + \sum_{i=1}^{N} t_s \dot{m}_{cmp} u_{hp}(i) - \sum_{i=1}^{N} m_{ohp}(i), \tag{3.44}$$

$$m_{mp}(N) = m_{mp}(0) = m_{mp}(0) + \sum_{i=1}^{N} t_s \dot{m}_{cmp} u_{mp}(i) - \sum_{i=1}^{N} m_{omp}(i), \tag{3.45}$$

$$m_{lp}(N) = m_{lp}(0) = m_{lp}(0) + \sum_{i=1}^{N} t_s \dot{m}_{cmp} u_{lp}(i) - \sum_{i=1}^{N} m_{olp}(i), \tag{3.46}$$

The terminal constraints are implemented as soft constraints because a fixed mass of gas flows into the cascade storage for every sampling instant when the compressor is on, which yields a discrete profile of possible values of quantity of gas. The soft terminal constraint thus allows feasibility under slight variations from the target quantities by accepting the nearest feasible value for the cascade storage gas quantity. A solution may otherwise not be automatically feasible with a hard constraint. The softened terminal constraint applied in this study is a restriction of the final mass of gas in the cascade storage to between 90%-100% of the initial gas quantity in a control period. Therefore from (3.44), (3.45) and (3.46)

$$0.9 \times m_{hp}(0) \leq m_{hp}(0) + \sum_{i=1}^{N} t_s \dot{m}_{cmp} u_{hp}(i) - \sum_{i=1}^{N} m_{ohp}(i) \leq m_{hp}(0), \tag{3.47}$$

$$0.9 \times m_{mp}(0) \leq m_{mp}(0) + \sum_{i=1}^{N} t_s \dot{m}_{cmp} u_{mp}(i) - \sum_{i=1}^{N} m_{omp}(i) \leq m_{mp}(0), \tag{3.48}$$

$$0.9 \times m_{lp}(0) \leq m_{lp}(0) + \sum_{i=1}^{N} t_s \dot{m}_{cmp} u_{lp}(i) - \sum_{i=1}^{N} m_{olp}(i) \leq m_{lp}(0). \tag{3.49}$$

3.3 CASE STUDY

3.3.1 The CNG fuelling station

The data used for the case study in this chapter comes from a fast-fill CNG station located in Johannesburg, South Africa. The fuelling station has a reciprocating compressor that supplies compressed gas to the cascade storage, which is dispensed through two dispensers. Gas from the gas utility company supplying the Johannesburg municipality is delivered to the station via a gas pipeline. Table (3.1) shows the relevant parameters of the station that are used with the optimization model. In the baseline operation, low quantities of gas trigger compressor-on status at the lower limit and high quantities of gas in the cascade storage trigger compressor-off status at the upper limit.

Table 3.1. CNG fuelling station data

Specification	value
High pressure reservoir capacity	2000 L
Medium pressure reservoir capacity	2000 L
Low pressure reservoir capacity	2000 L
Maximum Pressure for all reservoir levels	252 bar
High pressure reservoir minimum pressure	210 bar
Medium pressure reservoir minimum pressure	150 bar
Low pressure reservoir minimum pressure	75 bar
Priority panel	3 lines
Compressor capacity	900 Nm^3/hr
Compressor motor rating	132 kW

3.3.2 Time-of-use electricity tariff

The time-of-use (TOU) electricity tariff uses time differentiated pricing of electricity to reflect the periods when the demand is determined to be high, low or average, thus encouraging users to migrate their flexible loads away from high demand-high price periods [103]. This pricing profile may vary by time of day, day of the week or season of the year [81, 104]. The TOU tariff under which the CNG

station under consideration operates is the Miniflex TOU tariff by the South African electricity utility, Eskom. The electricity price under the Miniflex tariff is implemented on two levels; time of day price variation and seasonal price variation. In the seasonal pricing the winter months of June to August are classified as high demand season and prices of electricity per unit are higher, while the remaining months of the year, September to May are classified as low demand season with lower electricity prices. Further, daily electricity pricing is classified into peak, standard and off-peak times, which for the two seasons are such that

$$p_{eHD}(t) = \begin{cases} p_{offpeak} = 0.5157 \text{ R/kWh} & \text{if } t \in [0,6] \cup [22,24] \\ p_{standard} = 0.9446 \text{ R/kWh} & \text{if } t \in [9,17] \cup [19,22] \\ p_{peak} = 3.1047 \text{ R/kWh} & \text{if } t \in [6,9] \cup [17,19] \end{cases}, \tag{3.50}$$

$$p_{eLD}(t) = \begin{cases} p_{offpeak} = 0.4472 \text{ R/kWh} & \text{if } t \in [0,6] \cup [22,24] \\ p_{standard} = 0.7016 \text{ R/kWh} & \text{if } t \in [6,7] \cup [10,18] \cup [20,22] \\ p_{peak} = 1.0167 \text{ R/kWh} & \text{if } t \in [7,10] \cup [18,20] \end{cases}, \tag{3.51}$$

where p_{eHD} and p_{eLD} are the daily electricity prices for the high demand and low demand seasons respectively, $p_{offpeak}$ is the off-peak price, $p_{standard}$ the standard time price and p_{peak} the peak time price, R is the South African Rand and t is the time of the day in hours. Additional components of the tariff are not considered for the purpose of implementing the optimization model because they remain constant for all periods [98].

3.3.3 Gas demand

Figure 3.2 shows the metered gas demand profile for each of the three levels of the cascade storage bank for two days; one in the high electricity demand pricing season and the second in the low electricity demand pricing season. The mass flow of gas from the cascade storage reservoirs is measured at the dispenser and recorded in the operation log [105]. From Figure 3.2, there are similarities in the demand profile for the two days in the high electricity demand pricing season and low electricity demand pricing season. In both profiles, an increase in demand is observed during the morning hours up to 10:00, which can be attributed to motorist fuelling before beginning their daily movements. An increase in gas demand also occurs beginning at 14:00, due to motorists refilling their tanks prior to the

evening rush hour. For the CNG station under consideration, the customers are mainly public service vehicles, courier service vehicles and security patrol vans. Public service transportation demand may explain the up-tick in gas demand that precedes peak people movement periods of the day. Some motorists may also fuel their vehicles in the evenings, in preparation for movement in the next day, which may explain the demand profile observed in the evening hours. A sampling time of four minutes

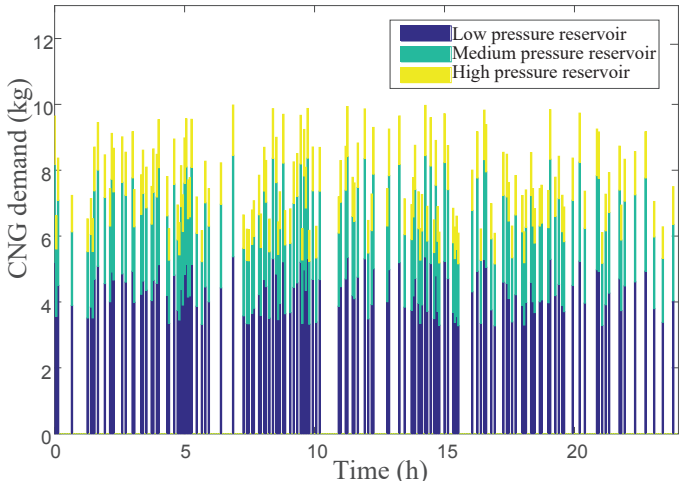

Figure 3.2(a): High electricity demand season

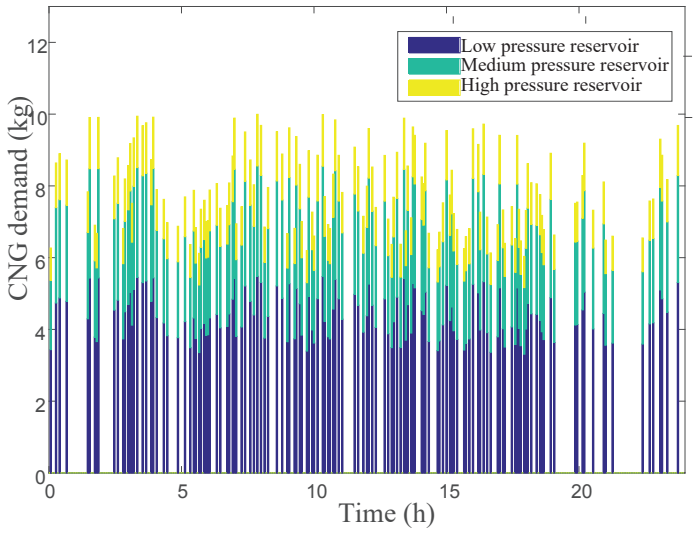

Figure 3.2(b): Low electricity demand season

Figure 3.2. CNG demand from the three cascade storage levels for single day in each electricity pricing season

is considered for this optimization problem for a control horizon of 24 hours.

3.4 RESULTS AND DISCUSSION

3.4.1 High demand electricity pricing season

3.4.1.1 Optimization without consideration for compressor switching frequency

Figure 3.3 shows the operation of the station compressor, when the optimal minimization of electricity cost is implemented without limiting the switching frequency in the objective function. Close to the end of the off-peak electricity pricing time at 06:00, the compressor is turned on to fill up the cascade storage reservoirs and avoid compressor operation during the peak electricity pricing period between 06:00 and 09:00. The controller successfully prevents operation of the compressor during this peak electricity pricing period which saves on electricity cost. Because the compressor stays off in the two hours of the peak electricity pricing time, the level of gas in the cascade reservoirs requires to be replenished, and the compressor is turned on several times during the standard electricity pricing time between 09:00 and 17:00. The quantity of gas in the cascade storage is also kept high before the onset of the evening peak between 17:00 and 19:00, to ensure that sufficient levels of gas in the cascade reservoirs are available at this time without turning on the compressor. The controller also succeeds in keeping the compressor off over the length of the evening peak electricity pricing time and beyond, thereby minimizing the cost of electricity further.

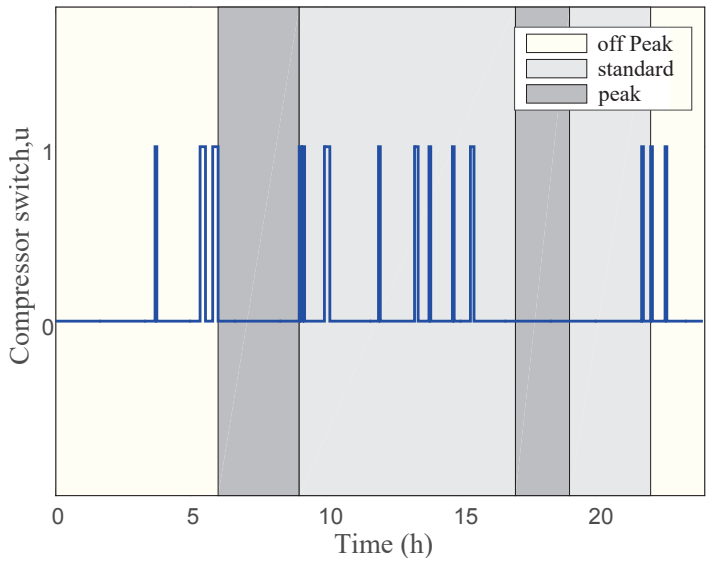

Figure 3.3(a): Compressor switch action

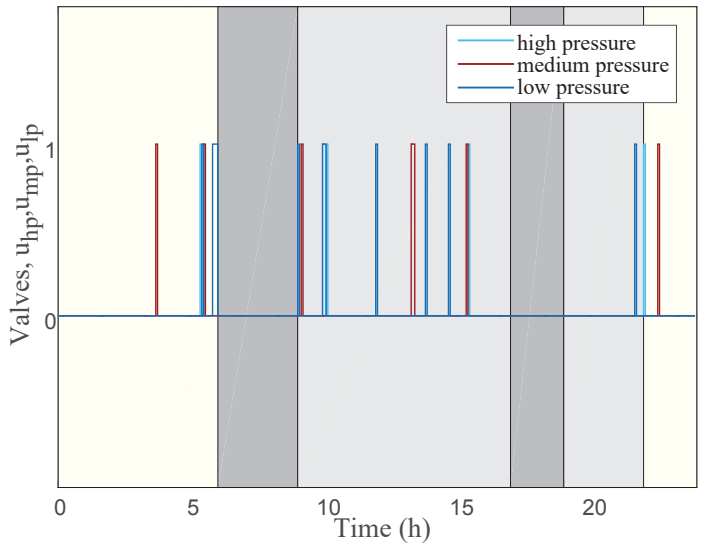

Figure 3.3(b): Valve action

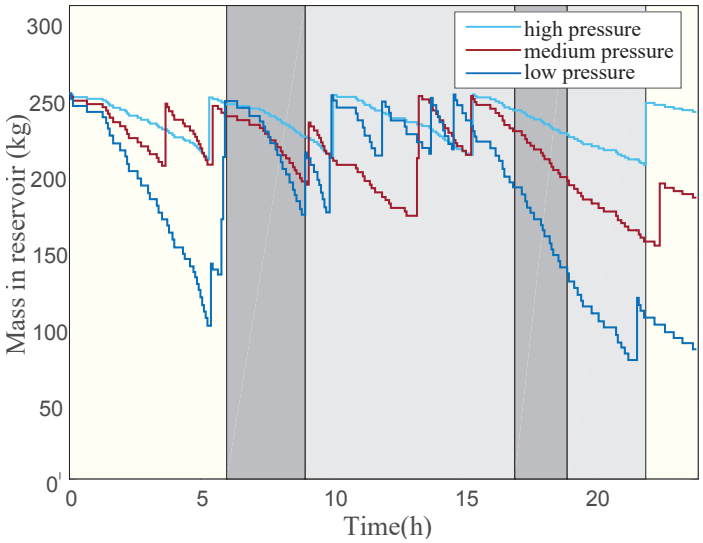

Figure 3.3(c): Mass of gas in reservoir

Figure 3.3. System operation profile in the high demand electricity pricing season without minimization of compressor switching frequency

The compressor is turned on minimally during the standard electricity pricing time close to 22:00 and in the evening off-peak electricity pricing period to meet the gas demand until the end of the control horizon. When the switching frequency of the compressor is not minimized, the compressor is turned on to meet the gas requirements in each cascade reservoir independently, resulting in frequent on/off

cycling of the compressor. Electricity cost incurred in this operation profile over the control horizon is R148.90, a substantial reduction from the baseline of R432.59. Although a significant reduction in electricity cost is realized in this optimization operation by avoiding operation of the compressor during peak electricity pricing times, the high switching frequency of up to 14 transient instances is detrimental to the components of the compressor, because of the increased wear and tear which will result in rising maintenance costs [91, 99].

3.4.1.2 Optimization while considering compressor switching frequency

Figure 3.4 and Figure 3.5 show the system operation profile when strategies for minimizing the compressor switching frequency are implemented in the objective function. For the Pretoria method, a weighting factor of ξ=0.01 is used while for the quadratic objective function method the weighting factor used is ψ=0.9. These weighting factors are selected to yield the same cost of electricity as in the optimization without compressor switching minimization, with the minimum possible number of transient instances. Both the quadratic objective function method and the Pretoria method lower the number of compressor on/off instances from a high of 14 in the optimization without minimization of the compressor switching frequency, to 4 as shown in Figure 3.4(a) and Figure 3.5(a). Further, the compressor-on status is successfully prevented from occurring during the peak electricity pricing time between 06:00 and 09:00 for both methods.

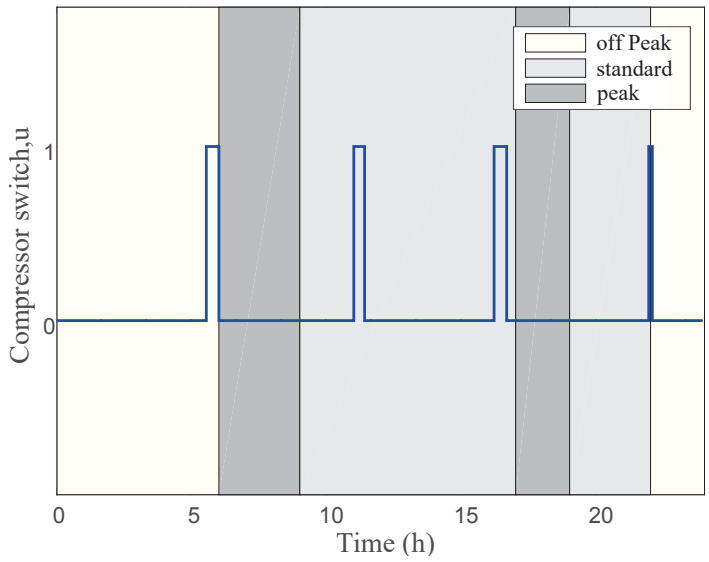

Figure 3.4(a): Compressor switch action

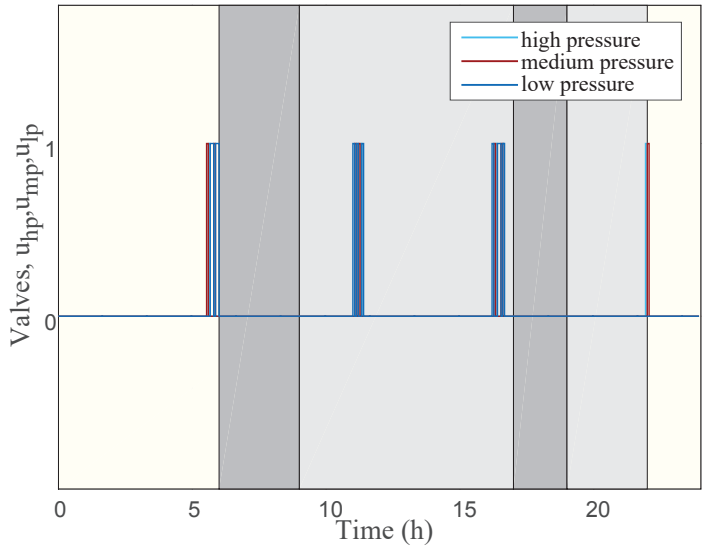

Figure 3.4(b): Valve action

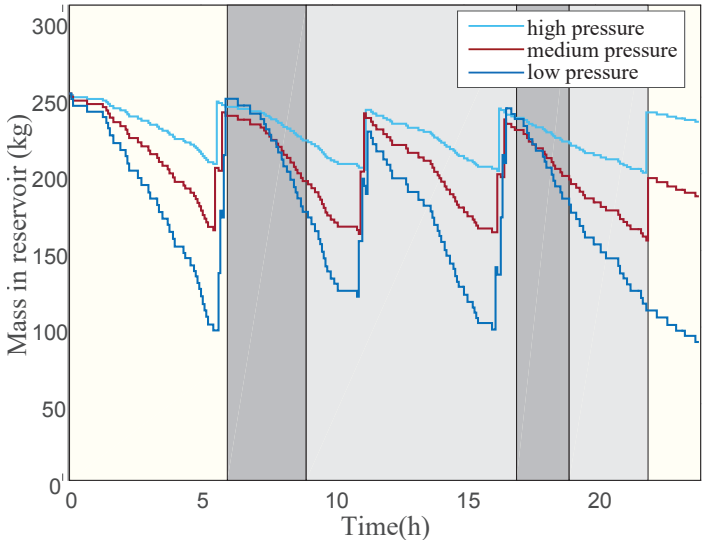

Figure 3.4(c): Mass of gas in reservoir

Figure 3.4. System operation profile in the high demand electricity pricing season using the Pretoria method of minimizing compressor switching

This is achieved in the optimal solution by having the compressor operate just before the onset of the peak electricity pricing time at 06:00, in order to fill up the cascade storage reservoir to meet demand in the peak electricity pricing period without switching on the compressor. Two compressor on-states are observed during the standard electricity pricing time of the TOU tariff, between 09:00 and 17:00.

This enables the CNG station to meet the mid morning gas demand, as well as replenish the cascade reservoirs before the onset of the second peak electricity pricing time at 17:00. Under the optimal solution from both methods, the compressor stays off during the evening peak electricity pricing time between 17:00 and 19:00 and further during the subsequent standard electricity pricing time between 19:00 and 22:00, and the compressor is switched on during the off-peak electricity pricing time after 22:00. Whenever an on-state of the compressor occurs, the solutions from both methods synchronize the filling of the three reservoirs of the cascade storage so that the compressor does not have to be switched on independently for each reservoir. This is how the optimal minimization of compressor switching frequency is achieved.

Figure 3.5(b) and Figure 3.4(b) show the coordination of valve action for the priority panel, to replenish gas quantities in the three levels of the cascade storage so that when the compressor is off, each cascade storage reservoir can sustain their independent gas demand until the next synchronized refill. This effect is further demonstrated by the state of mass of gas in the three resevoirs of the cascade storage shown in Figure 3.4(c) and Figure 3.5(c). When compared to optimal operation without minimization of compressor switching frequency, the reduction in transient states for the two methods represents a 71.4% reduction in one of the main contributing factors to wear and tear. Fewer transient states of the compressor mean a reduction in the probability of component failure through fatigue caused by a high frequency of mechanical disturbance [106, 107]. This in-turn lowers the maintenance and replacement rate of components which adds up to maintenance costs [108, 109].

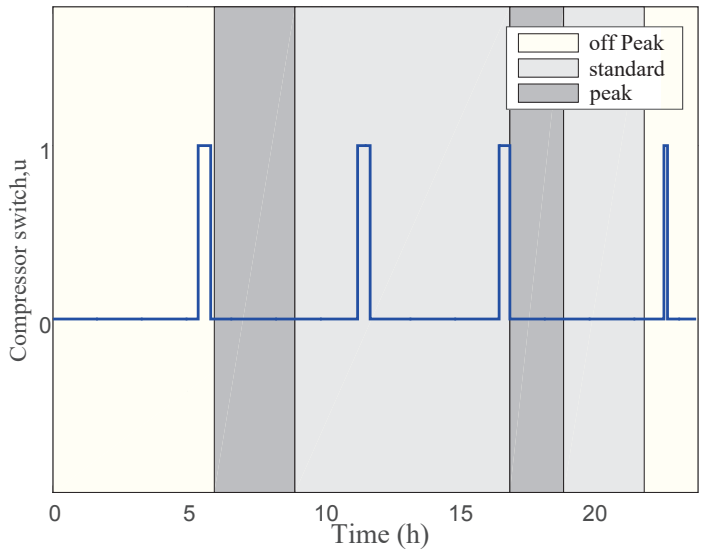

Figure 3.5(a): Compressor switch action

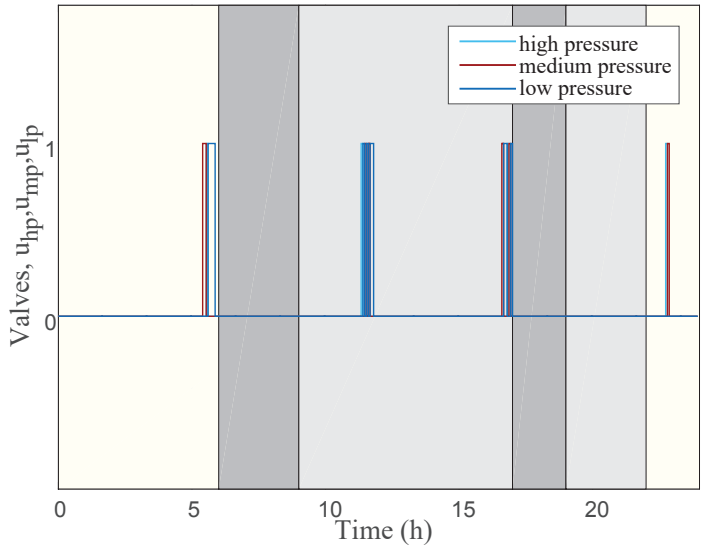

Figure 3.5(b): Valve action

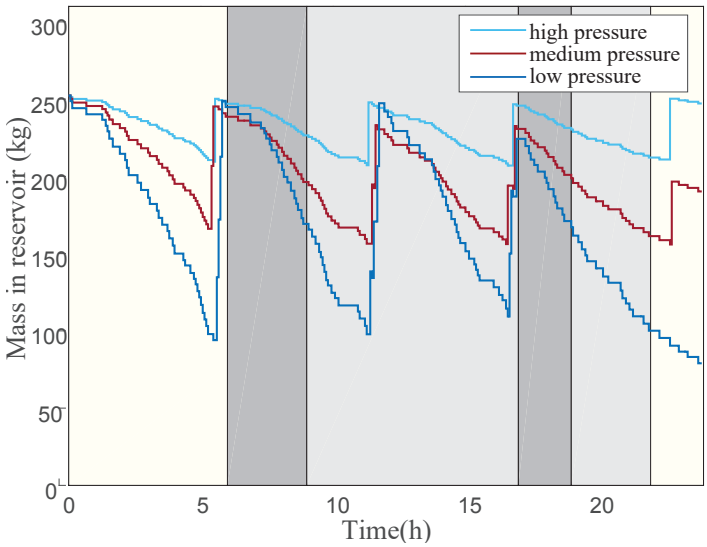

Figure 3.5(c): Mass of gas in reservoir

Figure 3.5. System operation profile in the high demand electricity pricing season using the quadratic objective function method of minimizing compressor switching

Table 3.2 shows a comparison of the performance of the three approaches to the optimal operation of the CNG station compressor. All the three methods achieve a reduction in electric power cost from a baseline of R432.59, to an optimally minimal cost of R148.90. The operation profile of the compressor in the three methods is such that the effective compressor operation time in each electricity pricing

period is the same for all three strategies, with the difference being only in the exact time the switching instances occur and the length of those instances, which is why the cost of electricity for the three strategies is equal. Although the strategy that minimizes electricity cost without considering switching frequency is less computationally complex and yields the same cost of electricity as the other methods, the number of transient instances of compressor status is too high, thereby increasing the probability of component fatigue and failure. Comparing the quadratic objective function method of compressor switching minimization to the Pretoria method shows that the time taken to compute the solution is shorter for the quadratic objective function method which can be linked to lower computational costs and hence the method can be deemed superior [110]. Consequently, it can be concluded that for the three methods under consideration, the one involving the quadratic objective function of compressor switching minimization has the most desirable performance profile for achieving the aim of electricity cost minimization and compressor care.

Table 3.2. Comparison of performance for the control strategies for a 24-hour control period

	Electricity cost (Rand)	*Switching instances*	*Computing time (Second)*
Optimal operation without switching minimization	148.90	16	0.5
Optimal operation with Pretoria switching minimization	148.90	4	71
Optimal operation with quadratic objective function switching minimization	148.90	4	21

3.4.2 Low demand electricity pricing season

The quadratic objective function approach, determined to be superior in Section 3.4.1, is implemented in the optimal operation of the CNG station for the case of the low electricity demand season which results in the system operation profile shown in Figure 3.6. Similar to the high electricity demand season operation, the solution for the low electricity demand season involves operation of the compressor prior to the onset of the peak electricity pricing time at 07:00. The compressor operates in the off-peak electricity pricing time and stays on a few minutes into the standard electricity pricing period between

06:00 and 07:00. This ensures that the cascade storage is replenished to meet demand during the peak electricity pricing period between 07:00 and 10:00 with the compressor off. The gas demand during the standard electricity pricing time between 10:00 and 18:00 is met through two compressor on instances, that also help meet gas demand until the onset of the off-peak electricity pricing time after 22:00. The compressor is turned on once during the off-peak electricity pricing period to meet the gas demand near the end of the control horizon.

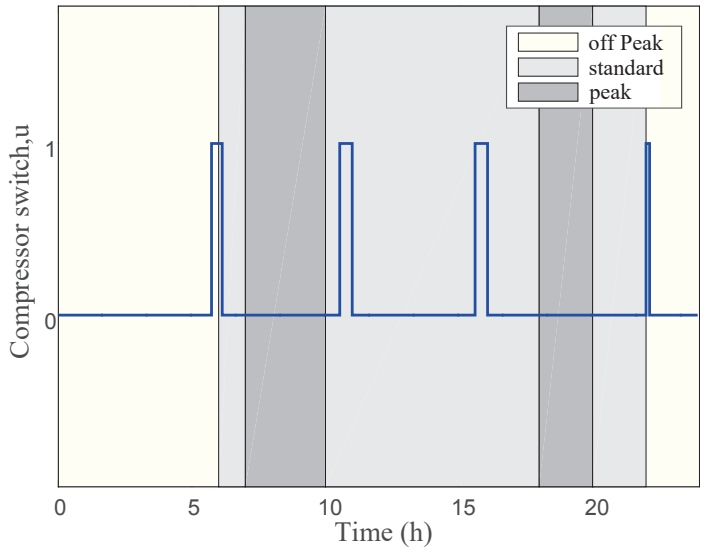

Figure 3.6(a): Compressor switch action

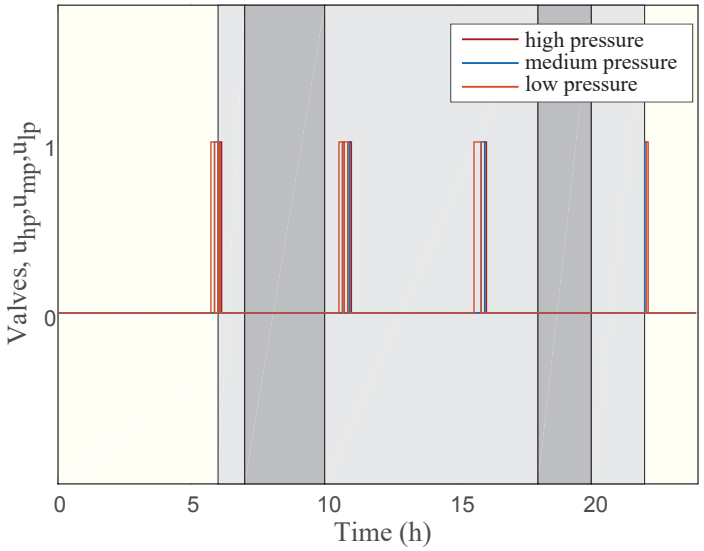

Figure 3.6(b): Valve action

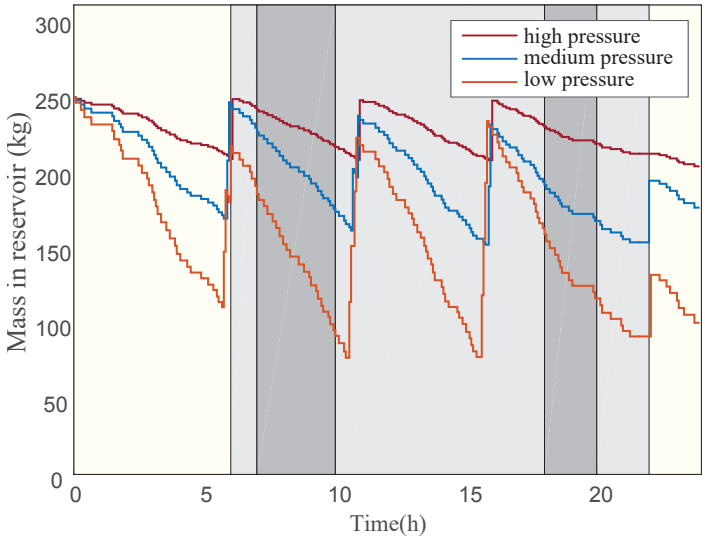

Figure 3.6(c): Mass of gas in reservoir

Figure 3.6. System operation in the low demand electricity pricing season using the quadratic objective function method

From a baseline electricity cost of R212.40 for the control horizon under low electricity demand pricing, the optimal operation profile reduces the cost of electricity to R122.40,which is a significant 42.3% reduction in the electric power cost for the control horizon. This is evidence that the application of optimal operation of the CNG compressor to minimize energy cost for the CNG station is applicable through both seasons of electricity demand pricing for the year.

3.4.3 Solutions with terminal constraints

It is evident from the Figures 3.3(c), 3.4(c), 3.5(c) and 3.6(c) that the quantity of gas held in the cascade storage reservoirs at the end of the control horizon does not match the initial quantities of gas in the cascade storage at the beginning of the control horizon. This means that the initial conditions of the subsequent control horizon will be different from the initial conditions of the current control horizon which may jeopardize the effectiveness of the control solution.A terminal constraint is implemented with the quadratic objective function method of minimizing electricity cost resulting in the profile of operation shown in Figure 3.7. When the terminal constraint is implemented, the optimal operation solution from the superior approach still succeeds in keeping the compressor from operating in both the

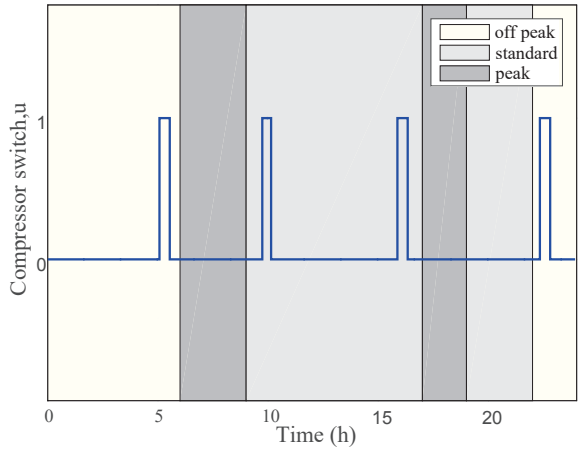

Figure 3.7(a)(i)

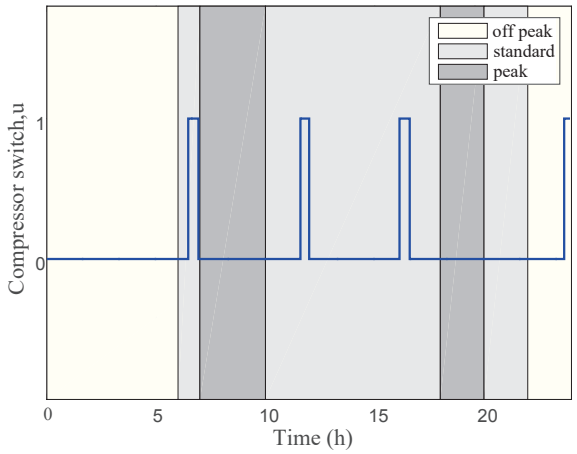

Figure 3.7(a)(ii)

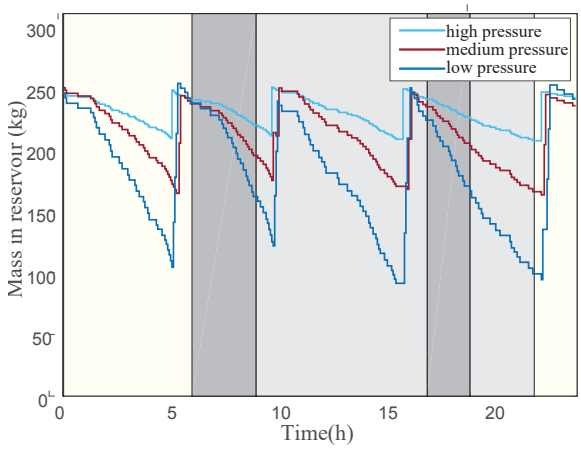

Figure 3.7(b)(i)

High electricity Demand season

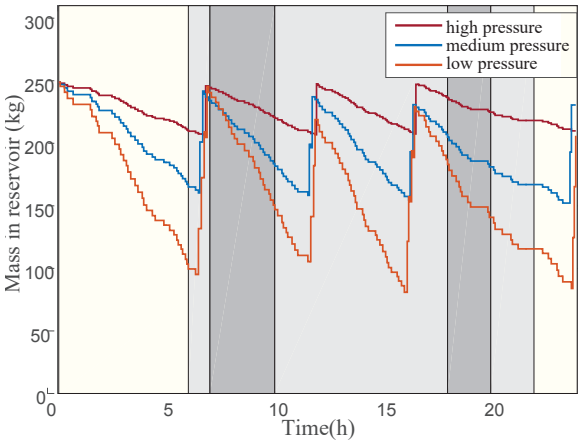

Figure 3.7(b)(ii)

Low electricity demand season

Figure 3.7. (a) Compressor switching and (b) mass of gas in reservoir results with terminal constraints for high and low electricity demand seasons

morning and evening peaks over the control horizon, for the both the high and low electricity demand pricing seasons. Further, the gas quantity held in the cascade storage is replenished to near initial condition levels at an electricity cost of R171.60 for the high electricity demand season and R139.84 for the low electricity demand which is as a result of additional compressor operation to restore gas levels to the initial condition.

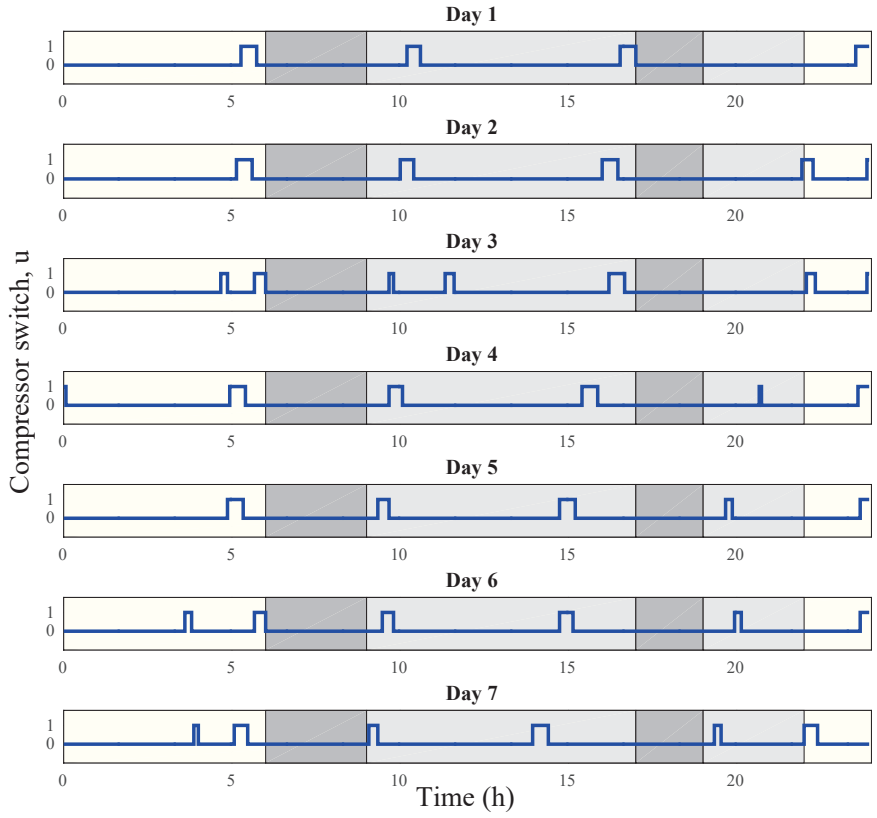

Figure 3.8(a)(i) Compressor operation in high electricity demand season

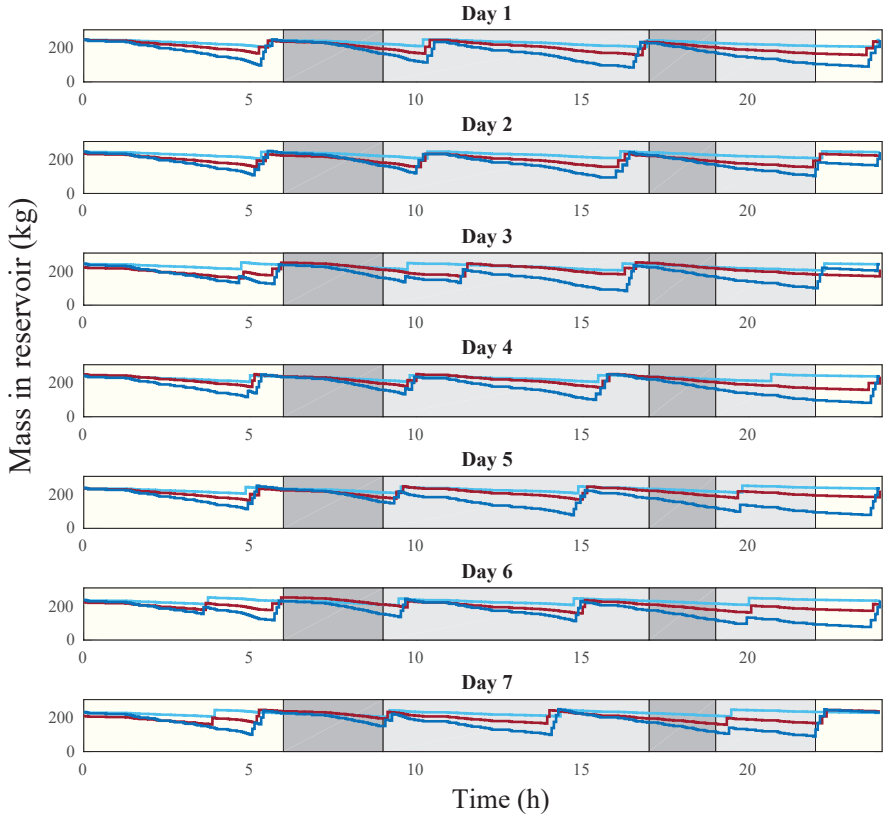

Figure 3.8(b)(i) Mass in storage in high electricity demand season.

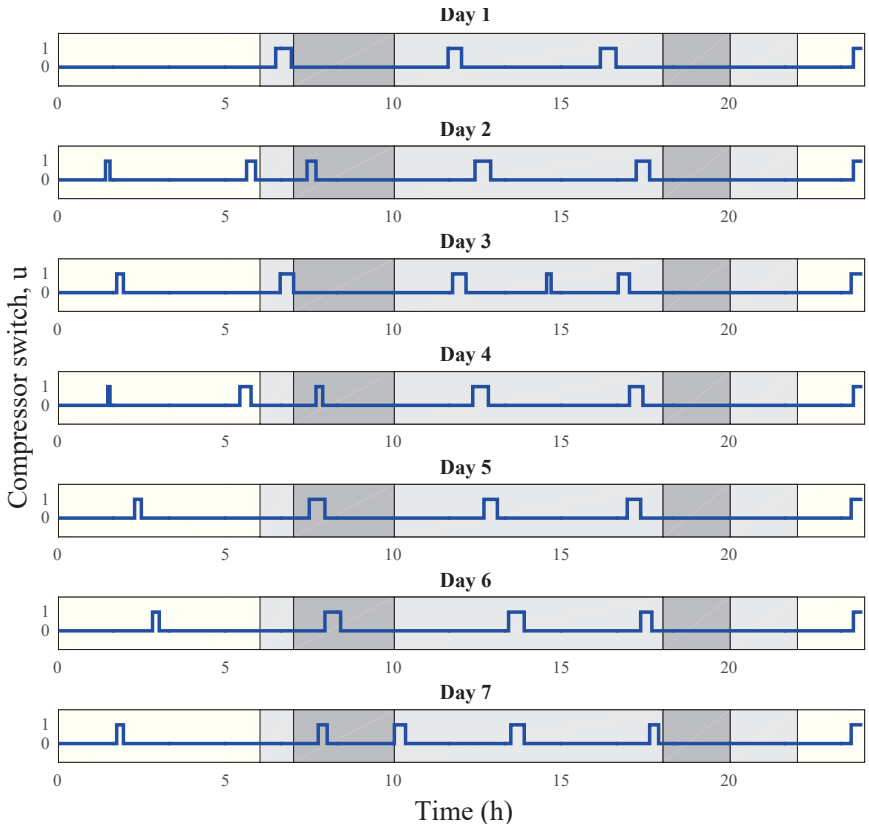

Figure 3.8(a)(ii) Compressor operation in low electricity demand season

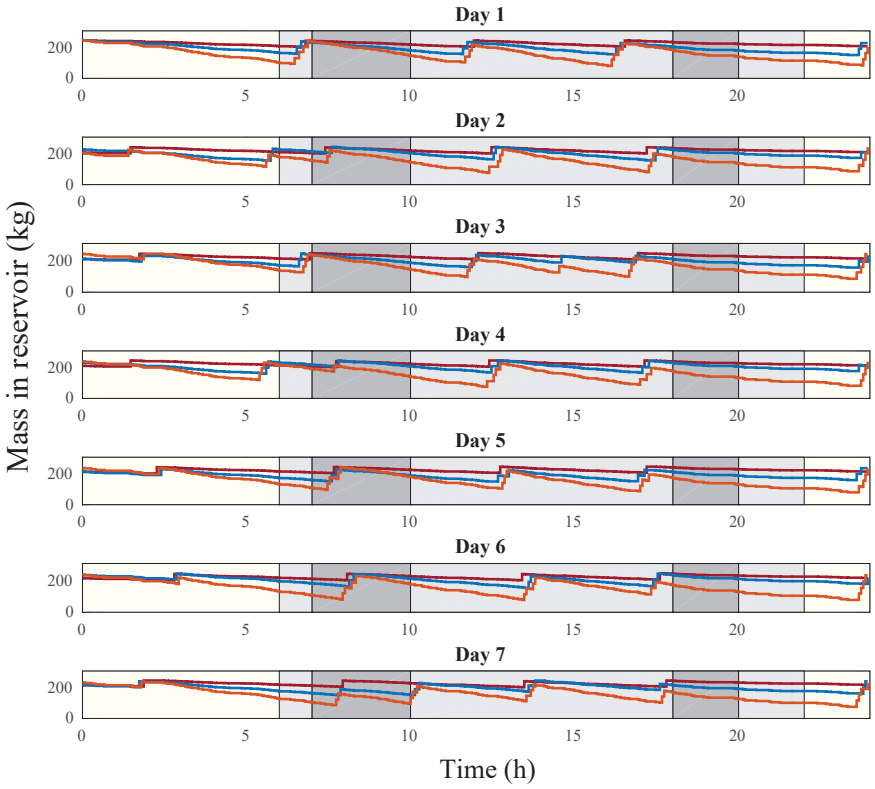

Figure 3.8(b)(ii) Mass in storage in low electricity demand season.

Figure 3.8. Solutions with terminal constraints for seven consecutive days.

The effect of the implementation of the terminal constraints is demonstrated in Figure 3.8 which shows the operation profile for seven consecutive days. In general, the level of gas in the cascade storage at the end of each day is similar to the initial conditions for that day. However variations from the initial conditions result in the compressor operation profile being slightly different for some days than others. This change in the compressor operation profile is observed in the form of the number and timing of compressor transient states during both the high electricity demand season and the low electricity demand period. Although the number of start/stop instances increases, it is still 50% lower than those observed when optimization is carried out without implementing a minimization of the switching frequency.

Over the seven days that the strategy including the terminal constraint is implemented, the compressor is still successfully kept from operating in the peak electricity pricing times of the day for the high demand electricity pricing season. The resulting average cost of electricity incurred for the week under evaluation is R176.13 per day, which is a 59.3% reduction from the baseline. The highest electricity cost for a day occurs on the fourth day at R179.91, while the lowest cost at R171.60 is incurred on the first day. For the low electricity demand pricing season, the compressor is turned on during the morning peak electricity pricing time for the 4th, 5th, 6th and 7th days. However, the average cost of electricity per day is still significantly lower than the baseline at R158.54 with the highest cost incurred on the 5th day at R172.54 and the lowest cost incurred on the 1st day at R143.16. The average savings on electricity cost from the baseline is 25% during the low demand electricity pricing period. This outcome demonstrates the versatility of the proposed strategy to deliver electricity cost savings under variant initial conditions.

3.5 CONCLUSION

Minimizing electricity costs incurred in the delivery of compressed natural gas can greatly promote the use of CNG as an alternative fuel to diesel and petrol. The results in this chapter show that 59.3% in electricity cost savings are realized, while considering both electricity cost and the sustainable operation of the CNG station compressor. These savings can be translated to a cost of gas delivery saving of 0.04 Rand cents per kilogram of CNG sold in the low demand electricity pricing period and 0.23 Rand cents per kilogram of CNG sold in the high demand electricity pricing period. These margins can add up to significant annual savings for the station operator, that can be invested in expansion of CNG infrastructure or passed on to customers to improve the attractiveness of CNG as a fuel.

The control solutions obtained through the use of the strategy proposed in this chapter can be used to set optimal operation schedules for CNG fuelling station compressors, which will save on the electricity costs, without compromising on wear and tear of the compressor. The solutions can be implemented by time scheduling compressor operation statuses on the station programmable logic controller, so that the compressor operates according to the solution of the optimal control schedule other than through limit-triggered cycling. It is necessary to implement safety interrupts for maximum and minimum pressure to deal with unexpected occurrences that may result in operation limits being violated.

The optimization model proposed in this chapter leads to improved economic efficiency of the CNG fuelling station and adds to the cost competitiveness of CNG as an alternative fuel. Reduced cost of gas delivery if passed on to consumers have the potential to encourage increased uptake CNG powered vehicles over liquid fossil fuel powered vehicles. Further, participation of CNG stations in demand response programs of the electricity grid can contribute to lowering overall green house gas emission from the electricity generation infrastructure which is one of the objectives of such programs by the power utilities.

CHAPTER 4 A HIERARCHICAL OPTIMAL OPERATION OF A COMPRESSED NATURAL GAS STATION FOR ENERGY AND FUELLING EFFICIENCY

4.1 CHAPTER OVERVIEW

In this chapter, a hierarchical model for the efficient operation of a CNG fast-fill station is presented. The model includes an upper layer, which is an optimisation of compressor scheduling to minimise energy cost, and a lower layer to control the valves of the priority panel and the gas dispenser so as to achieve desirable conditions of pressure for minimum vehicle filling time. In the upper layer, the scheduling of the compressor operation to minimise electricity cost incurred under a TOU tariff is realised while minimising compressor switching frequency and meeting the gas demand in the control horizon. The compressor operation schedule obtained is implemented on the lower layer as an input for the optimal control of vehicle fuelling to achieve minimum filling time using a model predictive control strategy (MPC). This study presents the first combined solution of the optimal minimisation of CNG station energy cost through compressor scheduling, with the optimal control of the vehicle filling pressure conditions from the cascade storage to achieve minimum filling time. The proposed approach will safeguard the gains from energy cost savings, by ensuring a simultaneous improvement in gas transfer performance which is of great importance to fuelling convenience. The work and case study highlight how adoption of alternative fuels intersects with electricity demand response programs, and how the operation optimisation for demand response must be enhanced with performance optimisation to secure the resulting complementary benefits.

For the rest of this chapter, Section 4.2 describes the modelling of the two layers of the optimal operation approach, Section 4.3 presents the data and parameters considered, while Section 4.4 is a discussion of the optimal operation results. Section 4.5 concludes this chapter.

4.2 SYSTEM MODELLING AND FORMULATION

4.2.1 The Energy Cost Minimisation Layer

Figure 4.1 shows the configuration of the CNG fast-fill station. Unlike in Figure 3.1, the dispenser valves details are illustrated because they form part of the lower layer control variables together with the priority panel valves. Under normal operation, the compressor receives natural gas from the utility's distribution pipeline at low to medium pressure, approximately 4–15 bar [39], and compresses it into a three level cascade storage system. The gas being compressed passes through a priority panel valve system that alternates the flow of CNG between the three levels of the cascade storage usually called the high pressure, medium pressure and low pressure levels according to their minimum allowed operating pressures [37]. The series of valves v_{hp}, v_{mp} and v_{lp} in the priority panel represent the inlet valves to the high pressure, medium pressure and low pressure tanks of the cascade storage respectively, similar to the case in Section 3.2. When the upper pressure limit for all the cascade storage level is achieved, the compressor switch u is turned off so that no more gas flows into the cascade storage. Vehicles arriving at the dispenser have their tanks filled through the dispenser valves v_{ohp}, v_{omp} and v_{olp} for the high pressure, medium pressure and low pressure cascade storage tanks, respectively. The gas flow is alternated so that a lower limit of flow rate determines the tank from which the vehicle is filled, starting with the lowest pressure tank to the medium pressure tank as the vehicle tank fills up and topping off with the high pressure tank [105]. As CNG leaves the cascade storage, the pressure in storage drops and when the minimum pressure limits are reached, the compressor switch u comes on to replenish the storage [111] and the cycle is repeated. The gas demand at the dispenser, m_o, determines the cycling of the compressor and thus the total cost of electricity incurred in a TOU electricity tariff. The energy cost minimisation layer is formulated as a mass flow problem. This means that the scheduling of the compressor operation is optimised around mass inflow to the cascade storage from the municipal supply line and mass outflow as determined by mass of gas demand at the dispenser over the control horizon.

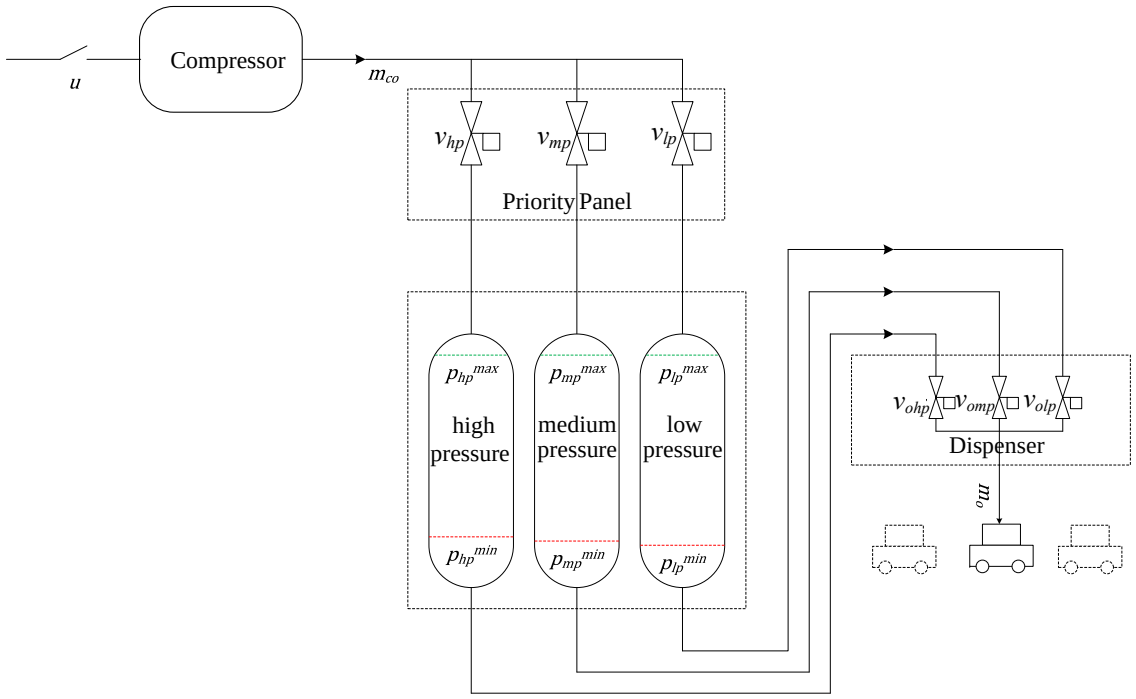

Figure 4.1. Layout of the fast-fill CNG station.

4.2.1.1 Objective Function

The objective of this layer is to minimise the cost of electricity incurred by the compressor operation over the control horizon so that the following objective function is used:

$$J = \sum_{t=1}^{N} P_{co} P_e(t) t_s u(t), \tag{4.1}$$

where t is the counter for the sampling instants, N is the total number of sampling instants over the control horizon, P_{co} is the compressor power rating in kW, $P_e(t)$ is a vector of the price of electricity per kWh in a TOU tariff, t_s is the sampling period and $u(t)$ is the status of the compressor switch which is the control variable such that

$$u(t) \in \{0,1\} \quad \text{for} \quad 1 \leq t \leq N. \tag{4.2}$$

It is important to modify the objective function so that the switching frequency of the compressor is minimised as well. This is because the frequency of on/off instances positively correlates to increased

wear and tear of moving components of the compressor [86, 90]. For the optimised minimum cost of electricity incurred over the control horizon, this study seeks to achieve the lowest number of switching instances for the compressor. One of the methods considered is the one used in the previous chapter, where the approach involves the reduction of the ramp rate between successive instances of the switch so that the element of the objective function dealing with minimising compressor frequency is

$$J_q = \sum_{t=1}^{N-1} \Big(u(t+1) - u(t) \Big)^2. \tag{4.3}$$

Elsewhere the approach based on the introduction of an auxiliary variable $s(t)$ [96, 97] was also considered. The auxiliary variable assumes a value of 1 when a switch-on occurs and tries to minimise the summation of the auxiliary variable over the control horizon such that

$$J_{pr} = \sum_{t=1}^{N} s(t), \tag{4.4}$$

and

$$u(1) - s(1) \leq 0, \tag{4.5}$$

$$u(t) - u(t-i) - s(t) \leq 0. \tag{4.6}$$

Although both methods have already been demonstrated to be effective, in this chapter, we introduce a new method where the operation is optimised to prefer the occurrence of on-instances in succession of each other by minimising the summation of the negative product of successive instances of the solution to the control variable u, so that the objective function becomes

$$J_U = \rho \sum_{t=1}^{N} P_{co} P_e t_s u(t) + (1-\rho) \sum_{t=1}^{N-1} \Big(-u(t)u(t+1) \Big), \tag{4.7}$$

where ρ is a weighting factor. The weighting factor can be set to reduce the number of switching instances so that the minimum number possible is attained for the same energy cost incurred such as was the case in Chapter 3. The method proposed in this chapter for minimising the frequency of compressor switching, involves a single mathematical operation and no additional constraints which reduces the computational complexity of the problem when compared with (4.3) and (4.4).

4.2.1.2 Constraints

The constraints for this upper layer minimising energy cost are based on the total mass storage capacity of the cascade storage as well as the terminal conditions so that

$$m_{min} \leq m(t) \leq m_{max}, \tag{4.8}$$

where m_{max} is the maximum mass limit of gas for the cascade storage corresponding to the maximum pressure limits, m_{min} is the minimum mass limit of gas for the cascade storage at the minimum pressure limits and the mass of gas in the cascade storage $m(t)$ is

$$m(t) = m(0) + t_s \sum_{i=0}^{t-1} \dot{m}_{co} u(i) - \sum_{i=0}^{t-1} m_o(i), \tag{4.9}$$

where $m_o(i)$ is the mass of gas flowing out of the cascade storage into a vehicle in a sampling instant and $\dot{m_{co}}$ is the mass flow rate of the compressor in kg/h which is obtained as [30]

$$\dot{m}_{co} = \rho_{std} \times Q_{std} = (\frac{Mw_g}{Mw_a}) \times \rho_{a,std} \times Q_{std}, \tag{4.10}$$

where ρ_{std} is the density of CNG in kg/m^3, Mw_g is the molecular weight of the CNG, Mw_a is the molecular weight of air, $\rho_{a,std}$ is the air density in kg/m^3 and Q_{std} is the capacity of the compressor in m^3/h. The values of ρ_{std}, $\rho_{a,std}$ and Q_{std} are under standard conditions (0^oC temperature and $10^5 pascals$ pressure) [87].

The mass limits of gas for the cascade storage capacity constraints m_{min} and m_{max} are derived from working pressure limits of the cascade storage and the physical properties of the gas

$$pV = znRT, \tag{4.11}$$

where p is the value of the pressure rating in $bars$, V is the total volume of the cascade storage in L, z is the compressibility factor, R is the ideal gas constant and n the quantity of gas in moles which is correlated with the mass as

$$n = \frac{m}{M}, \tag{4.12}$$

where M is the molar mass. The working mass limits for the cascade storage therefore become

$$m_{max} = \frac{MVP_{max}}{zRT} \quad m_{min} = \frac{MVP_{min}}{zRT}. \tag{4.13}$$

4.2.1.3 Algorithm

To solve the problem using OPTI toolbox SCIP solver interfaced in Matlab [101], the upper layer energy cost minimisation layer problem is formulated in the form

$$\text{minimise}_x \quad f(x), \tag{4.14}$$

$$\text{subject to} \quad Ax \leq b, \tag{4.15}$$

$$l_b \leq x \leq u_b, \tag{4.16}$$

$$x \in \{0,1\}. \tag{4.17}$$

The objective function in (4.7) is expressed as

$$f(x) = \left(\rho P_{co} P_e t_s \times \Big(u(1)+u(2)+\cdots+u(N)\Big)\right) - \left((1-\rho)\times\Big(u(1)\times u(2)+u(2)\times u(3)+\cdots+u(N-1)\times u(N)\Big)\right). \tag{4.18}$$

From the constraint (4.8) and the dynamic equation of mass (4.9), these linear inequalities can be expressed as

$$\boldsymbol{Ax} \leq \boldsymbol{b_1}, \tag{4.19}$$

$$-\boldsymbol{Ax} \leq \boldsymbol{b_2}, \tag{4.20}$$

where

$$\boldsymbol{A} = \begin{bmatrix} -t_s\dot{m}_{co} & 0 & \cdots & 0 \\ -t_s\dot{m}_{co} & -t_s\dot{m}_{co} & \cdots & 0 \\ \vdots & \vdots & \ddots & \vdots \\ -t_s\dot{m}_{co} & -t_s\dot{m}_{co} & \cdots & -t_s\dot{m}_{co} \end{bmatrix}_{N\times N}, \tag{4.21}$$

$$\boldsymbol{b_1} = \begin{bmatrix} m(0) - m_{min} - m_o(1) \\ m(0) - m_{min} - \Big(m_o(1) + m_o(2)\Big) \\ \vdots \\ m(0) - m_{min} - \Big(m_o(1) + m_o(2) + \cdots + m_o(N)\Big) \end{bmatrix}_{N\times 1}, \tag{4.22}$$

$$\boldsymbol{b_2} = \begin{bmatrix} m_{max} - m(0) + m_o(1) \\ m_{max} - m(0) + \Big(m_o(1) + m_o(2)\Big) \\ \vdots \\ m_{max} - m(0) + \Big(m_o(1) + m_o(2) + \cdots + m_o(N)\Big) \end{bmatrix}_{N\times 1}. \tag{4.23}$$

The linear inequality constraints in the form of $\boldsymbol{Ax} \leq \boldsymbol{b}$ become

$$\boldsymbol{A} = \begin{bmatrix} \boldsymbol{A} \\ -\boldsymbol{A} \end{bmatrix}_{2N\times N}, \boldsymbol{b} = \begin{bmatrix} \boldsymbol{b_1} \\ \boldsymbol{b_2} \end{bmatrix}_{2N\times 1}. \tag{4.24}$$

The control vector for the problem, x, can be written in the standard form

$$\boldsymbol{x} = [u(1), u(2) \cdots u(N)]^T_{N\times 1}. \tag{4.25}$$

4.2.2 Gas Flow Optimisation Layer

A model predictive control (MPC) strategy is implemented on the lower layer with a prediction horizon N_p and the sampling time t_{ss}. The status of the compressor switch u is obtained from the solution of optimisation of the upper layer. Whenever switch u is on, gas flows into the three tank storage via valves v_{hp}, v_{mp} and v_{lp} of the priority panel. The gas flows in from the compressor at a constant mass flow rate $\dot{m}_{co}$. Each of the three tanks has maximum and minimum pressures, p_{hp}^{max}, p_{mp}^{max}, p_{lp}^{max} and p_{hp}^{min}, and p_{mp}^{min} and p_{lp}^{min}, respectively. Gas flows into the vehicle from the storage tanks via the dispenser valves v_{ohp}, v_{omp} and v_{olp}. The initial pressure for each vehicle tank p_{veh} is a known quantity from the demand data while the initial pressure for the high pressure tank p_{hp}, medium pressure tank p_{mp} and low pressure tank p_{lp} are measured from the final conditions after the previous control action.

4.2.2.1 Objective Function

The objective of this layer is to minimise the difference between the vehicle tank pressure $p_{veh}(k+j)$ and the target pressure $p_T(k+j)$ which corresponds to the quantity of gas ordered by the customer for the vehicle at step j based on the current sampling instant k. This ensures continuous flow of gas from the cascade storage tanks to the vehicle tank. Additionally, we minimise the summation of dispenser valve action instances, which ensures minimisation of filling time. This is because lowering the total number of instances required for the dispenser valves to be on in order to fill the vehicle tank, corresponds to a shorter filling time of the vehicle tank. Therefore, the controller prefers the cascade filling profile with the least number of total dispenser valve open instances. The objective function based on the current sampling instant k is therefore to minimise

$$J_L(k) = (\varsigma) \sum_{j=0}^{N_p-1} \left(p_T(k+j) - p_{veh}(k+j) \right) + (1-\varsigma) \sum_{j=0}^{N_p-1} \left(v_{ohp}(k+j) + v_{omp}(k+j) + v_{olp}(k+j) \right), \tag{4.26}$$

where ς is a weighting factor and $v_{ohp}(k+j)$, $v_{omp}(k+j)$ and $v_{olp}(k+j)$ are the dispenser statuses for the high pressure, medium pressure and low pressure cascade storage tanks, respectively. Gas flow from the cascade storage tanks to the vehicle tank, $\dot{m}_{veh}(k+j)$ ensures that the vehicle pressure approaches the target pressure value and is the sum of flow rates from the three tanks, so that based on the current sampling instant k

$$\dot{m}_{veh}(k+j) = \dot{m}_{hp}(k+j)v_{ohp}(k+j) + \dot{m}_{mp}(k+j)v_{omp}(k+j) + \dot{m}_{lp}(k+j)v_{olp}(k+j). \tag{4.27}$$

The equations for the instantaneous flow rates $\dot{m}_{hp}(k+j)$, $\dot{m}_{mp}(k+j)$ and $\dot{m}_{lp}(k+j)$ between the high, medium and low pressure tanks of the cascade storage, respectively, and the vehicle tank, are based on the ideal gas model for an adiabatic system [112] and are governed by the pressure ratios between the storage tanks and the vehicle tank. i.e.,

$$\begin{aligned} \dot{m}_{hp}(k+j) =& C_d \rho_{hp}(k+j) A_{orifice} \left(\frac{p_{veh}(k+j)}{p_{hp}(k+j)} \right)^{\frac{1}{\gamma}} \left\{ \left(\frac{2\gamma}{\gamma-1}\right) \left(\frac{p_{hp}(k+j)}{\rho_{hp}(k+j)}\right) \left(1 - \left(\frac{p_{veh}(k+j)}{p_{hp}(k+j)}\right)^{\frac{\gamma-1}{\gamma}} \right) \right\}^{\frac{1}{2}} \\ & \text{for} \quad \frac{p_{veh}(k+j)}{p_{hp}(k+j)} \leq \left(\frac{2}{\gamma+1} \right)^{\frac{\gamma}{\gamma-1}}, \end{aligned} \tag{4.28}$$

and

$$\dot{m}_{hp}(k+j) = C_d\sqrt{\gamma p_{hp}(k+j)\rho_{hp}(k+j)A_{orifice}}\left(\frac{2}{\gamma+1}\right)^{\frac{\gamma+1}{2(\gamma-1)}} \text{for} \quad \frac{p_{veh}(k+j)}{p_{hp}(k+j)} \geq \left(\frac{2}{\gamma+1}\right)^{\frac{\gamma}{\gamma-1}}, \tag{4.29}$$

and similarly for the $\dot{m}_{mp}(k+j)$

$$\begin{aligned}\dot{m}_{mp}(k+j) =& C_d\rho_{mp}(k+j)A_{orifice}\left(\frac{p_{veh}(k+j)}{p_{mp}(k+j)}\right)^{\frac{1}{\gamma}}\left\{(\frac{2\gamma}{\gamma-1})(\frac{p_{mp}(k+j)}{\rho_{mp}(k+j)})\left(1-(\frac{p_{veh}(k+j)}{p_{mp}(k+j)})^{\frac{\gamma-1}{\gamma}}\right)\right\}^{\frac{1}{2}} \\ &\text{for} \quad \frac{p_{veh}(k+j)}{p_{mp}(k+j)} \leq \left(\frac{2}{\gamma+1}\right)^{\frac{\gamma}{\gamma-1}},\end{aligned} \tag{4.30}$$

and

$$\dot{m}_{mp}(k+j) = C_d\sqrt{\gamma p_{mp}(k+j)\rho_{mp}(k+j)A_{orifice}}\left(\frac{2}{\gamma+1}\right)^{\frac{\gamma+1}{2(\gamma-1)}} \text{for} \quad \frac{p_{veh}(k+j)}{p_{mp}(k+j)} \geq \left(\frac{2}{\gamma+1}\right)^{\frac{\gamma}{\gamma-1}}, \tag{4.31}$$

and for $\dot{m}_{lp}(k+j)$

$$\begin{aligned}\dot{m}_{lp}(k+j) =& C_d\rho_{lp}(k+j)A_{orifice}\left(\frac{p_{veh}(k+j)}{p_{lp}(k+j)}\right)^{\frac{1}{\gamma}}\left\{(\frac{2\gamma}{\gamma-1})(\frac{p_{lp}(k+j)}{\rho_{lp}(k+j)})\left(1-(\frac{p_{veh}(k+j)}{p_{lp}(k+j)})^{\frac{\gamma-1}{\gamma}}\right)\right\}^{\frac{1}{2}} \\ &\text{for} \quad \frac{p_{veh}(k+j)}{p_{lp}(k+j)} \leq \left(\frac{2}{\gamma+1}\right)^{\frac{\gamma}{\gamma-1}},\end{aligned} \tag{4.32}$$

and

$$\dot{m}_{lp}(k+j) = C_d\sqrt{\gamma p_{lp}(k+j)\rho_{lp}(k+j)A_{orifice}}\left(\frac{2}{\gamma+1}\right)^{\frac{\gamma+1}{2(\gamma-1)}} \text{for} \quad \frac{p_{veh}(k+j)}{p_{lp}(k+j)} \geq \left(\frac{2}{\gamma+1}\right)^{\frac{\gamma}{\gamma-1}}, \tag{4.33}$$

where γ is the ratio of specific heats

$$\gamma = \frac{c_p}{c_v}, \tag{4.34}$$

and c_p is the specific heat capacity of the gas at constant pressure while c_v is specific heat capacity of the gas at constant volume. C_d is the coefficient of discharge of the dispenser valve orifice, $A_{orifice}$ is the area of the dispenser valve orifice in m^2 and ρ_{hp}, ρ_{mp} and ρ_{lp} are the densities of the gas in the high pressure ,medium pressure and low pressure reservoirs respectively in kg/m^3.

4.2.2.2 Constraints

The valves at the dispenser and the priority panel, as the control variables, are subject to operational constraints. The valves of the priority panel open one at a time when the compressor is filling the cascade storage reservoirs which gives the constraint in (4.35). The valves of the dispenser also open one at a time during the filling of the vehicle from the cascade storage as represented by the constraint in (4.36).

$$v_{hp}(k+j) + v_{mp}(k+j) + v_{lp}(k+j) - u(k+j) = 0, \tag{4.35}$$

$$v_{ohp}(k+j) + v_{omp}(k+j) + v_{olp}(k+j) \leq 1, \tag{4.36}$$

$$v_{ohp}(k+j), v_{omp}(k+j), v_{olp}(k+j), v_{hp}(k+j), v_{mp}(k+j), v_{lp}(k+j), u(k+j) \in \{0,1\}.$$

Further, the vehicle tank pressure p_{veh} and the pressure in the three cascade reservoirs p_{hp}, p_{mp} and p_{lp}, as the states of the gas flow optimisation layer, are also subject to operational constraints. The limits of pressure for the vehicle tank and each of the reservoirs of the cascade storage are such that

$$p_{hp}^{min} \leq p_{hp}(k+j) \leq p_{hp}^{max}, \tag{4.37}$$

$$p_{mp}^{min} \leq p_{mp}(k+j) \leq p_{mp}^{max}, \tag{4.38}$$

$$p_{lp}^{min} \leq p_{lp}(k+j) \leq p_{lp}^{max}, \tag{4.39}$$

$$p_{veh}(k+N_p+1-j) \geq p_T(k), \tag{4.40}$$

Equations (4.37)–(4.39) ensure that the maximum and minimum working pressures of the cascade storage tanks are not exceeded, while (4.40) ensures that, at the end of the control horizon, the vehicle tank is filled to the target pressure corresponding to the requested quantity of gas by the customer.

Based on the described flow of gas for the proposed approach, the general differential equations for pressure change in the vehicle and cascade storage reservoirs are

$$\frac{d}{dt}p_{veh}(t) = \dot{m}_{veh}(t)K_1, \tag{4.41}$$

$$\frac{d}{dt}p_{hp}(t) = -\dot{m}_{hp}(t)K_{hp}v_{ohp}(t) + \dot{m}_{co}v_{hp}(t), \tag{4.42}$$

$$\frac{d}{dt}p_{mp}(t) = -\dot{m}_{mp}(t)K_{mp}v_{omp}(t) + \dot{m}_{co}v_{mp}(t), \tag{4.43}$$

$$\frac{d}{dt}p_{lp}(t) = -\dot{m}_{lp}(t)K_{lp}v_{olp}(t) + \dot{m}_{co}v_{lp}(t), \tag{4.44}$$

where the constants K_1, K_{hp}, K_{mp} and K_{lp} are

$$K_1 = T\left(\frac{c_p}{c_v}\frac{R}{V_{veh}}\right), \quad K_{hp} = T\left(\frac{c_p}{c_v}\frac{R}{V_{hp}}\right), \quad K_{mp} = T\left(\frac{c_p}{c_v}\frac{R}{V_{mp}}\right) \quad \text{and} \quad K_{lp} = T\left(\frac{c_p}{c_v}\frac{R}{V_{lp}}\right), \tag{4.45}$$

where V_{veh}, V_{hp}, V_{mp} and V_{lp} are the volumes of the vehicle tank in L, high pressure reservoir, medium pressure reservoir and low pressure reservoir, respectively. This yields the following discrete equations of pressure, for the current sampling instant k

$$p_{veh}(k+j) = p_{veh}(k) + t_{ss}K_1\sum_{\tau=k}^{k+j}\dot{m}_{veh}(\tau), \tag{4.46}$$

$$p_{hp}(k+j) = p_{hp}(k) - t_{ss}K_{hp}\sum_{\tau=k}^{k+j}\dot{m}_{veh}(\tau)v_{ohp}(\tau) + t_{ss}\dot{m}_{co}\sum_{\tau=k}^{k+j}v_{hp}(\tau), \tag{4.47}$$

$$p_{mp}(k+j) = p_{mp}(k) - t_{ss}K_{mp}\sum_{\tau=k}^{k+j}\dot{m}_{veh}(\tau)v_{omp}(\tau) + t_{ss}\dot{m}_{co}\sum_{\tau=k}^{k+j}v_{mp}(\tau), \tag{4.48}$$

$$p_{lp}(k+j) = p_{lp}(k) - t_{ss}K_{lp}\sum_{\tau=k}^{k+j}\dot{m}_{veh}(\tau)v_{olp}(\tau) + t_{ss}\dot{m}_{co}\sum_{\tau=k}^{k+j}v_{lp}(\tau). \tag{4.49}$$

4.2.2.3 Algorithm

The Mixed Integer Distributed Ant Colony Optimisation (MIDACO) solver was chosen for the solution of the lower layer MPC problem because it was found to be significantly more time efficient in solving this mixed integer nonlinear programming (MINLP) problem, compared to the OPTI toolbox SCIP solver used in Chapter 3 and in the upper layer integer programming problem in Section 4.2.1.3 [113]. To solve the gas flow optimisation layer problem using the Mixed Integer Distributed Ant Colony Optimisation (MIDACO) solver, the components of the problem have to be formulated as

$$\begin{aligned} &\text{minimise} && f(x) && \text{(objective function)} && (4.50)\\ &\text{subject to} && g(x) = 0 && \text{(equality constraints)} && (4.51)\\ &&& h(x) \geq 0 && \text{(inequality constraints)} && (4.52) \end{aligned}$$

The control vector consists of the conditions of the three priority panel valves and the three dispenser valves, and for each sampling instant k, x can be written in the standard form

$$\begin{aligned} \boldsymbol{x} = [&v_{hp}(k+1), v_{hp}(k+2), \cdots v_{hp}(k+N_p), v_{mp}(k+1), v_{mp}(k+2), \cdots v_{mp}(k+N_p), v_{lp}(k+1),\\ &v_{lp}(k+2), \cdots v_{lp}(k+N_p), v_{ohp}(k+1), v_{ohp}(k+2), \cdots v_{ohp}(k+N_p), v_{omp}(k+1),\\ &v_{omp}(k+2), \cdots v_{omp}(k+N_p), v_{olp}(k+1), v_{olp}(k+2), \cdots v_{olp}(k+N_p),]^T_{6N_p\times 1}. \end{aligned} \tag{4.53}$$

The objective function (4.26),

$$\begin{aligned} \boldsymbol{f(x)} = [&\varsigma \times \Big(P_T - P_{veh}(k+1) + P_T - P_{veh}(k+2) \cdots P_T - P_{veh}(k+N_p)\Big) + (1-\varsigma) \times \Big(v_{ohp}(k+1) +\\ &v_{omp}(k+1) + v_{olp}(k+1) + v_{ohp}(k+2) + v_{omp}(k+2) + v_{olp}(k+2) \cdots\\ &v_{ohp}(k+N_p) + v_{omp}(k+N_p) + v_{olp}(k+N_p)\Big)]. \end{aligned} \tag{4.54}$$

The equality constraint (4.35) yields the $g(x) = 0$ set for the algorithm so that

$$\boldsymbol{g(x)} = \begin{bmatrix} v_{hp}(k+1)+v_{mp}(k+1)+v_{lp}(k+1)-u(k+1)\\ v_{hp}(k+2)+v_{mp}(k+2)+v_{lp}(k+2)-u(k+2)\\ \vdots\\ v_{hp}(k+N_p)+v_{mp}(k+N_p)+v_{lp}(k+N_p)-u(k+N_p) \end{bmatrix}_{N_p\times 1}, \tag{4.55}$$

while the inequality (4.36) yields the first set of $h(x) \geq 0$ such that

$$\boldsymbol{h_1(x)} = \begin{bmatrix} 1-\Big(v_{ohp}(k+1)+v_{omp}(k+1)+v_{olp}(k+1)\Big) \\ 1-\Big(v_{ohp}(k+2)+v_{omp}(k+2)+v_{olp}(k+2)\Big) \\ \vdots \\ 1-\Big(v_{ohp}(k+N_p)+v_{omp}(k+N_p)+v_{olp}(k+N_p)\Big) \end{bmatrix}_{N_p \times 1} . \tag{4.56}$$

The next set of inequality constraints is derived from (4.37)–(4.39) such that

$$\boldsymbol{h_2(x)} = \begin{bmatrix} p_{hp}^{max}-p_{hp}(k+1) \\ \vdots \\ p_{hp}^{max}-p_{hp}(k+N_p) \\ p_{mp}^{max}-p_{mp}(k+1) \\ \vdots \\ p_{mp}^{max}-p_{mp}(k+N_p) \\ p_{lp}^{max}-p_{lp}(k+1) \\ \vdots \\ p_{lp}^{max}-p_{lp}(k+N_p) \\ p_{hp}(k+1)-p_{hp}^{min} \\ \vdots \\ p_{hp}(k+N_p)-p_{hp}^{min} \\ p_{mp}(k+1)-p_{mp}^{min} \\ \vdots \\ p_{mp}(k+N_p)-p_{mp}^{min} \\ p_{lp}(k+1)-p_{lp}^{min} \\ \vdots \\ p_{lp}(k+N_p)-p_{lp}^{min} \end{bmatrix}_{6N_p \times 1} . \tag{4.57}$$

The final element of the inequality constraints is derived from (4.40), yielding

$$\boldsymbol{h_3(x)} = \Big[\, p_{veh}(k+N+1-j)-p_T(k) \,\Big]_{1\times 1} . \tag{4.58}$$

The combined set of inequality constraints therefore becomes

$$\boldsymbol{h}(\boldsymbol{x}) = \begin{bmatrix} \boldsymbol{h_1}(\boldsymbol{x}) \\ \boldsymbol{h_2}(\boldsymbol{x}) \\ \boldsymbol{h_3}(\boldsymbol{x}) \end{bmatrix}_{(7N_p+1)\times 1} . \tag{4.59}$$

At the current sampling instant k, an open loop optimisation problem is solved by the controller for the prediction horizon N_p. Only the first elements of the control variables v_{hp}, v_{mp}, v_{lp}, v_{ohp}, v_{omp} and v_{olp} are implemented on the CNG filling station plant. The vehicle pressure p_{veh} and the pressure in the cascade storage tanks p_{hp}, p_{mp} and p_{lp}, which are the system states, are measured and the values fed back to the MPC controller, forming the initial states for the following sampling instant $k+1$. The input variables are then updated and the cycle repeated until all control actions for the intended period are implemented.

The MPC controller workflow is such that:

1. For the current sampling instant k, the controller minimises the objective function (4.26) and finds an optimum solution for the control variables v_{hp}, v_{mp}, v_{lp}, v_{ohp}, v_{omp} and v_{olp}, subject to the constraints set out in Section 4.2.2.2.
2. From the solution, only the first elements of the solution $v_{hp}(k|k)$, $v_{mp}(k|k)$, $v_{lp}(k|k)$, $v_{ohp}(k|k)$, $v_{omp}(k|k)$ and $v_{olp}(k|k)$ are implemented.
3. The states $p_{veh}(k+1)$, $p_{hp}(k+1)$, $p_{mp}(k+1)$ and $p_{lp}(k+1)$ are measured to be fed back.
4. The value of k is set to $k = k+1$ and system states, inputs and outputs are updated.
5. Steps 1–4 are repeated until k reaches a value predetermined to mark the end of the control period.

4.3 CASE STUDY

The case study involves a roadside vehicle fuelling station based in Johannesburg South Africa, that is currently in operation, located in an industrial zone, as shown on the map in Figure 4.2. The average hourly demand profile for a 24-hour period, which is the upper layer control horizon N, is shown in Figure 4.3. The station serves vehicles mainly in the public transportation sector and fleets of courier and security firms. Both individual and fleet customers arrive one by one on their individual need basis,

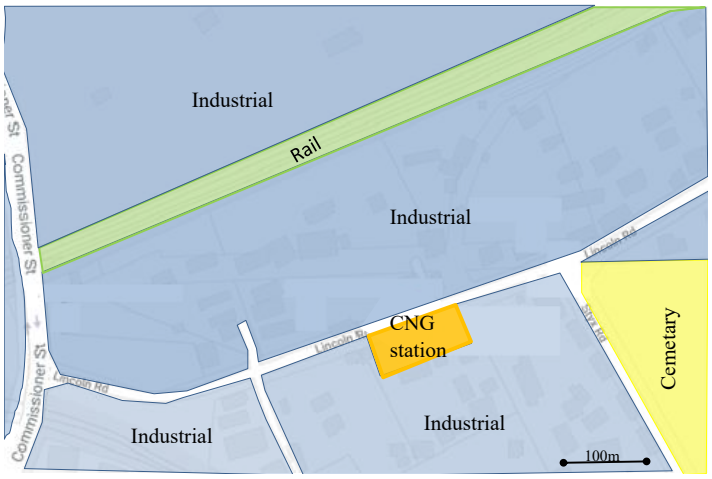

Figure 4.2. Station location and land use map.

and there is currently no scheduled fleet refuelling at this station. Vehicles serviced by the fuelling station are hybrid fuelled, with combined CNG and diesel/petrol powered engines. The vehicles are run on CNG and resort to diesel and petrol power when the CNG in their tanks runs out. The station itself obtains gas from a municipal line, which is compressed by a 132 kW motor powered compressor, into three levels of the cascade storage, which are 2000 L each. The three level tanks have a maximum operating pressure of 250 bar and are in the baseline operated at minimum pressures of 75 bar, 150 bar and 210 bar for the low pressure, medium pressure and high pressure reservoirs, respectively. The compressor pumps gas into the storage at a rate of 900 m^3/h. Although the station has two installed compressors and three dispensers, the station only operates one compressor and fills vehicles from one dispenser, since the current number of customers visiting the station is modest and no congestion or queuing problem has arisen. The station compressor operates between the limits of the quantity of gas in storage with the compressor being switched on at the lower limit to fill the cascade storage, and once the compressor is on, stays on to fill the cascade storage to the upper limit. The compressed natural gas station purchases electricity from South Africa's national utility firm Eskom based on a time-of-use tariff known as the Miniflex tariff which is priced in South African Rands as

$$p_e(t) = \begin{cases} p_{offpeak} = 0.5157 \text{ R/kWh} & \text{if } t \in [0,6] \cup [22,24] \\ p_{standard} = 0.9446 \text{ R/kWh} & \text{if } t \in [9,17] \cup [19,22] \\ p_{peak} = 3.1047 \text{ R/kWh} & \text{if } t \in [6,9] \cup [17,19] \end{cases} \tag{4.60}$$

The tariff is divided into peak, offpeak and standard times during the day, reflecting the times during the day when electricity demand is high, low and intermediate, respectively.

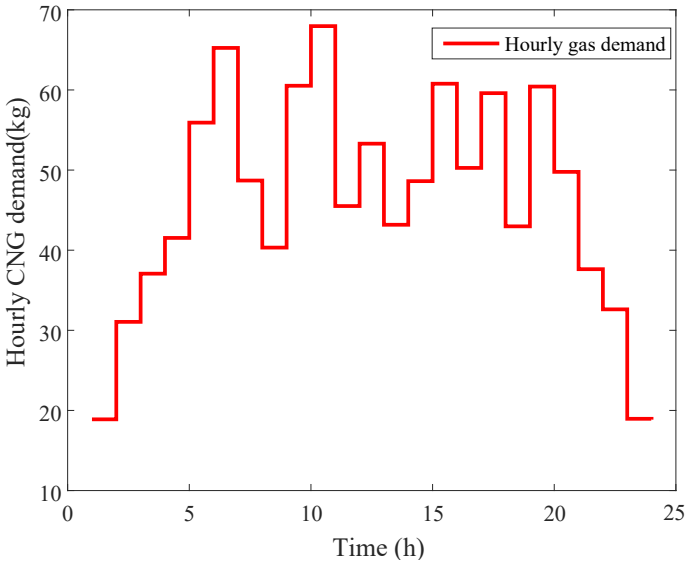

Figure 4.3. Average hourly gas demand profile for the Johannesburg CNG fuelling station.

A sampling time of 15 minutes is used for the upper layer of this study with a control horizon of 24 hours. For the lower layer MPC problem, a sampling time of 20 seconds for a receding prediction horizon N_p of five minutes is used. During existing baseline operation, vehicle tank filling starts at the low pressure reservoir and the transfer to medium and high pressure reservoirs occurs when the flow rate between the reservoir and the vehicle tank falls to a set point. This study seeks to allow the flexibility of the transfer of vehicle filling between the reservoirs through optimised control of the dispenser valves in the lower layer. The priority panel valves and the dispenser valves are modelled as binary valves with orifice diameters of 5 mm each. There are two sizes of vehicle cylinders for the vehicles fuelled in the 24 hour control horizon at 80 and 100 litres respectively. The initial vehicle tank pressure is assumed to be 1 bar since the vehicles are hybrid CNG and petrol/diesel powered and typically refill CNG tanks on empty.

The solution of the upper layer compressor schedule obtained from optimisation for the average 24-hour demand is applied to the MPC receding horizon control of vehicle filling, for a day in which 143 vehicles fuel at the CNG station with gas demand as shown in Figure 4.4. Table 4.1 shows additional parameters and constants

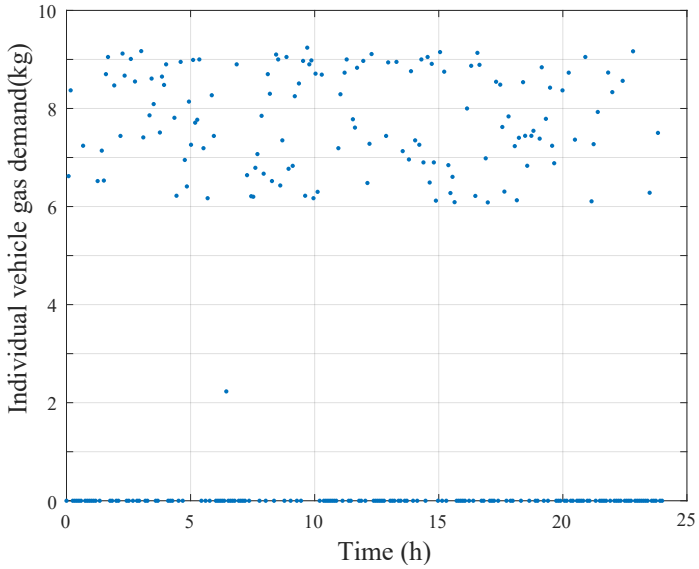

Figure 4.4. Individual vehicle gas demand over 24 hours.

Table 4.1. Additional parameters and constants.

Parameter	Value
$\rho_{a,std}$	1.225 kg/m^3
C_d	0.61
γ	1.304
Mw_a	0.028966 g
Mw_g	0.0164 g
R	0.083145 LbarK^{-1}mol^{-1}
T	294.15 K

Figure 4.5 demonstrates the functioning of the compressor under the baseline cycling operation. The compressor cycles between the minimum and maximum limits of the storage to maintain the level of gas within designed operation limits. Indeed, in Figure 4.5(a), it is clear that the compressor operates during the peak electricity pricing period in the morning, as well as during the standard electricity pricing period during the rest of the day. This means that, under baseline operation, the station does not take advantage of the low electricity prices of the offpeak electricity pricing periods. The total cost of electricity incurred as a result of this baseline operation profile is R440.23. The main component of this cost is the cost of electricity consumed as a result of the compressor-on status during the significantly expensive peak electricity pricing period and an optimal avoidance of this occurrence should lower the cost considerably.

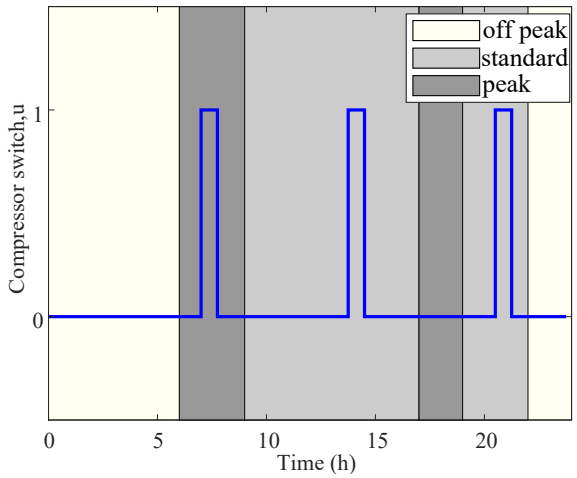

Figure 4.5(a): Compressor switch action

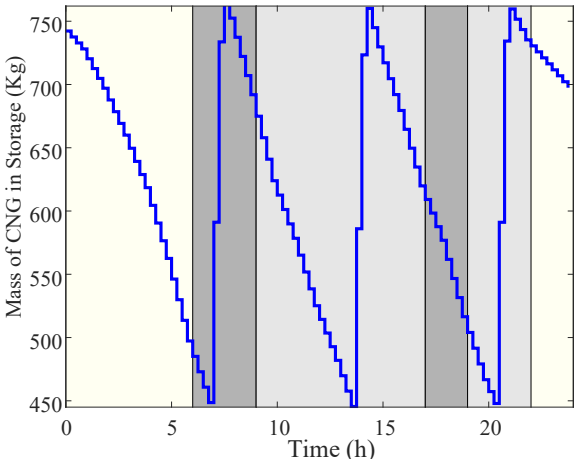

Figure 4.5(b): Total mass of gas in storage

Figure 4.5. Baseline operation profile.

4.4 RESULTS

4.4.1 Energy cost minimisation layer results.

The optimised results for the operation schedule of the compressor are shown in Figure 4.6. The proposed approach is successful in preventing compressor-on instances during both peak electricity demand periods for the average 24-hour gas demand of the control horizon. Preceding the first peak demand period between 06:00 and 09:00, the compressor switches on to replenish the gas in storage so as to sustain demand during the peak electricity pricing period during which the compressor stays off. There are two instances when the compressor is turned on during the standard electricity pricing period to meet the gas demand as well as to refill the cascade storage before the second peak electricity demand period of the 24 hours. Prior to the second peak, the cascade storage is refilled. The level of gas is thereafter enough to sustain the demand until the end of the second standard electricity pricing time at 22:00.

The delay in switching on the compressor after the second peak demand period is a desirable outcome of the optimisation strategy. This is in response to the pricing of the standard electricity demand period that is higher than the pricing during the offpeak electricity demand period, which causes the controller to prefer delaying compressor-on status beyond the peak electricity demand period [114]. The delay

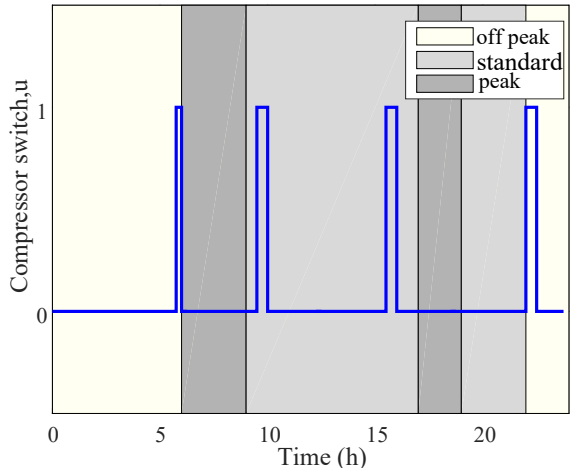

Figure 4.6(a): Compressor switch action

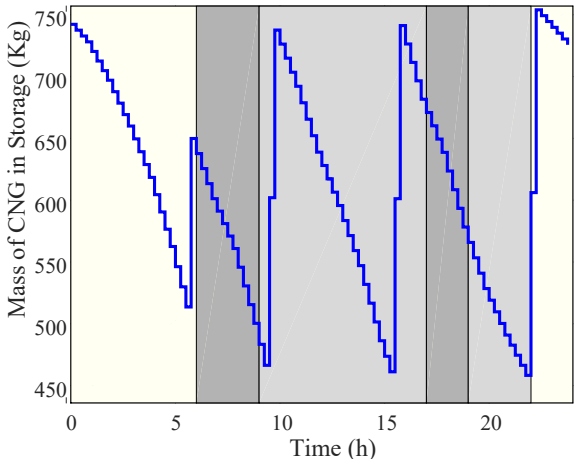

Figure 4.6(b): Total mass of gas in storage

Figure 4.6. Optimised compressor operation result for the average 24-hour horizon.

is an important quality of the realised schedule as it reduces the contribution of the CNG station to the grid comeback load associated with the surge in electricity demand immediately following the end of the peak pricing period [115, 116]. A total of four switching instances occur over the control horizon, which is comparable with observed results for alternative strategies observed in Chapter 3. This implies the superiority of the current method as it matches the performance of previously proposed techniques with the added benefit of fewer mathematical operations, thereby achieving the goal of reducing computational complexity of the problem. The computing time achieved for the upper layer using the proposed approach was 15.15 seconds, compared to 20.22 seconds for the method using (4.3) and 35.58 seconds for the method in (4.4). The strategy reduces the cost of electricity over the 24-hour horizon from the baseline R440.23 to R175.74, which represents a 60.08% reduction in energy cost. This is a significant reduction in cost of operation through a strategy that involves only a change in the operation schedule, without additional investment in new hardware.

4.4.2 Gas Flow Optimisation Layer Results

The compressor scheduling results from the energy cost minimisation layer are passed onto the lower layer, for the implementation of the MPC strategy in the vehicle tank filling for each of 143 vehicles fuelled over 24 hours. These upper layer results determine the status of the compressor switch for a particular sampling instant in the lower layer. In the lower layer problem, four scenarios emerge,

with each having a different priority panel and dispenser status combination. To ascertain the validity of the proposed approach, the system operation must remain valid and consistent with the system constraints under the four scenarios. These four scenarios are, vehicle tank filling with compressor off, vehicle tank filling with compressor on, compressor on without a vehicle filling at the dispenser, and compressor off without a vehicle filling at the dispenser.

4.4.2.1 Vehicle Filling with the Compressor Off

The results of optimised MPC filling process when a vehicle is at the dispenser and the compressor is off are shown in Figure 4.7. The results show the filling profile of the fourth vehicle of the 143 filled over the 24–hour control horizon of the upper layer. The priority panel remains inactive since no gas flows into the cascade storage from the compressor given the off-status of the compressor switch, which is scheduled from the optimisation of the upper layer. All levels of cascade storage are utilised in the implemented control actions of the filling process to attain the pressure corresponding to the target level of gas to be filled in the vehicle.

The dispenser valves from the three cascade storage tanks switch between each other to fill the vehicle's tank, as shown in Figure 4.7(b), producing the optimal pressure profile of the filling shown in Figure 4.7(c). In Figure 4.7(b), the MPC controller shuffles the operation of the dispenser valves between the three levels of the cascade storage in the filling process which is dependent on the pressure ratio between the vehicle tank and the reservoirs. This is different from the baseline operation where filling is sequentially scheduled and switching occurs at the set point of the dropping flow rate. A comparison of the pressure increase in the vehicle tank under the optimal control strategy and the baseline can be seen in Figure 4.7(c). A filling time of 200 seconds is achieved, which is shorter than the 220 seconds achieved under the baseline operation.

4.4.2.2 Vehicle Filling with the Compressor On

When the vehicle is filled as the compressor is filling the cascade storage, the profile of operation is shown in Figure 4.8. The results show the profile of the filling process for 38th vehicle of the 143 filled over the 24-hour control horizon. A smooth filling profile is obtained with a filling time of 200 seconds, which is shorter by 20 seconds from the baseline filling profile.

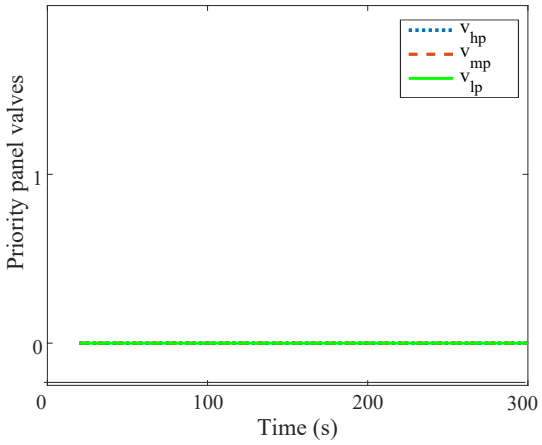

Figure 4.7(a): Priority panel valves

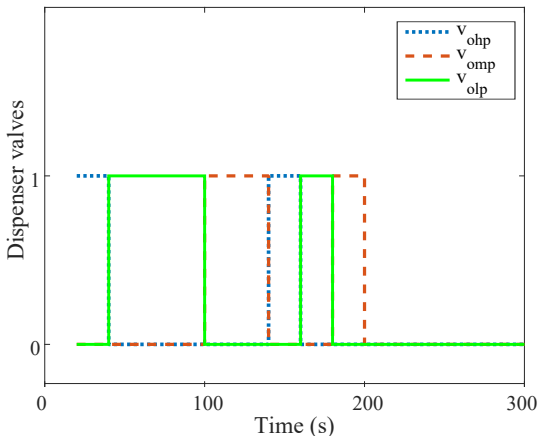

Figure 4.7(b): Dispenser valves

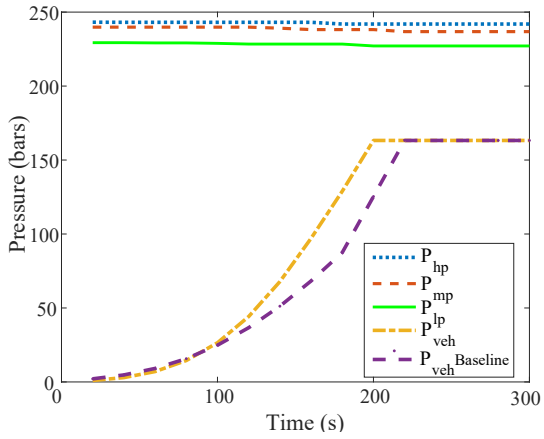

Figure 4.7(c): Pressure

Figure 4.7. Vehicle filling without the compressor (fourth vehicle of 143).

Similar to the filling of the vehicle while the compressor is off, the dispenser valves switches between levels of cascade storage to produce the optimal filling profile of the vehicle tank so that the targeted quantity of gas is transferred. The priority panel valves alternate the filling of the gas from the compressor into the cascade storage between the three levels.

For both cases in Sections 4.4.2.1 and 4.4.2.2, the proposed control strategy produces an efficient accelerated filling of the vehicle tank by switching optimally between the dispenser valves to achieve the minimum possible number of total dispenser valve-on instances to reach the targeted transfer of gas to the vehicle, which corresponds to the shortest possible filling time under the given constraints. This filling profile represents the optimal increase in pressure in the vehicle tank as achieved through

the MPC strategy of the lower layer.

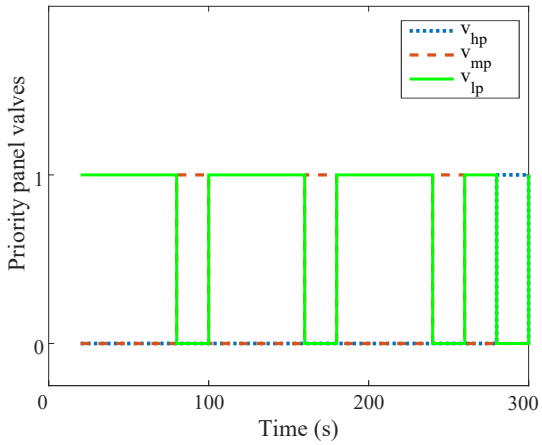

Figure 4.8(a): Priority panel valves

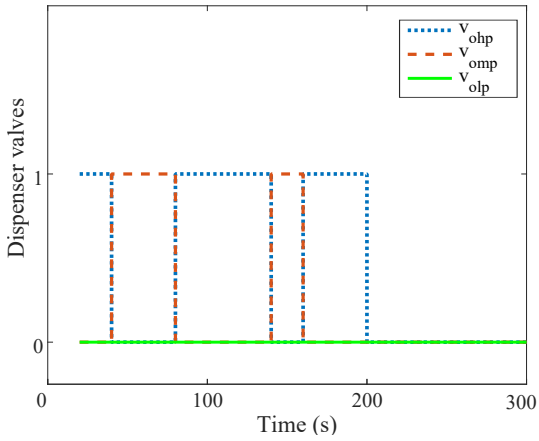

Figure 4.8(b): Dispenser valves

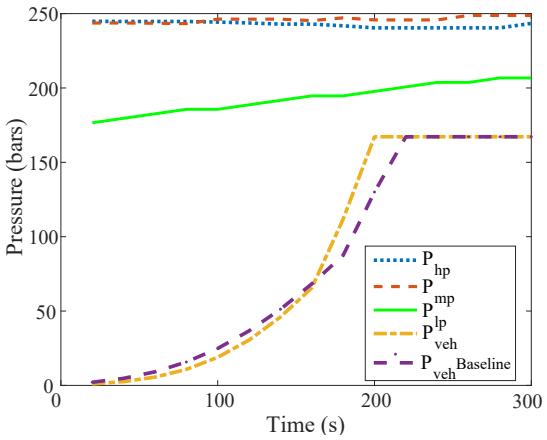

Figure 4.8(c): Pressure

Figure 4.8. Vehicle filling with the compressor on (38th vehicle of 143).

Under this novel optimised MPC filling approach, the improvement in filling time is achieved with a median of 20 seconds reduction in filling time for an average saving of 16.92 seconds for the 143 vehicles. This outcome confirms that, by altering the operation of the dispenser valves through optimisation, better CNG fuelling performance can be achieved, which would further justify the optimisation of the CNG station operations, beyond the minimising of electricity costs.

4.4.2.3 Cascade Reservoir Filling without Vehicle Fuelling

As dictated by the energy cost optimisation layer schedule, during the interval when there is no vehicle fuelling at the dispenser but the compressor is on, the profile for the filling of the cascade storage from the compressor is shown in Figure 4.9. A preference to keep the high pressure reservoir of the cascade

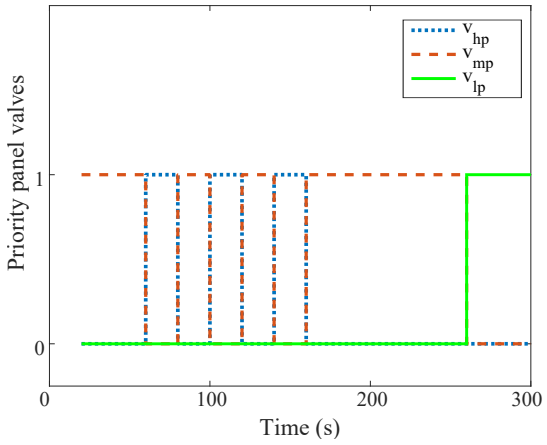

Figure 4.9(a): Priority panel valves

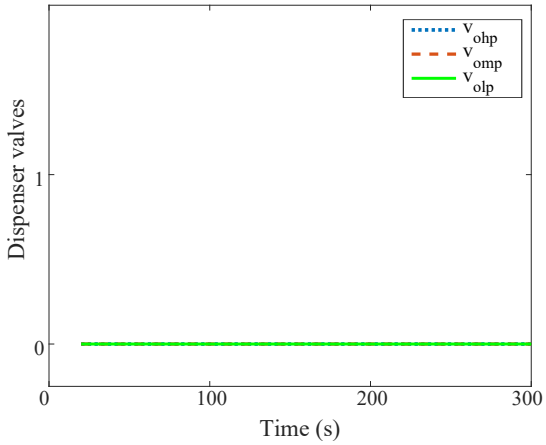

Figure 4.9(b): Dispenser valves

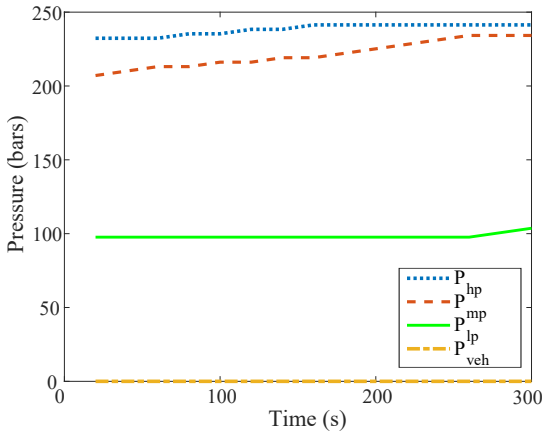

Figure 4.9(c): Pressure

Figure 4.9. Compressor operation without vehicle being filled.

storage at high pressure is observed under the MPC strategy for the lower layer. The pressure level is flexibly controlled to fulfil the optimal control goals of vehicle filling and meet the conditions of the operation constraints. By successfully keeping the dispenser valves in the off position, the strategy demonstrates feasibility under this condition and achieves the expected performance profile for the given operational constraints.

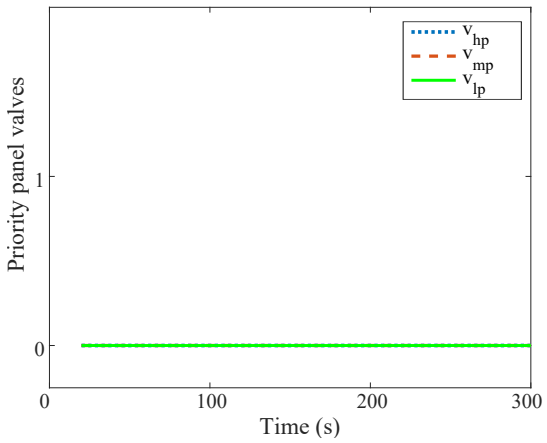

Figure 4.10(a): Priority panel valves

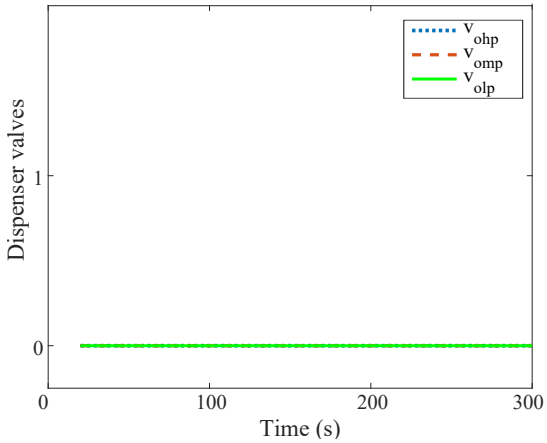

Figure 4.10(b): Dispenser valves

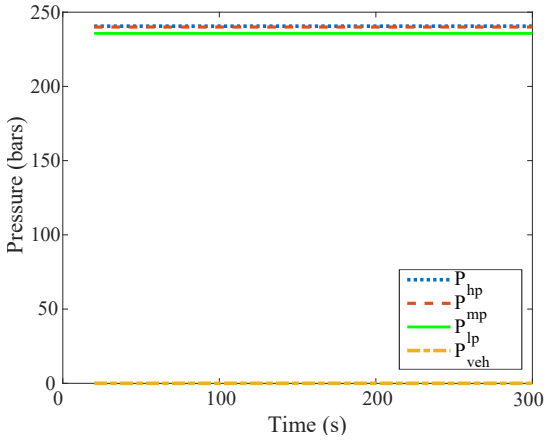

Figure 4.10(c): Pressure

Figure 4.10. Profile with compressor off and no vehicle at the dispenser.

4.4.2.4 Control Action during Idle Time

It is necessary to report on the system performance during idle time when the compressor is off and there is no vehicle fuelling at the dispenser. The state of the control variables and the pressure in the cascade storage for the lower layer is shown in Figure 4.10. The results show that the dispenser valves and priority panel valves remain in the off position over the entire control period demonstrating that the MPC strategy for the lower layer remains feasible when there is no inflow or outflow of gas from the cascade storage of the filling station. This indicates that the strategy is sufficiently constrained for all operation scenarios of the CNG filling station.

The proposed two-layer optimisation for the reduction of energy cost and improvement filling efficiency shows a feasibility demonstrated in the results with a significant reduction in energy cost and vehicle filling time. The achieved reduction in the cost of electricity for the CNG fast-fill station by 60.08% can be passed on to consumers on cost per unit because of the lowered cost of gas delivery. Further, a shorter filling time is achieved for vehicles fuelling at the station with a median reduction in filling time of 20 seconds and an average reduction by 16.92 seconds for all the vehicles through the MPC strategy for the lower layer. Reduced fuelling time is a welcome improvement in fuelling convenience that could serve to maintain existing CNG vehicle customers and lower the level of concern for new CNG vehicle users. The benefits from the optimisation of the two layers can be viewed as complementary to one another, given the cascaded improvement in financial and technical performance of the CNG station that has been realised.

4.4.3 Sensitivity Analysis

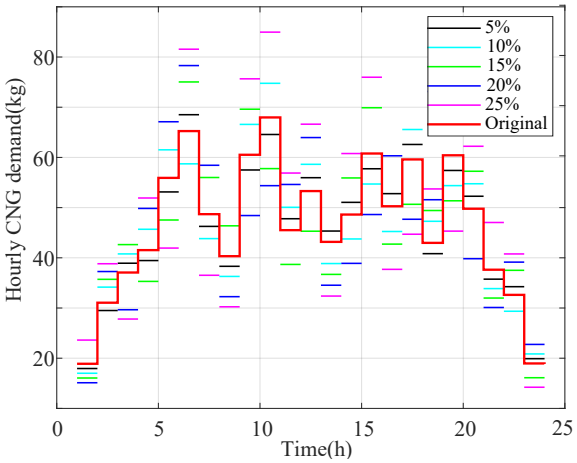

Figure 4.11(a): Percentage disturbances to demand

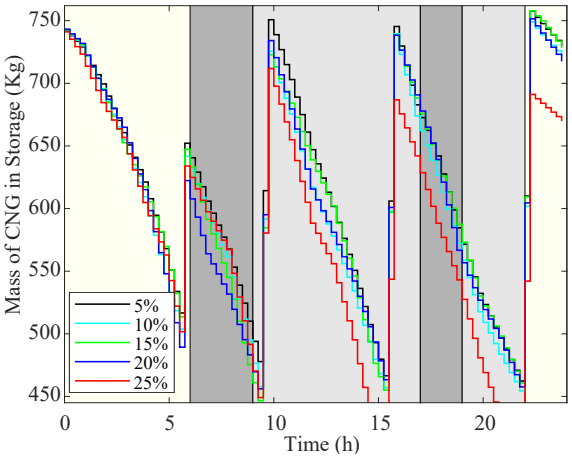

Figure 4.11(b): Mass of gas in storage.

Figure 4.11. System performance under random gas demand disturbances.

An analysis was carried out to scrutinise the validity of the model's output under disturbances, which originate from scenarios that alter the input parameters. A random change in the gas demand, which is an important parameter for compressor scheduling, is the most probable source of disturbance for the proposed optimal operation approach and could affect the feasibility of the compressor schedule solution. Consequently, an inspection of the possible effects of random disturbances, implemented as random percentage increase or decrease in hourly gas demand, on the quantity of gas in storage was done. The disturbance demand profiles are shown in Figure 4.11(a).

It is evident in Figure 4.11(b) that the solution of the compressor schedule obtained through the optimal scheduling remains valid through the series of variations in hourly gas demand of up to 20%. This means that the limits of the quantity of gas stored in the cascade storage are not violated if the schedule obtained is implemented, even if some variation in demand occur. However, when effecting the optimal schedule solution to the existing station controller, it is necessary to include safety interrupts to tackle circumstances where large disturbances cause a violation of operating limits, as shown in Figure 4.11(b) for the 25% variation in demand. These interrupts would correct the violation by either shutting off the compressor outside of schedule when the maximum quantity of gas limit in the cascade storage is reached, or by turning on the compressor outside of schedule when the minimum limit is reached as a result of unexpected gas demand circumstances. The feedback characteristic of the MPC strategy in the lower layer allows for the controller to adapt to disturbances in the system inputs [117], which means that when disturbances in the quantity of gas condition in the cascade storage occur, the controller updates operation control to attain the lower layer objectives.

Table 4.2 shows the fuelling time for each of the two vehicles in Sections 4.4.2.1 and 4.4.2.2 when gas level disturbances in one of the three cascade storage cylinders are implemented. By feeding back the conditions of the system states to the controller input, the approach allows for new calculation of future control action so as to meet the set optimisation goals. The solutions from the proposed approach to optimal CNG station operation have thus been shown to be valid for the predicted operating conditions as well as under some variations to these conditions.

Table 4.2. Vehicle filling time.

Gas Level Disturbance	4^{th} **Vehicle(s)**	38^{th} **Vehicle(s)**
5%	200	200
10%	200	200
15%	200	200
20%	200	200

4.5 CONCLUSIONS

Participation of CNG delivery infrastructure in demand response programs not only saves cost for the station operators and CNG users, but it is also a participation in contributing to the wider goals of such programs in increasing grid reliability and efficiency for all electricity users in society. Cities seeking

to expand the use of alternative fuels as cleaner means of transportation also need the associated infrastructure to develop responsibly with regard to use of electricity, which is an indispensable resource.

This chapter provides an expansive perspective of the operation profile of an optimised CNG fast-fill station, which is the major component of gas delivery infrastructure, incorporating both energy savings and pressure conditions management. The proposed approach achieves a huge reduction in the cost of electricity for the CNG fast-fill station, and delivers on shorter filling time for vehicles fuelling at the station. The results demonstrate savings of up to 60.08% in electricity cost for the upper layer as well as average savings of 16.92 seconds in vehicle fuelling time for the lower layer. Further, the sensitivity analysis shows an ability of the solutions obtained to withstand some disturbances in the inputs, which is important for the station operation reliability.

Implementation of energy cost reduction strategies by energy users should remain sensitive to other performance considerations in the core area of the business. For compressed natural gas vehicle users, vehicle fuelling time cannot be jeopardised as it is one of the main consideration consumers make when deciding on adoption of cleaner gaseous alternative fuels. The study demonstrates that benefits associated with adoption of CNG can be amplified by optimally operating delivery infrastructure with respect to existing demand response programs while simultaneously improving customer convenience. As an introductory study on the implementation of a combined energy cost and filling time optimisation, this study is a timely highlight to an important intersection between different approaches to better use of energy and system performance.

CHAPTER 5 OPTIMAL COMPRESSOR SIZING, OPERATION AND POWER DISPATCH OF A DUAL POWERED CNG FUELLING STATION

5.1 CHAPTER OVERVIEW

The optimal operation of the CNG fast-fill station, with the objective of minimizing energy cost in time-of-use (TOU) electricity tariff environments has been the main subject of the preceding two chapters. The TOU tariff for the grid electricity is a demand response program implemented to incentivize the change in electricity consumption behaviour by customers, enabling the grid operator to lower demand peaks and better match electricity load to the generation capacity [66, 118]. The distribution of the peak load to alternative times reduces the overall load fluctuation which has been shown to be a cost effective strategy of raising grid reliability and stability [9, 63]. In Chapter 3 the CNG fast-fill station was modelled as a mass balance system, where the plant dynamics were balanced between the inflow from the compressor pumping gas into the cascade storage, initial conditions in the cascade storage tanks and the outflow from the gas demand over the station for a 24 hour control horizon. In order to minimize the number of on/off instances the compressor would undergo in the optimized solution, a quadratic element minimizing the ramp rate of the compressor switch status was compared with the method involving the use of an auxilliary variable first proposed by [96] for electric motor systems named the Pretoria method. Further, the expected operation of the priority panel under the optimal solution for the scheduled compressor operation was reported and a comparison of the strategies for limiting compressor on/off instances was performed. In Chapter 4, a hierarchical approach to the optimal operation of the CNG station was carried out, where in the lower layer, the

optimal operation of valves for a three-line priority panel and dispenser, to achieve minimum filling time under an upper layer optimization of compressor scheduling. While the outcomes reported are important additions to existing research on the optimization of infrastructure in the CNG delivery chain that other researchers have contributed to [119, 120, 121], there still exist ignored opportunities to further enhance the CNG station performance by taking advantage of complementary benefits of CNG station compressor capacity matching to the demand, optimal dispatch of multiple sources of power and optimization of the filling process.

The work in this chapter seeks to compare the performance of optimally sized FSD and VSD compressors used in a CNG fast fill station, as well as minimize the cost of energy used to run the compressor by optimally dispatching the grid electricity and natural gas (NG) generator power to the compressor in consideration of the TOU tariff of grid electricity. The compressor is the main contributor to electricity consumption at the station [33] and could be optimally sized to meet the existing demand lowering over-sizing inefficiencies, this is both an equipment and technology consideration under the POET approach to energy efficiency. Further, the use of a four line priority panel in place of a three line priority panel introduces the option of direct filling of vehicle tanks from the compressor, that can be beneficial in reducing the filling time of vehicle tanks, when the flow rate from the cascade storage tanks is low. The aim is to achieve minimized energy cost in a CNG station powered by grid and NG generator and at the same time meet gas demand and minimize the vehicle tank filling time, by deploying both a combined optimal sizing and optimal operation approach. In the proposed operation configuration, the station compressor power will be supplied from the grid and the NG generator so that minimal cost of energy is incurred over the control horizon by considering the TOU tariff of the grid and the pricing of natural gas fuel for the NG generator. The results of the study contribute further to the cost efficiency of CNG refuelling infrastructure as well as ensure efficient gas transfer is achieved for the CNG vehicle users.

In the rest of this chapter, Section 5.2 is a description of the optimal sizing and optimal operation models for both the FSD and VSD compressors, Section 5.3 contains the case data and parameters, and Section 5.4 contains the results and discussion of the outcomes. Section 5.5 is the conclusion of the chapter.

5.2 SYSTEM MODELLING AND FORMULATION

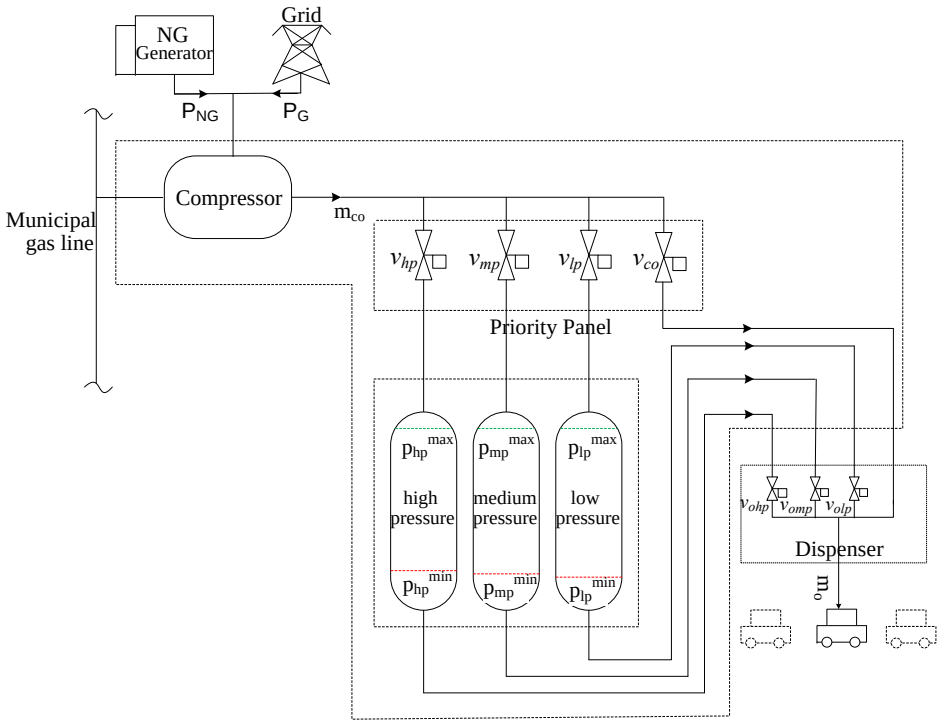

Figure 5.1. Layout of the fast-fill CNG station

Figure 5.1 shows the schematic of the proposed configuration of the CNG station. The compressor is powered from two sources; the grid electricity and the NG generator. Gas from the compressor flows through the priority panel, going to either the three levels of the cascade storage or directly to the vehicle cylinder at the dispenser. The four line priority panel offers availability of the superior flow rate from the compressor for filling vehicle tanks when the flow from the cascade storage is low, which is in contrast to the exclusive filling of vehicle tanks from the cascade storage in the three line priority panel configuration.

To achieve the objectives of the proposed approach, firstly, the models for achieving optimally minimal energy cost involves optimally minimizing the flow rate of the station compressor so that minimum energy is consumed while also making sure that the gas demand is met. Minimizing the size of the compressor to achieve higher operation efficiency and minimize electricity consumption at the CNG station is consistent with the equipment efficiency considerations of the POET classifications approach to energy efficiency, because it tackles capacity and specification optimization of energy consumed by the CNG station [122]. Secondly, an optimum dispatch of grid and NG generator with consideration for

the TOU pricing of electricity and NG generator fuel costs further contributes to energy cost reduction. This constitutes an operation consideration of energy efficiency under the POET classification. Finally, an optimum gas flow control profile for the four line priority panel configuration achieves minimum vehicle tank filling time.

5.2.1 Model for the fixed speed drive

Optimal sizing for the FSD drive compressor seeks to determine the optimum fixed flow rate of the compressor that sustains availability of gas flow to the cascade storage and the four-line priority panel configuration of the CNG station such that all gas demand at the dispenser is met, by optimizing conditions of the cascade storage and compressor switch. The optimally sized FSD compressor and four line priority panel configuration is also optimally operated to minimize the cost of electricity drawn by the compressor from the grid and NG generators and also produce minimum-time vehicle tank filling profiles.

5.2.1.1 Objective function

The objective of the model is to minimize the size of the compressor by minimizing the flow rate necessary to meet the gas demand needs at the dispenser and to simultaneously minimize the cost of electricity consumed from both the grid and NG generator as well as minimize the filling time of the vehicle tanks. The objective function is thus

$$J_{FSD} = (\psi_1)\dot{m}_{co} + (\psi_2)\sum_{t=1}^{N-1} t_s\Big(P_G(t)P_e(t)u(t) + P_{NG}(t)P_{GWH}u(t)\Big) + (\psi_3)\sum_{t=1}^{N-1}(p_T(t) - p_{veh}(t)) + (\psi_4)\sum_{t=1}^{N-1}\big(u(t+1) - u(t)\big)^2, \tag{5.1}$$

where $\dot{m}_{co}$ is the compressor flow rate in kg/h, t_s is the sampling time, $P_G(t)$ is the instantaneous power drawn from the grid in kW, $P_e(t)$ is the TOU tariff electricity price per kW, $u(t)$ is the compressor switch, $P_{NG}(t)$ is the instantaneous power drawn from the NG generator in kW, P_{GWH} is the unit cost of NG generator power per kW, $p_T(t)$ is the target vehicle pressure for current vehicle in $bars$, $p_{veh}(t)$ is the vehicle pressure at the current sampling in $bars$,ψ_j ($j \in \{1,2,3,4\}$) are weighting factors and N is the control horizon.

5.2.1.2 Constraints

The power consumption of the compressor is supplied from the grid and the NG generator such that,

$$P_G(t) + P_{NG}(t) = P_{FSD}(t)u(t), \tag{5.2}$$

where $P_{FSD}(t)$ is the power consumed by the fixed speed drive compressor which is a function of the gas mass flow rate $\dot{m}_{co}$, which is a control variable that is constant in the control horizon such that [123],

$$P_{FSD}(t) = \frac{n_v}{n_v - 1} R \frac{T}{\eta_c} \left[\left(\frac{p_i(t)}{p_{inlet}} \right)^{\left(\frac{n_v - 1}{n_v}\right)} - 1 \right] \dot{m}_{co} \qquad i \in \{hp, mp, lp, veh\}, \tag{5.3}$$

where n_v is the polytrophic coefficient, R is the gas constant, T is the inlet gas temperature in K, η_c is the compressor efficiency, p_{inlet} is the compressor inlet pressure from the municipal gas line and p_i is the pressure in the target tank which is either one of the cascade reservoirs or the vehicle tank.

Gas flows from the cascade storage tanks and the compressor to the vehicle tank at a mass flow rate $\dot{m}_{veh}(t)$ which is the sum of flow rates from the three cascade reservoirs and the compressor, so that

$$\dot{m}_{veh}(t) = \dot{m}_{hp}(t)v_{ohp}(t) + \dot{m}_{mp}(t)v_{omp}(t) + \dot{m}_{lp}(t)v_{olp}(t) + \dot{m}_{co}v_{co}(t), \tag{5.4}$$

where v_{ohp}, v_{omp} and v_{olp} are the dispenser valves to the high medium and low pressure reservoirs of the cascade storage respectively and v_{co} is the priority panel valve linking the compressor to the dispenser for direct vehicle tank filling from the compressor. The flow rates $\dot{m}_{hp}(t)$, $\dot{m}_{mp}(t)$ and $\dot{m}_{lp}(t)$ between the high, medium and low pressure reservoirs of the cascade storage and the vehicle tank respectively, are based on the ideal gas model for an adiabatic system [112] and are governed by the pressure ratios between the storage tanks and the vehicle tank. i.e.,

$$\begin{aligned}
&\dot{m}_i(t) = C_d \rho_i(t) A_{orifice} \left(\frac{p_{veh}(t)}{p_i(t)} \right)^{\frac{1}{\gamma}} \times \\
&\left\{ (\frac{2\gamma}{\gamma-1})(\frac{p_i(t)}{\rho_i(t)}) \left(1 - (\frac{p_{veh}(t)}{p_i(t)})^{\frac{\gamma-1}{\gamma}} \right) \right\}^{\frac{1}{2}} \\
&\text{for} \quad \frac{p_{veh}(t)}{p_i(t)} \leq \left(\frac{2}{\gamma+1} \right)^{\frac{\gamma}{\gamma-1}}, i \in \{hp, mp, lp\},
\end{aligned} \tag{5.5}$$

and

$$\begin{aligned}
&\dot{m}_i(t) = C_d \sqrt{\gamma p_i(t) \rho_i(t) A_{orifice}} \left(\frac{2}{\gamma+1} \right)^{\frac{\gamma+1}{2(\gamma-1)}} \\
&\text{for} \quad \frac{p_{veh}(t)}{p_i(t)} \geq \left(\frac{2}{\gamma+1} \right)^{\frac{\gamma}{\gamma-1}}, i \in \{hp, mp, lp\},
\end{aligned} \tag{5.6}$$

where γ is the ratio of specific heats

$$\gamma = \frac{c_p}{c_v}, \tag{5.7}$$

and c_p is the specific heat capacity of the gas at constant pressure while c_v is the specific heat capacity of the gas at constant volume. C_d is the coefficient of discharge of the dispenser valve orifice, $A_{orifice}$ is the area of the dispenser valve orifice in m^2 and ρ_i is the density of the gas in the respective cascade storage reservoir in kg/m^3, which relates to the instantaneous tank pressure through the equation [112]

$$\rho_i = \frac{P_i(t)}{RT\gamma}, \quad i \in \{hp, mp, lp\}. \tag{5.8}$$

When the compressor is on, the valves of the four line priority panel open in turns to fill the vehicle tank directly or replenish the cascade storage reservoirs as described by the equality constraint (5.9). The dispenser valves as well as the valve for direct filling of vehicles from the compressor also open in turns to fill the vehicle tank and shut off when the target pressure is reached as described by equality

constraints (5.10) and (5.11) respectively.

$$v_{hp}(t) + v_{mp}(t) + v_{lp}(t) + v_{co}(t) = u(t), \tag{5.9}$$

$$v_{ohp}(t) + v_{omp}(t) + v_{olp}(t) + v_{co}(t) = 1, \quad \text{for} \quad p_{veh}(t) < p_T(t) \tag{5.10}$$

$$v_{ohp}(t) + v_{omp}(t) + v_{olp}(t) + v_{co}(t) = 0, \quad \text{for} \quad p_{veh}(t) \geq p_T(t) \tag{5.11}$$

$$v_{ohp}(t), v_{omp}(t), v_{olp}(t), v_{hp}(t), v_{mp}(t), v_{lp}(t), v_{co}(t) \in \{0,1\}.$$

where v_{hp}, v_{mp} and v_{lp} are the priority panel valves to the high pressure, medium pressure and low pressure cascade storage tanks respectively and v_{ohp}, v_{omp} and v_{olp} are the corresponding dispenser valves and v_{co} is the priority panel valve linking the compressor to the dispenser for direct vehicle tank filling from the compressor. Gas pressure in the cascade reservoirs p_{hp}, p_{mp} and p_{lp}, and gas pressure in the vehicle tank p_{veh} are limited by inequality constraints (5.12), (5.13), (5.14) and (5.15).

$$p_{hp}^{min} \leq p_{hp}(t) \leq p_{hp}^{max}, \tag{5.12}$$

$$p_{mp}^{min} \leq p_{mp}(t) \leq p_{mp}^{max}, \tag{5.13}$$

$$p_{lp}^{min} \leq p_{lp}(t) \leq p_{lp}^{max}, \tag{5.14}$$

$$p_{veh}(t) \geq p_T(t) \quad \text{for} \quad \frac{t}{t_{max}} = jt_{max} \quad j \in \{1,2,3\cdots\} \tag{5.15}$$

(5.12), (5.13), (5.14) are the working pressure limits of the cascade storage tanks, with p_{hp}^{min}, p_{mp}^{min} and p_{lp}^{min} being the minimum limits and p_{hp}^{max}, p_{mp}^{max} and p_{lp}^{max} being the maximum limits for the three cascade storage levels respectively in *bars*. The inequality constraint (5.15) ensures that filling of each vehicle tank is complete within maximum allowed filling time for one vehicle t_{max}. The general

dynamic equations for pressure-changes in the vehicle and cascade storage reservoirs are

$$\frac{d}{dt}p_{veh}(t) = \dot{m}_{veh}(t)K_1, \tag{5.16}$$

$$\frac{d}{dt}p_{hp}(t) = -\dot{m}_{hp}(t)K_{hp}v_{ohp}(t) + \dot{m}_{co}v_{hp}(t), \tag{5.17}$$

$$\frac{d}{dt}p_{mp}(t) = -\dot{m}_{mp}(t)K_{mp}v_{omp}(t) + \dot{m}_{co}v_{mp}(t), \tag{5.18}$$

$$\frac{d}{dt}p_{lp}(t) = -\dot{m}_{lp}(t)K_{lp}v_{olp}(t) + \dot{m}_{co}v_{lp}(t), \tag{5.19}$$

where K_1, K_{hp}, K_{mp} and K_{lp} are constants such that

$$\begin{aligned} K_1 &= T\left(\frac{c_p}{c_v}\frac{R}{V_{veh}}\right), \quad K_{hp} = T\left(\frac{c_p}{c_v}\frac{R}{V_{hp}}\right), \\ K_{mp} &= T\left(\frac{c_p}{c_v}\frac{R}{V_{mp}}\right) \quad \text{and} \quad K_{lp} = T\left(\frac{c_p}{c_v}\frac{R}{V_{lp}}\right), \end{aligned} \tag{5.20}$$

where V_{veh}, V_{hp}, V_{mp} and V_{lp} are the volumes of the vehicle tank, high pressure reservoir, medium pressure reservoir and low pressure reservoir respectively in L. This results in the following discrete equations of pressure,

$$p_{veh}(t+1) = p_{veh}(t) + t_s K_1 \sum_{\tau=1}^{t} \dot{m}_{veh}(\tau), \tag{5.21}$$

$$p_{hp}(t+1) = p_{hp}(t) - t_s K_{hp} \sum_{\tau=1}^{t} \dot{m}_{veh}(\tau)v_{ohp}(\tau) + t_s \sum_{\tau=1}^{t} \dot{m}_{co}v_{hp}(\tau), \tag{5.22}$$

$$p_{mp}(t+1) = p_{mp}(t) - t_s K_{mp} \sum_{\tau=1}^{t} \dot{m}_{veh}(\tau)v_{omp}(\tau) + t_s \sum_{\tau=1}^{t} \dot{m}_{co}v_{mp}(\tau), \tag{5.23}$$

$$p_{lp}(t+1) = p_{lp}(t) - t_s K_{lp} \sum_{\tau=1}^{t} \dot{m}_{veh}(\tau)v_{olp}(\tau) + t_s \sum_{\tau=1}^{t} \dot{m}_{co}v_{lp}(\tau). \tag{5.24}$$

5.2.1.3 Algorithm

In order to solve the optimization problem using the Mixed Integer Distributed Ant Colony Optimisation (MIDACO) solver, the components of the problem have to be formulated as

$$\begin{aligned} &\text{minimise} \quad f(x) \quad \text{(objective function)} && (5.25)\\ &\text{subject to} \quad g(x) = 0 \quad \text{(equality constraints)} && (5.26)\\ &\qquad\qquad h(x) \geq 0 \quad \text{(inequality constraints)} && (5.27) \end{aligned}$$

The vector containing the control variables consists of the the three valves from the priority panel to the cascade storage and three valves in the dispenser from the cascade storage to the vehicle, as well as the fourth valve connecting the vehicle tank directly to the compressor. Further, the power drawn from the grid P_G and the power from the NG generator P_{NG} are also control variables as well as the fixed compressor flow rate $\dot{m}_{co}$. Therefore, x for the FSD can be written in the standard form

$$\begin{aligned} \boldsymbol{x_{FSD}} = [&v_{hp}(1), v_{hp}(2), \cdots v_{hp}(N), v_{mp}(1), v_{mp}(2), \cdots v_{mp}(N),\\ &v_{lp}(1), v_{lp}(2), \cdots v_{lp}(N), v_{ohp}(1), v_{ohp}(2), \cdots v_{ohp}(N),\\ &v_{omp}(1), v_{omp}(2), \cdots v_{omp}(N), v_{olp}(1), v_{olp}(2), \cdots v_{olp}(N),\\ &v_{co}(1), v_{co}(2) \cdots v_{co}(N), P_G(1), P_G(2) \cdots P_G(N),\\ &P_{NG}(1), P_{NG}(2) \cdots P_{NG}(N), \dot{m}_{co}]^T_{(9N+1)\times 1}. \end{aligned} \tag{5.28}$$

The objective function (5.1) becomes,

$$\begin{aligned} \boldsymbol{f_{FSD}} = \Bigg[&\psi_1 \dot{m}_{co} + \psi_2 t_s \Bigg(P_G(1)P_e(1)u(1) + P_G(2)P_e(2)u(2) \cdots + P_G(N)P_e(N)u(N) +\\ &P_{NG}(1)P_{GWH}(1)u(1) + P_{NG}(2)P_{GWH}(2)u(2) \cdots + P_{NG}(N)P_{GWH}(N)u(N) \Bigg) +\\ &\psi_3 \Bigg(\Big(P_T(1) - P_{veh}(1)\Big) + \Big(P_T(2) - P_{veh}(2)\Big) \cdots + \Big(P_T(N) - P_{veh}(N)\Big) \Bigg) +\\ &\psi_4 \Bigg(\Big(u(2) - u(1)\Big)^2 + \Big(u(3) - u(2)\Big)^2 \cdots + \Big(u(N) - u(N-1)\Big)^2 \Bigg) \Bigg], \end{aligned} \tag{5.29}$$

while the equality constraints (5.2), (5.9), (5.10), and (5.11) in the form $g(x) = 0$ are expressed as

$$\boldsymbol{g_1(x)} = \begin{bmatrix} P_G(1)+P_{NG}(1)-P_{FSD}(1) \\ P_G(2)+P_{NG}(2)-P_{FSD}(2) \\ \vdots \\ P_G(N)+P_{NG}(N)-P_{FSD}(N) \end{bmatrix}_{N\times 1}, \tag{5.30}$$

$$\boldsymbol{g_2(x)} = \begin{bmatrix} v_{hp}(1)+v_{mp}(1)+v_{lp}(1)+v_{co}(1)-u(1) \\ v_{hp}(2)+v_{mp}(2)+v_{lp}(2)+v_{co}(2)-u(1) \\ \vdots \\ v_{hp}(N)+v_{mp}(N)+v_{lp}(N)+v_{co}(N)-u(N) \end{bmatrix}_{N\times 1}, \tag{5.31}$$

$$\boldsymbol{g_3(x)} = \begin{bmatrix} v_{ohp}(1)+v_{omp}(1)+v_{olp}(1)+v_{co}(1)-1 \\ v_{ohp}(2)+v_{oomp}(2)+v_{lp}(2)+v_{co}(2)-1 \\ \vdots \\ v_{ohp}(N)+v_{omp}(N)+v_{olp}(N)+v_{co}(N)-1 \end{bmatrix}_{N\times 1} \quad \text{for } p_{veh} < p_T, \tag{5.32}$$

$$\boldsymbol{g_4(x)} = \begin{bmatrix} v_{ohp}(1)+v_{omp}(1)+v_{olp}(1)+v_{co}(1) \\ v_{ohp}(2)+v_{oomp}(2)+v_{lp}(2)+v_{co}(2) \\ \vdots \\ v_{ohp}(N)+v_{omp}(N)+v_{olp}(N)+v_{co}(N) \end{bmatrix}_{N\times 1} \quad \text{for } p_{veh} \geq p_T, \tag{5.33}$$

therefore

$$\boldsymbol{g_{FSD}(x)} = \begin{bmatrix} \boldsymbol{g_1(x)} \\ \boldsymbol{g_2(x)} \\ \boldsymbol{g_3(x)} \\ \boldsymbol{g_4(x)} \end{bmatrix}_{4N\times 1}. \tag{5.34}$$

The inequality constraints arising from pressure limits for the cascade storage (5.12), (5.13) and (5.14) are denoted as

$$\boldsymbol{h_1(x)} = \begin{bmatrix} p_{hp}^{max} - p_{hp}(1) \\ p_{hp}^{max} - p_{hp}(2) \\ \vdots \\ p_{hp}^{max} - p_{hp}(N) \\ p_{mp}^{max} - p_{mp}(1) \\ p_{mp}^{max} - p_{mp}(2) \\ \vdots \\ p_{mp}^{max} - p_{mp}(N) \\ p_{lp}^{max} - p_{lp}(1) \\ p_{lp}^{max} - p_{lp}(2) \\ \vdots \\ p_{lp}^{max} - p_{lp}(N) \\ p_{hp}(1) - p_{hp}^{m}in \\ p_{hp}(2) - p_{hp}^{m}in \\ \vdots \\ p_{hp}(N) - p_{hp}^{m}in \\ p_{mp}(1) - p_{mp}^{m}in \\ p_{mp}(2) - p_{mp}^{m}in \\ \vdots \\ p_{mp}(N) - p_{mp}^{m}in \\ p_{lp}(1) - p_{lp}^{m}in \\ p_{lp}(2) - p_{lp}^{m}in \\ \vdots \\ p_{lp}(N) - p_{lp}^{m}in \end{bmatrix}_{6N\times 1}, \tag{5.35}$$

while (5.15) is expressed as

$$\boldsymbol{h_2(x)} = \begin{bmatrix} p_{veh}(t_{max}) - p_T(t_{max}) \\ p_{veh}(2t_{max}) - p_T(2t_{max}) \\ \vdots \\ p_{veh}(N) - p_T(N) \end{bmatrix}_{\frac{N}{t_{max}}\times 1} \tag{5.36}$$

and hence

$$\boldsymbol{h_{FSD}(x)} = \begin{bmatrix} \boldsymbol{h_1(x)} \\ \boldsymbol{h_2(x)} \end{bmatrix}_{(6N+\frac{N}{t_{max}})\times 1}. \tag{5.37}$$

5.2.2 Model for the variable speed drive

Optimal sizing of the VSD seeks to determine the optimum instantaneous flow rate of the compressor which corresponds to minimum energy consumption while meeting the gas demand. Similar to the FSD optimization model in Section 5.2.1, the optimal VSD flow rate profile is combined with minimization of electricity cost from the grid and NG generator and optimization of the vehicle filling profile to achieve the minimum filling time. The objective function is therefore expressed as,

$$J_{VSD} = (\xi_1)\sum_{t=1}^{N-1} \dot{m}_{co}(t) + (\xi_2)\sum_{t=1}^{N-1} t_s\Big(P_G(t)P_e(t)u(t) + P_{NG}(t)P_{GWH}u(t)\Big) + (\xi_3)\sum_{t=1}^{N-1}(p_T(t) - p_{veh}(t)), \tag{5.38}$$

where ξ_1, ξ_2 and ξ_3 are weighting factors. The flow rate $\dot{m}_{co}(t)$ in the case of the VSD is time variant, in contrast with the constant flow rate for the case of the FSD. Additionally, the compressor switch in the VSD case is considered to be in an always-on mode, with the gas flow rate available to vary over the control horizon.

5.2.2.1 Constraints

The constraints for the VSD optimization model are similar to the FSD constraints in Section 5.2.1.2 such that the power consumption of the compressor is supplied from the grid and the NG generator so that,

$$P_G(t) + P_{NG}(t) = P_{VSD}(t)u(t), \tag{5.39}$$

where $P_{VSD}(t)$ is the power drawn by the variable speed drive compressor in kW, which is a function of the instantaneous compressor flow rate $\dot{m}_{co}(t)$ in m^3/h, which varies according to [123],

$$P_{VSD}(t) = \frac{n_v}{n_v - 1} R \frac{T}{\eta_c} \left[\left(\frac{p_i(t)}{p_{inlet}} \right)^{\left(\frac{n_v-1}{n_v}\right)} - 1 \right] \dot{m}_{co}(t) \qquad i \in \{hp, mp, lp, veh\}. \tag{5.40}$$

Similarly, gas flows from the cascade storage tanks and the compressor to the vehicle tank at a mass flow rate $\dot{m}_{veh}(t)$ which is the sum of flow rates from the three cascade reservoirs and the compressor, so that

$$\dot{m}_{veh}(t) = \dot{m}_{hp}(t) v_{ohp}(t) + \dot{m}_{mp}(t) v_{omp}(t) + \dot{m}_{lp}(t) v_{olp}(t) + \dot{m}_{co}(t) v_{co}(t). \tag{5.41}$$

Further, the flow rates $\dot{m}_{hp}(t)$, $\dot{m}_{mp}(t)$ and $\dot{m}_{lp}(t)$ between the high, medium and low pressure reservoirs of the cascade storage and the vehicle tank, are governed by the pressure ratios between the storage tanks and the vehicle tank. i.e.,

$$\begin{aligned} &\dot{m}_i(t) = C_d \rho_i(t) A_{orifice} \left(\frac{p_{veh}(t)}{p_i(t)} \right)^{\frac{1}{\gamma}} \times \\ &\left\{ \left(\frac{2\gamma}{\gamma-1}\right)\left(\frac{p_i(t)}{\rho_i(t)}\right)\left(1 - \left(\frac{p_{veh}(t)}{p_i(t)}\right)^{\frac{\gamma-1}{\gamma}}\right) \right\}^{\frac{1}{2}} \\ &\text{for} \quad \frac{p_{veh}(t)}{p_i(t)} \leq \left(\frac{2}{\gamma+1}\right)^{\frac{\gamma}{\gamma-1}}, i \in \{hp, mp, lp\}, \end{aligned} \tag{5.42}$$

and

$$\begin{aligned} &\dot{m}_i(t) = C_d \sqrt{\gamma p_i(t) \rho_i(t) A_{orifice}} \left(\frac{2}{\gamma+1}\right)^{\frac{\gamma+1}{2(\gamma-1)}} \\ &\text{for} \quad \frac{p_{veh}(t)}{p_i(t)} \geq \left(\frac{2}{\gamma+1}\right)^{\frac{\gamma}{\gamma-1}}, i \in \{hp, mp, lp\}. \end{aligned} \tag{5.43}$$

The limits for the operation of the priority panel and dispenser valves in the case of variable speed drive are the same as the valve operation of the fixed speed drive operation (5.9), (5.10) and (5.11). However, for the VSD, the compressor switch $u(t)$, is set to a static on-position with compressor gas output varying. Further, the limits of gas pressure in the cascade storage and vehicle filling remain the same as denoted by (5.12), (5.13) (5.14) and (5.15) for the three reservoir levels respectively. Additionally, the dynamic equations of pressure in the vehicle tank and cascade storage reservoirs remain the same as (5.21), (5.22), (5.23) and (5.24).

5.2.2.2 Algorithm

The sizing and optimization problem for the VSD compressor is also solved using the Mixed Integer Distributed Ant Colony Optimisation (MIDACO) solver, and the components of the problem have to be formulated in the form

$$\begin{aligned} \text{minimise} \quad & f(x) \quad \text{(objective function)}, && (5.44)\\ \text{subject to} \quad & g(x) = 0 \quad \text{(equality constraints)}, && (5.45)\\ & h(x) \geq 0 \quad \text{(inequality constraints)}. && (5.46) \end{aligned}$$

The $\boldsymbol{x}$ vector representing the VSD control variables consists of the seven priority panel and dispenser valves, the instantaneous power drawn from the grid and natural gas generator and the varying compressor flowrate so that it is expressed as

$$\begin{aligned} \boldsymbol{x_{VSD}} = [&v_{hp}(1), v_{hp}(2), \cdots v_{hp}(N), v_{mp}(1), v_{mp}(2), \cdots v_{mp}(N),\\ &v_{lp}(1), v_{lp}(2), \cdots v_{lp}(N), v_{ohp}(1), v_{ohp}(2), \cdots v_{ohp}(N),\\ &v_{omp}(1), v_{omp}(2), \cdots v_{omp}(N), v_{olp}(1), v_{olp}(2), \cdots v_{olp}(N),\\ &v_{co}(1), v_{co}(2) \cdots v_{co}(N), P_G(1), P_G(2) \cdots P_G(N),\\ &P_{NG}(1), P_{NG}(2) \cdots P_{NG}(N), \dot{m}_{co}(1), \dot{m}_{co}(2) \cdots \dot{m}_{co}(N)]^T_{10N\times 1}. \end{aligned} \tag{5.47}$$

and the objective function (5.38) is expressed as

$$\begin{aligned} \boldsymbol{f_{VSD}} = \Bigg[&\xi_1 \Big(\dot{m}_{co}(1) + \dot{m}_{co}(2) \cdots + \dot{m}_{co}(N) \Big) + \xi_2 t_s \Big(P_G(1) P_e(1) u(1) + P_G(2) P_e(2) u(2) \cdots +\\ &P_G(N) P_e(N) u(N) + P_{NG}(1) P_{GWH}(1) u(1) + P_{NG}(2) P_{GWH}(2) u(2) \cdots +\\ &P_{NG}(N) P_{GWH}(N) u(N) \Big) + \xi_3 \Bigg(\Big(P_T(1) - P_{veh}(1) \Big) + \Big(P_T(2) - P_{veh}(2) \Big) \cdots +\\ &\Big(P_T(N) - P_{veh}(N) \Big) \Bigg) \Bigg], \end{aligned} \tag{5.48}$$

The power-flow equality constraint (5.39) and the VSD equivalents to the the equality constraints (5.9), (5.10) and (5.11) for valve action are expressed as

$$\boldsymbol{g_5(x)} = \begin{bmatrix} P_G(1)+P_{NG}(1)-P_{VSD}(1) \\ P_G(2)+P_{NG}(2)-P_{VSD}(2) \\ \vdots \\ P_G(N)+P_{NG}(N)-P_{VSD}(N) \end{bmatrix}_{N\times 1}, \tag{5.49}$$

$$\boldsymbol{g_6(x)} = \begin{bmatrix} v_{hp}(1)+v_{mp}(1)+v_{lp}(1)+v_{co}(1)-u(1) \\ v_{hp}(2)+v_{mp}(2)+v_{lp}(2)+v_{co}(2)-u(1) \\ \vdots \\ v_{hp}(N)+v_{mp}(N)+v_{lp}(N)+v_{co}(N)-u(N) \end{bmatrix}_{N\times 1}, \tag{5.50}$$

$$\boldsymbol{g_7(x)} = \begin{bmatrix} v_{ohp}(1)+v_{omp}(1)+v_{olp}(1)+v_{co}(1)-1 \\ v_{ohp}(2)+v_{oomp}(2)+v_{lp}(2)+v_{co}(2)-1 \\ \vdots \\ v_{ohp}(N)+v_{omp}(N)+v_{olp}(N)+v_{co}(N)-1 \end{bmatrix}_{N\times 1} \quad \text{for } p_{veh} < p_T, \tag{5.51}$$

$$\boldsymbol{g_8(x)} = \begin{bmatrix} v_{ohp}(1)+v_{omp}(1)+v_{olp}(1)+v_{co}(1) \\ v_{ohp}(2)+v_{oomp}(2)+v_{lp}(2)+v_{co}(2) \\ \vdots \\ v_{ohp}(N)+v_{omp}(N)+v_{olp}(N)+v_{co}(N) \end{bmatrix}_{N\times 1} \quad \text{for } p_{veh} \geq p_T, \tag{5.52}$$

therefore

$$\boldsymbol{g_{VSD}(x)} = \begin{bmatrix} \boldsymbol{g_5(x)} \\ \boldsymbol{g_6(x)} \\ \boldsymbol{g_7(x)} \\ \boldsymbol{g_8(x)} \end{bmatrix}_{(4N+1)\times 1}. \tag{5.53}$$

The VSD inequality constraint for vehicle filling similar to FSD's (5.15) is expressed as

$$\boldsymbol{h_3(x)} = \begin{bmatrix} p_{veh}(t_{max}) - p_T(t_{max}) \\ p_{veh}(2t_{max}) - p_T(2t_{max}) \\ \vdots \\ p_{veh}(N) - p_T(N) \end{bmatrix}_{\frac{N}{t_{max}} \times 1} \tag{5.54}$$

and the inequality constraints arising from pressure limits for the cascade storage (5.12), (5.13) and (5.14) are denoted as

$$\boldsymbol{h_4(x)} = \begin{bmatrix} p_{hp}^{max} - p_{hp}(1) \\ p_{hp}^{max} - p_{hp}(2) \\ \vdots \\ p_{hp}^{max} - p_{hp}(N) \\ p_{mp}^{max} - p_{mp}(1) \\ p_{mp}^{max} - p_{mp}(2) \\ \vdots \\ p_{mp}^{max} - p_{mp}(N) \\ p_{lp}^{max} - p_{lp}(1) \\ p_{lp}^{max} - p_{lp}(2) \\ \vdots \\ p_{lp}^{max} - p_{lp}(N) \\ p_{hp}(1) - p_{hp}^{m}in \\ p_{hp}(2) - p_{hp}^{m}in \\ \vdots \\ p_{hp}(N) - p_{hp}^{m}in \\ p_{mp}(1) - p_{mp}^{m}in \\ p_{mp}(2) - p_{mp}^{m}in \\ \vdots \\ p_{mp}(N) - p_{mp}^{m}in \\ p_{lp}(1) - p_{lp}^{m}in \\ p_{lp}(2) - p_{lp}^{m}in \\ \vdots \\ p_{lp}(N) - p_{lp}^{m}in \end{bmatrix}_{6N \times 1} . \tag{5.55}$$

Therefore,

$$\boldsymbol{h_{VSD}(x)} = \begin{bmatrix} \boldsymbol{h_3(x)} \\ \boldsymbol{h_4(x)} \end{bmatrix}_{(6N+\frac{N}{t_{max}})\times 1}. \tag{5.56}$$

5.3 CASE STUDY

A CNG fuelling station located in the Johannesburg municipality in the Gauteng province of South Africa is considered in this study. The station serves CNG powered vehicles such as public transportation vans, courier delivery vehicles and security patrol fleets. Most of the vehicles fuelled at this station are dual-fuel vehicles, with CNG being used in conjunction with either petrol or diesel. As such, vehicles use CNG stored in the on-board cylinder until the gas is depleted and then switch to petrol or diesel to power the internal combustion engine until the CNG is replenished. Currently, the station runs on a 132kW compressor with a rated flow rate of 900 m3/h under standard conditions, which is cycled between the limits of gas in storage under the baseline operation. The station has a three line priority panel for filling gas from the compressor to the cascade storage and a three valve dispenser connecting vehicle tanks to the three levels of the cascade storage. Gas delivered via the municipal gas-line is compressed into the three levels of the cascade storage reservoirs with a capacity of 2000L each. The cascade reservoirs are operated between the lower limits of 75 bars, 150 bars and 210 bars for the low pressure, medium pressure and high pressure levels respectively, and a maximum pressure of 250 bars for the three levels. The station is supplied with electricity from the national utility provider Eskom under the Miniflex TOU tariff[1], divided into daily peak, standard and offpeak times denoting the electricity pricing levels for different times during the day, such that

$$p_e(t) = \begin{cases} p_{offpeak} = 0.5157 \text{ R/kWh} & \text{if } t \in [0,6] \cup [22,24] \\ p_{standard} = 0.9446 \text{ R/kWh} & \text{if } t \in [9,17] \cup [19,22] \\ p_{peak} = 3.1047 \text{ R/kWh} & \text{if } t \in [6,9] \cup [17,19] \end{cases} \tag{5.57}$$

At the CNG station under consideration, a 150 kW NG generator is installed on site as a standby source of power for when interruptions to grid power occur. The price per kWh of power generated through the NG generator at 60% efficiency, is estimated to be 0.85 R/kWh based on the highest price

[1] http://eskom.co.za/tariffs

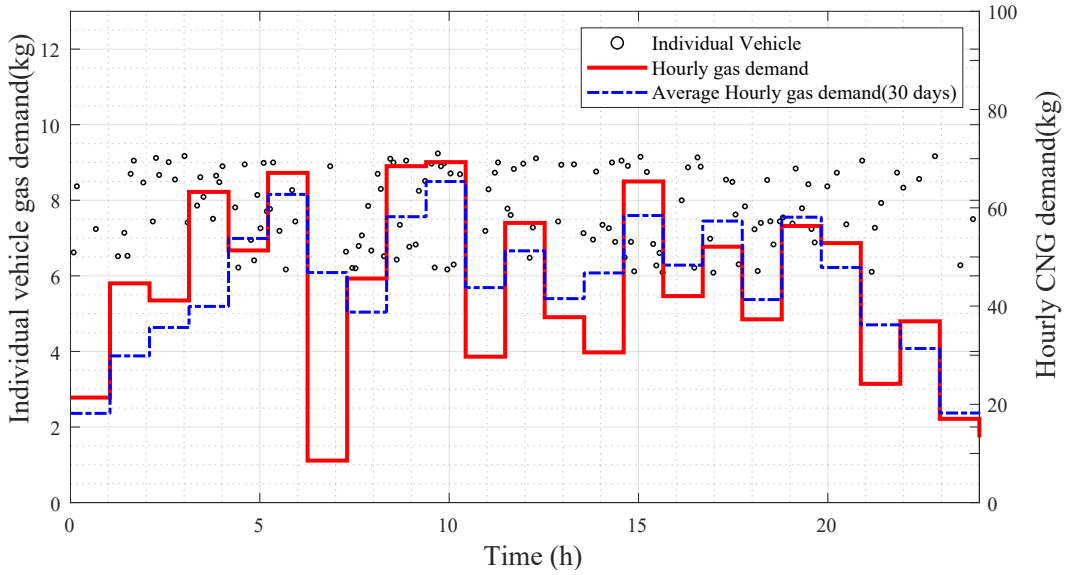

Figure 5.2. Gas demand profile.

per Gigajuole of natural gas in South Africa[2]. Under the proposed optimal operation model, the NG generator is availed for optimal power dispatch in the regular operation of the station compressor. This means that powering the station compressor optimally will include the option to use the NG power, when grid electricity prices are higher than cost of power from the NG generator.

The gas demand at the station is shown in Figure 5.2. The plot shows the average hourly demand for a period of one month, overlayed with the hourly demand of a single day in the 30 day period and the scatter plot shows the individual vehicle gas demand for this day. The demand profile shows a higher gas demand prior to and during peak people movement times of the day. Under the baseline operation, the compressor stays off as vehicles are filled from the cascade storage and is switched on when the quantity of gas in the cascade reservoir hits the lower limit. The compressor stays on until the upper limit of quantity of gas in the cascade storage is reached and the compressor is switched off. This cycling of the compressor results in an operation profile shown in Figure 5.3. It is clear from Figure 5.3(a) that under the baseline operation, the compressor is in operation during the peak electricity pricing period of the morning and further switches on twice during the standard electricity pricing period, thereby failing to take advantage of lower electricity pricing available in the offpeak electricity pricing period. This operation profile results in energy consumption of 212.08 kWh for the control horizon, at a total electricity cost of R432.59, mainly contributed by the on status during the

[2]http://www.energy.gov.za/files/media/explained/Energy-Price-Report-2017.pdf

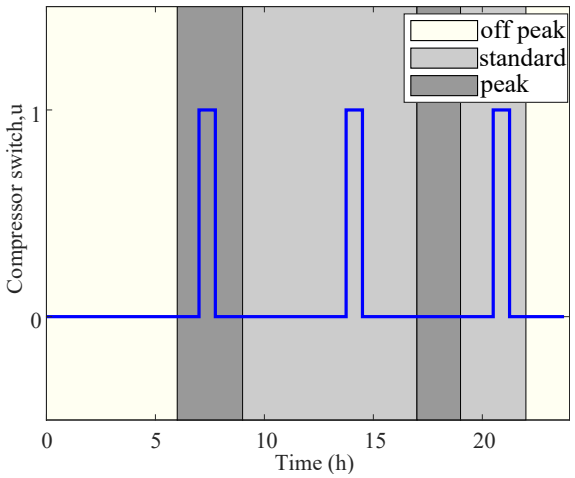

Figure 5.3(a): Compressor switch status

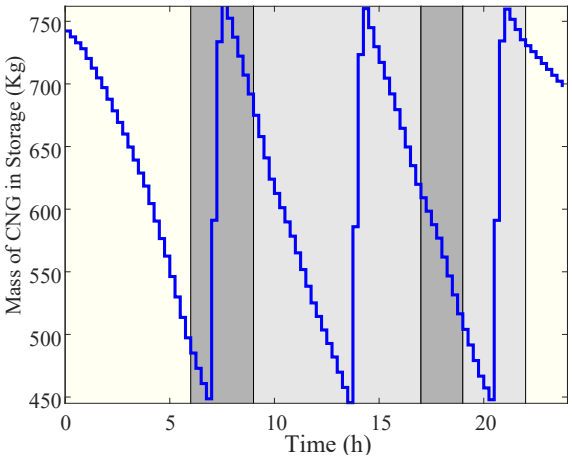

Figure 5.3(b): Mass of gas in the cascade storage

Figure 5.3. Baseline Operation profile.

significantly steep-priced morning peak period. The proposed strategy is expected to overcome this challenge by employing a combination of optimal scheduling of compressor-on status, the optimal sizing of FSD and VSD compressors for lower power consumption and the use of the NG generator to optimally achieve the minimum possible power cost over the 24 hour operation. Furthermore, the strategy involves optimization of gas transfer from the cascade storage and compressor under the resulting operation profile so that a comprehensive improvement in the CNG fuelling station performance is realized. Table 5.1 contains further parameters and constant values used in the solution of the optimization problem.

Table 5.1. Additional parameters and constants.

Parameter	Value	Parameter	Value
$\rho_{a,std}$	1.225 kg/m^3	Mw_g	0.0164 g
C_d	0.61	R	0.083145 LbarK^{-1}mol^{-1}
γ	1.304	T	294.15 K
Mw_a	0.028966 g		

5.4 RESULTS

The optimization problem for minimal compressor flow rates, optimal power dispatch and optimal control of gas transfer was solved using the MIDACO solver in the MatLab environment for a control horizon of 24 hours, with a sampling time of 20s.

5.4.1 Sizing and power consumption

Figure 5.4 shows the optimal flow rate and operation profile in the solution of the sizing problem for the compressor considering the FSD and VSD scenarios. Firstly the optimal compressor fixed flow rate for the FSD case is found to be 253 m^3/hour. This is a significantly lower value compared to the baseline 900 m^3/hour flow rate compressor currently in use. The optimal solution means that this flow rate represents the ideal capacity of the compressor required, to achieve minimum energy consumption for gas compression at the CNG station, while meeting the demand within the specified constraints. The operation profile of the compressor switch show longer operation times for the compressor which is consistent with a lower flow rate meeting the demand previously supplied by a higher flow rate compressor. Further, the compressor is operated during the morning and evening offpeak electricity pricing times and once during the standard electricity pricing times, in contrast with the baseline operation where the compressor is on during peak electricity pricing time, thereby avoiding cost penalties associated with operation during high electricity price times. Secondly, the optimal variable flow rate for the VSD case in Figure 5.4(b) shows how the optimal flow rate of the compressor, obtained from the solution of the model, evolves over the control horizon to meet demand, minimize electricity cost and accomplish gas transfer within the given constraints. The compressor operates continuously with higher flow rate occurring during the offpeak electricity pricing times and lower flow rate during the peak and standard electricity pricing times of the control horizon. Since the flow rate directly correlates to power consumption, this outcome means lower power consumption during higher electricity pricing times.

The power consumption profile from the grid and the NG generator is shown in Figure 5.5. In the FSD case, where operation of the compressor is intermittent according to the optimal compressor schedule obtained from the proposed model, the grid power is in use for the compressor-on instances occurring during the grid's offpeak electricity pricing periods, which takes advantage of the lower prices of grid

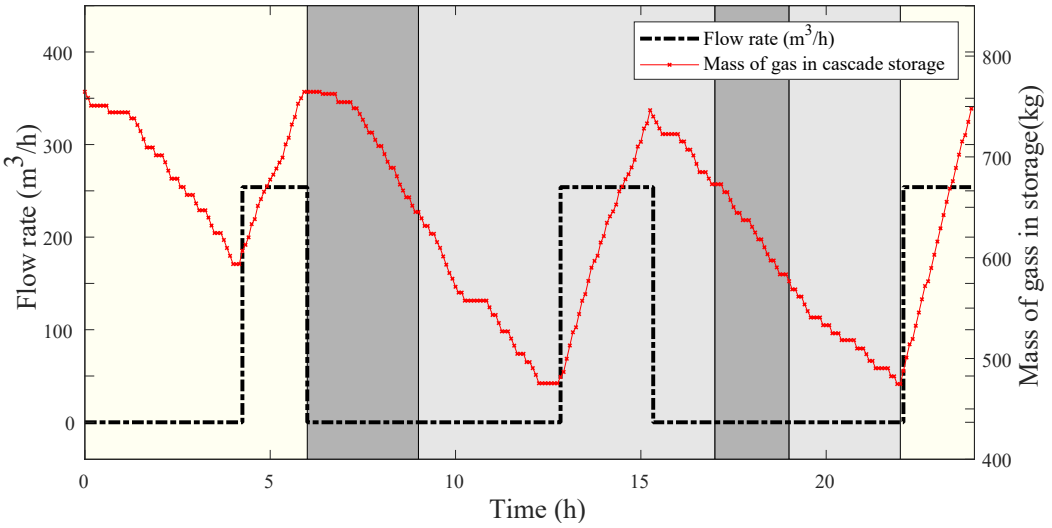

Figure 5.4(a): Fixed speed drive

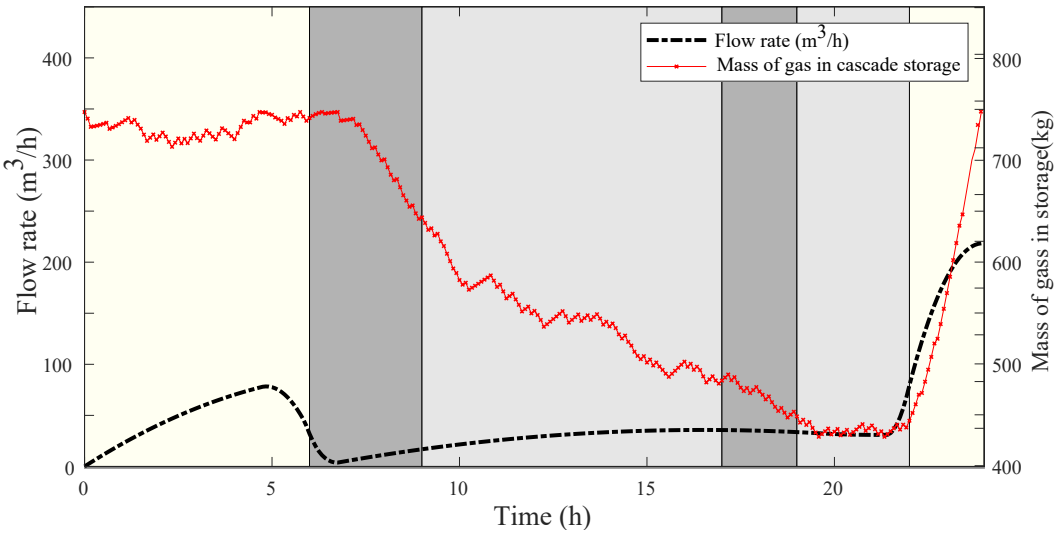

Figure 5.4(b): Variable speed drive

Figure 5.4. Optimal flow rates for FSD and VSD and cascade storage mas of gas

power on offer, to replenish the cascade storage. During the standard electricity pricing period, when the compressor is turned on, the NG generator is used instead of grid power as it costs less per unit of power than the grid electricity price during this time. The total energy consumed by the optimally sized, optimally scheduled and optimally power dispatched FSD driven compressor is 207.73 kWh costing R135.28. Although the reduction in energy consumption from the baseline is marginal, the combined effect of optimal sizing and optimal scheduling and power dispatch yields a significant reduction in energy cost. In the case of the VSD, power draw from the grid rises gradually during the

morning offpeak electricity pricing period to replenish the cascade storage as vehicles continue to fill up. When the peak electricity pricing period commences at 06:00, the NG generator, whose power costs less per unit than the peak and standard electricity price, supplies the power requirements of the VSD compressor over the rest of the standard electricity pricing period as well as the evening peak and standard electricity pricing periods. After 22:00 when the offpeak electricity pricing period for the grid resumes, the VSD compressor draws power from the grid once again, as it replenishes the cascade storage to the initial condition levels at the end of the control horizon. The total energy consumed under the optimally varied and optimally power dispatched VSD compressor is 143.34 kWh at a total cost of R93.70. This remarkable reduction in energy consumption and electricity cost is consistent with the flexibility of the variable speed drives, which allows for huge savings in energy costs as a result of optimal matching with prevailing load requirements, thereby reducing power inefficiencies [65]. The level of energy cost savings also demonstrates the compounding of energy cost savings where sizing optimization, operation optimization and optimal power dispatch strategies are applied under demand response programs. Table 5.2 summarizes the energy consumption and electricity cost outcomes of the baseline scenario against the optimally sized and optimally operated FSD and VSD compressors from the proposed model.

Table 5.2. Energy consumption data.

Scenario	Energy consumption (kWh)	Electricity Cost (R)
Baseline	212.08	432.59
Optimal FSD	207.73	135.28
Optimal VSD	143.34	93.70

From Table 5.2, the optimally sized and optimally power-dispatched VSD compressor yields the most desirable outcomes in energy consumption and energy cost. VSDs have been shown to be the most effective way to achieve energy efficiency in air compression systems, providing more than 30% in energy consumption savings in air compression applications [124, 125]. In the current study, a comparison of energy consumption between the baseline and the proposed interventions shows energy consumption savings of 32.41% when VSD technology is used to replace the baseline fixed speed drive, which is a significant reduction in energy use for the CNG fuelling station. The reduction in energy use for the VSD is also significantly higher than the savings in energy consumption achieved through optimal sizing of the FSD compressor. The lowering of energy consumption is useful for the reduction in operation costs of the CNG station, and on a wider picture, it is a useful contribution

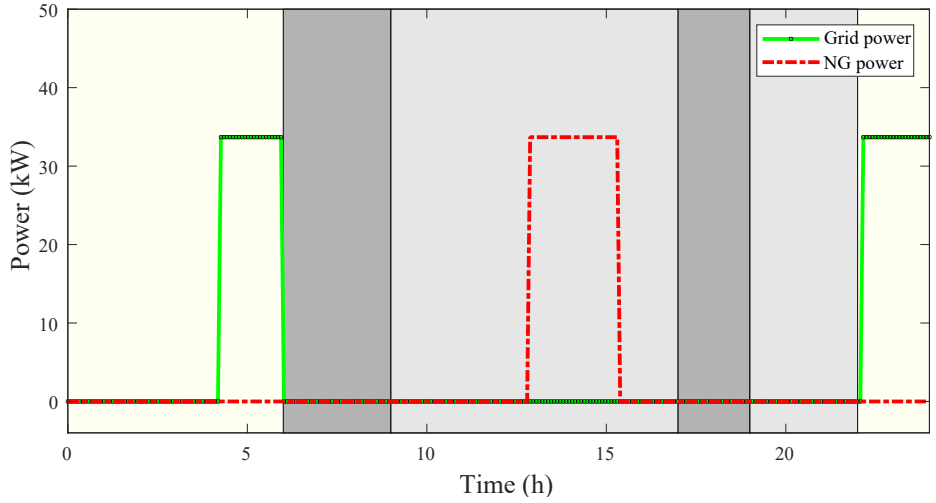

Figure 5.5(a): Fixed speed drive

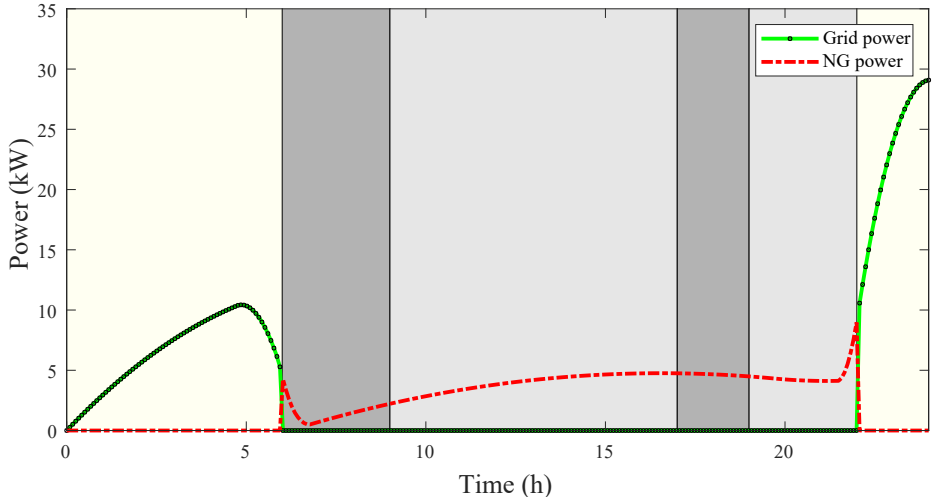

Figure 5.5(b): Variable speed drive

Figure 5.5. Optimal power dispatch for FSD and VSD and cascade storage mas of gas

of the CNG station to better use of energy for the benefit of all grid electricity customers. Under the model proposed in this study, the lowering of energy cost through lower energy consumption is compounded with optimal dispatch of the dual-power supply between the NG generator and the TOU tariff priced grid electricity. For the FSD case a 68.72% savings in energy cost are realized which can be attributed to an optimal dispatch of the two power sources, since for this case, the reduction in energy consumption through optimal sizing is marginal. The results of the compounded energy savings and energy cost saving strategy are demonstrated by the results for the VSD case, where a remarkable 78% in energy cost savings is achieved. This reduction in energy cost is contributed to by both lower

energy use and optimal dispatch of the grid and NG power around the TOU and gas fuel pricing for the grid and NG generator respectively. It is therefore reasonable to conclude that the VSD option in the energy efficiency intervention for the CNG station is the superior one, as it is the most effective in reaping the benefits of capacity and operation optimization. Consequently, an analysis of the economic implication of implementing such an intervention is necessary in order to facilitate decision making by CNG station operators.

5.4.2 Gas transfer

The results of the optimization of gas transfer are demonstrated in the gas filling profiles in Figure 5.6. The results show the optimal filling profile of the first vehicle in the control horizon, demonstrating a shorter filling time is realized for the VSD scenario compared to the FSD scenario. Because of the VSDs always-on operation of the compressor, the controller utilizes the four line priority panel for direct vehicle tank filling from the compressor through valve v_{co}. By having the option to connect the vehicle tank directly to the compressor when the optimum solution requires it, the VSD optimal operation has a continuously available choice to achieve the shortest possible filling time above the optimal sequencing of the cascade storage valves. This is unlike the case of the FSD where the optimal solution yielded an intermittent operation of the compressor where most of the vehicles are fuelled during the compressor-off times thereby not having available the option to fill directly from the compressor through valve v_{co} in the optimal filling profile.

The effects of this difference are further demonstrated in Figure 5.7, where the average gas transfer time per kilogram is plotted. It is clear from this plot that the availability of the compressor flow rate at all times helps to shorten the filling time of the VSD scenario further than the optimal filling profile of the FSD and the baseline. This additional benefit of the VSD and four line priority panel configuration is a desirable enhancement of the performance of the CNG fast-fill station, which the optimal control method proposed in the current study is able to achieve. In general, the average time saving for the filling process is 24.24 seconds per vehicle for the FSD case and 26.43 seconds for the VSD scenario in comparison with the baseline. These savings represent a notable advantage of the optimization strategy of the filling process proposed in this study.

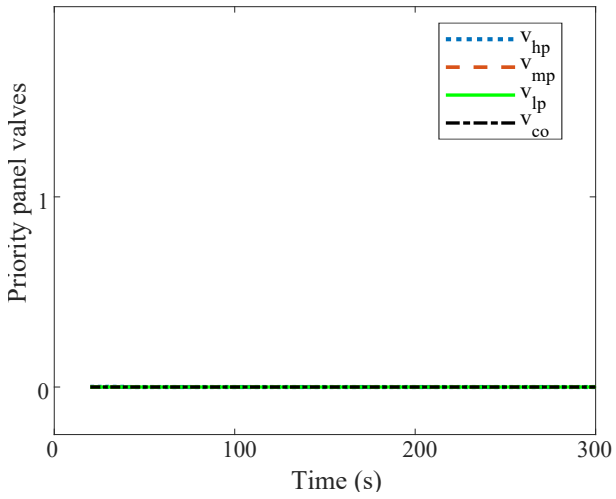

Figure 5.6(a)(i) FSD priority panel

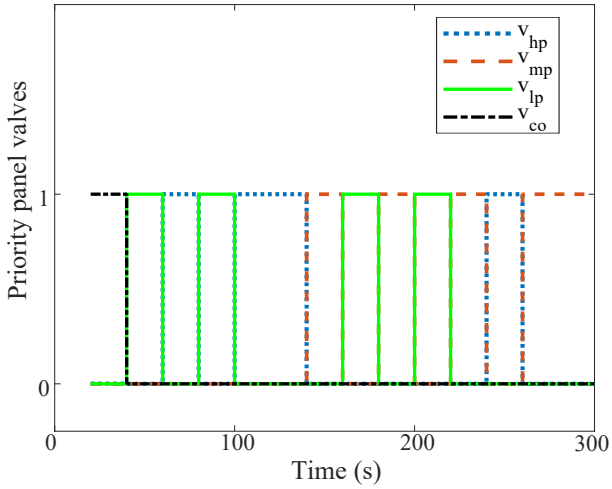

Figure 5.6(a)(ii) VSD priority panel

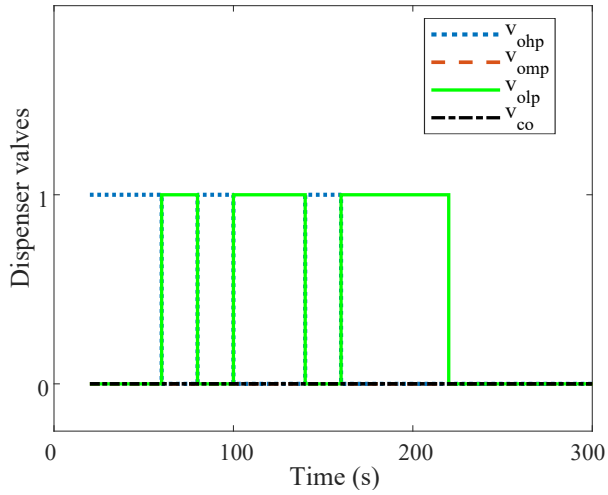

Figure 5.6(b)(i) FSD dispenser

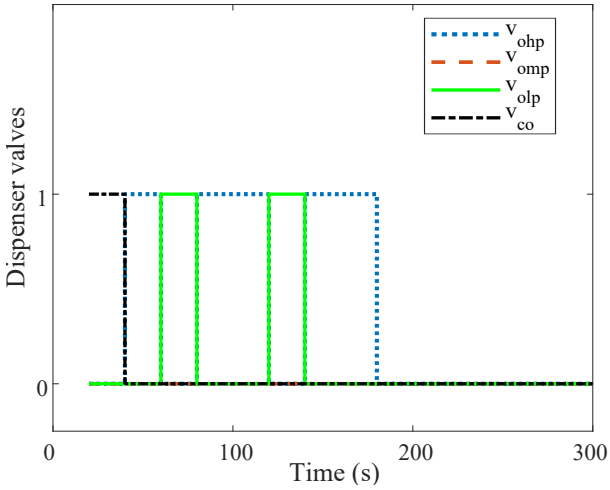

Figure 5.6(b)(ii) VSD dispenser

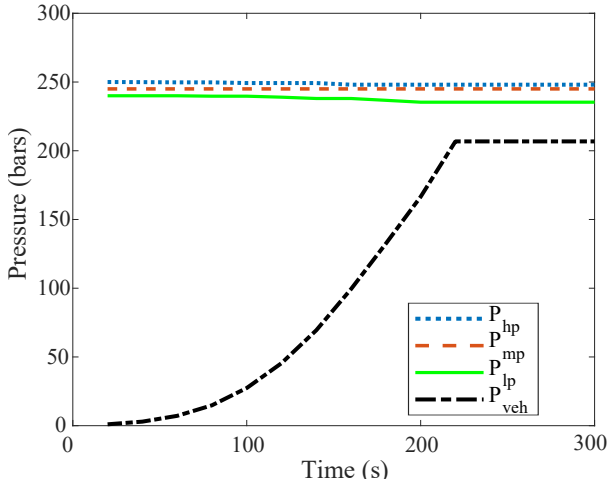

Figure 5.6(c)(i) FSD pressure

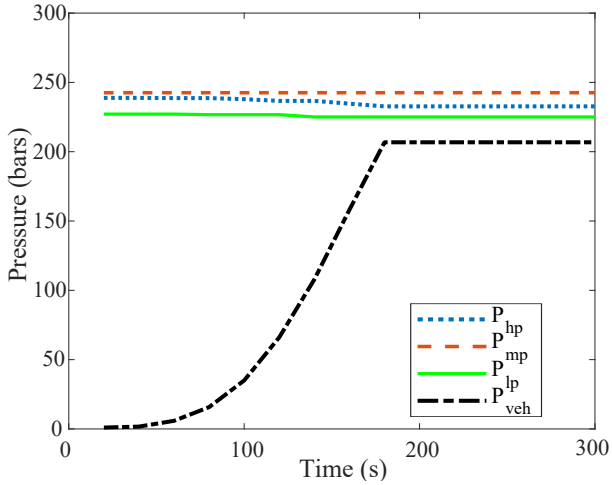

Figure 5.6(c)(ii) VSD pressure

Figure 5.6. Gas transfer profile to vehicle tank

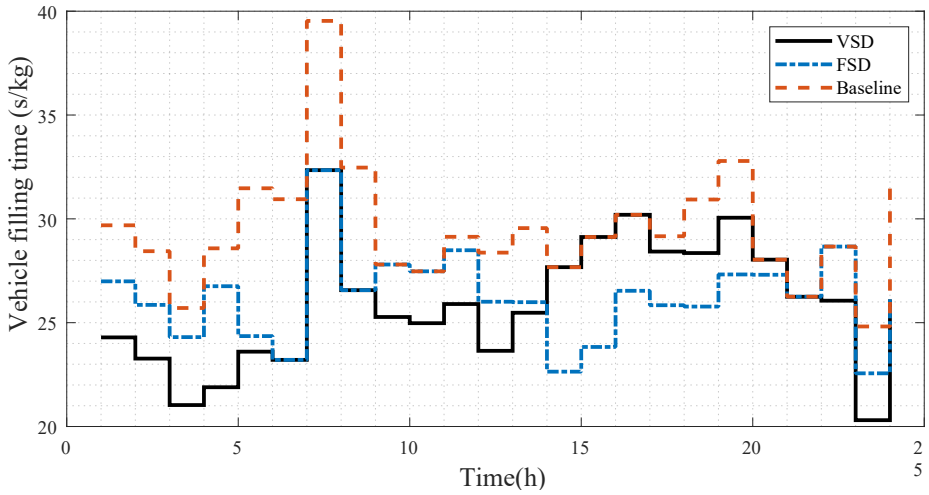

Figure 5.7. Gas transfer time

5.4.3 Economic analysis

The optimally operated VSD has been identified in this study as the superior approach for energy efficiency and energy cost reduction, and an economic analysis in the form of payback period evaluation is carried out to determine the time it takes to recover the initial investment in the intervention, through the returns from energy cost savings. The baseline case considered is the limit-based compressor cycling operation, whose profile is shown on Figure 5.3, powered exclusively from the grid. The savings from the proposed dual-powered VSD optimized model over the 24 hour control horizon are used to obtain the annualized benefits. The system maintenance cost is assumed to be constant. The discounted present value technique is used in the cash flow analysis such that [126]

$$DPV = \frac{FV}{(1+r)^n} \quad , \tag{5.58}$$

where DPV represents the discounted present value of future cash flow, r is the discount rate, n is the number of years and FV is the nominal value of the cash flow amount in a future period [127, 128].

Variable speed drives are costly and thus careful evaluation of cost and benefits is necessary to determine the appropriateness of implementing this type of intervention. From the cash flow data on Table 5.3, the break even point is realized after a period of 3 years and 1 month. This is an reasonable time for

the station operator to implement the optimal solution using the VSD with many years of energy cost savings expected beyond the payback period.

Table 5.3. Payback period

Years	0	1	2	3	4	5
Variable speed drive	(206048.00)					
Controller	(22900.00)					
Installation cost	(20604.80)					
Maintenance cost		(2495.53)	(2495.53)	(2495.53)	(2495.53)	(2495.53)
VSD and Optimal Operation benefit		123694.00	135568.62	148583.21	162847.20	178480.53
	(249552.80)	121198.47	133073.10	146087.68	160351.67	175985.00
Discount factor @ 4.62%	1.00	0.96	0.91	0.87	0.83	0.80
Discounted cashflows	(249552.80)	115846.37	121579.63	127576.14	133848.85	140411.31

Discounted payback period	Years	Discounted cashflows	Cumulative cashflows
	0	(249552.80)	(249552.80)
	1	115846.37	(133706.43)
	2	121579.63	(12126.80)
	3	127576.14	115449.34
	4	133848.85	249298.19
	5	140411.31	389709.50
Payback is	3 years 1 month		

5.5 CONCLUSION

The optimal matching of CNG station compressor capacity to the established gas demand and the optimal operation of the compressor powered from optimally dispatched NG generator and grid power have been pursued in this chapter to push the energy efficiency of the CNG fast-fill station higher and push the energy costs lower. The approach which involves optimal sizing of an FSD compressor and optimal variation of flow rate for a VSD compressor yields remarkable results that show the significant opportunities for cost saving and energy efficiency that exist for CNG station which is an important component of the gas delivery infrastructure.

The results of the study show that the flexibility of the VSD in combination with the proposed four line priority panel, yield not only significant energy savings and significant energy cost reduction, but also desirable reduction in vehicle filling time. This outcome secures the reputation of the proposed energy efficiency intervention for the CNG station as it realizes winnings for the CNG station operator in form

of cost savings and at the same time does not compromise on customer satisfaction with vehicle filling time.

Transition to less polluting energy choices in transportation requires that the expanding infrastructure for alternative fuels implements measures that reinforce the sector as a responsible user of grid electricity which is under growing strain due to explosion in demand and the capital intensive nature of developing new generation to keep up with the demand. This study demonstrates the benefit of optimal power dispatch and CNG fast-fill station participation in demand response programs in the form of TOU tariff for the CNG station operator through reduced operation costs, complemented by an optimization of gas delivery to the benefit of CNG powered vehicle users.

CHAPTER 6 CONCLUSIONS

This thesis presents a design of approaches to efficient operation of the fast-fill compressed natural gas vehicle fuelling station with regards to energy use. The compressed natural gas delivery network is a primary energy network that interacts in consequential ways with the electricity grid which is a secondary energy delivery network. The work can be classified in three categories: one involving the optimal shifting of compressor operations to achieve minimum electricity costs while satisfying gas demand in the context of a demand response program, the second involving the optimal operation of the compressed natural gas station components for optimal product delivery where demand response interventions are adopted by the operator and the third involving equipment and technology level interventions in energy efficiency, to go with operation level interventions and product delivery optimization.

The model of gas flow through the system is developed and implemented to determine optimal gas replenishment schedules for the cascade storage through the switching on and off of the compressor, that results in minimum possible cost of electricity purchased in the TOU tariff. The pressure conditions for the gas filling process are modelled so as to achieve the optimal deployment of the dispenser and priority panel valves that produce the minimum filling time for the vehicle cylinders. The use of the NG generator as a DSM mitigation device is evaluated under optimal sizing and operation conditions of compressors using FSD and VSD technologies to realize minimum cost of power for the CNG filling operation, in combination with minimum filling time optimization.

6.1 SUMMARY

The pursuit of a lower carbon future is an important endeavour for humanity in the present times, driven by the increasing human population, which requires the development of solutions to both energy

insecurity as well as environmental pollution. The energy intensive transport industry has consistently been one of the sectors that are most culpable in contributing to the present crisis from the view point of energy sourcing and energy use. Adoption of alternative to the traditional liquid fossil fuels has shown significant promise in increasing the rate at which the transportation industry is securing a better energy profile for the coming years. Compressed natural gas, being one of the main alternative fuels, has therefore been experiencing growth in usage and popularity, which has brought with it the need to expand the network for gas delivery. Simultaneously, the electricity delivery network continues to suffer the effects of increasing demand and expensive generation development, which has necessitated the use of demand management as a tool to securing the stability of the grid. DSM programs have availed incentives for customers to participate in the shaping of grid load profiles, especially through the use of pricing differentiation for different usage patterns. Because gas delivery is reliant on electricity for powering different nodes in the network of pipelines and compressors, the intersection of sustainability interventions in the transportation industry and in electricity grid supply become important to consider.

Three approaches to managing energy use in the gas delivery to vehicular consumers are provided in this work, with the aim to align the expansion of the use of compressed natural gas as an alternative fuel, with the demand response goals of DSM programs adopted by power utility providers.

- An approach to optimally schedule the compressor operation to minimize electricity cost in a scenario with an electricity time-of-use tariff is designed in Chapter 3. The controller is designed to determine optimal operation profile of the compressor that achieves minimum energy cost given the electricity pricing profile and further maintains the quantity of gas in each of the three cascade storage reservoirs at the levels that satisfy the established demand, through the deployment of the three line priority panel. Accordingly, this is an entry level response to demand side management of the compressed natural gas station, that is realized through implementation of a new operation scheduling profile previously not existent.
- In Chapter 4, the concern of the proposed approach is to address gas transfer from the cascade storage to the vehicle, to go with the optimal minimization of electricity cost consumption of the station compressor through optimized scheduling of the on-status with respect to the utility time-of-use tariff. A lower layer model predictive controller is designed to control the valves of the three line priority panel for the filling of each cascade storage reservoir, and the dispenser valves for the filling of the vehicle tanks in an optimal manner with the aim of achieving minimum

vehicle tank filling time. The gas transfer process is dependent on the pressure ratio between the reservoir and the vehicle tank, and a mixed integer non-linear programming problem is modelled to realize the optimal filling profiles. The lower layer uses the output of the upper layer compressor-on status scheduling as an input for the gas transfer optimal control problem. The results of this hierarchical approach to the gas transfer and energy cost efficiency problems show the ideal outcomes for product delivery under demand response interventions.

- In Chapter 5, a proposed change in the sizing and technology of the compressor drive is evaluated. FSD and VSD based solutions are modelled to solve for energy consumption levels for each case. Furthermore, this technology-based approach to better energy use is combined with an optimal operation of the compressor, considering the TOU tariff of the grid and the cost of fuel for the NG generator, introduced as a DSM mitigation device. Additionally, the optimal control of gas transfer is solved for a proposed four line priority panel configuration so that the filling time is minimized. Indeed, the results obtained from this combined-strategies proposal show a remarkable reduction in energy cost for the CNG station due to a combination of lower energy consumption and optimal economic operation of the compressor. The VSD options emerges as the superior choice in comparison with the optimally sized FSD for the parameters of performance under consideration. The vehicle fuelling time is also minimized from the baseline, as a result of the optimal control of the filling process through the dispenser and four-line priority panel.

6.2 RECOMMENDATIONS AND FUTURE WORK

The strategies to the energy efficient operation of the CNG station presented in this study demonstrate the existence of ignored economic opportunities in the interaction of a primary energy delivery network and the electricity grid. The results demonstrate that there are significant savings that can be realized through adoption of energy efficiency strategies for the operators of the CNG vehicle fuelling station, which not only lowers the cost of gas delivery, but also ensures the energy consuming nodes of the gas delivery network participate in DSM, for the benefit of all grid users and the environment.

Even though the objectives of this research have been met, there are useful further opportunities to improve on the impact of similar interventions for the CNG network and the grid.

1. Incorporating a renewable source of compressed natural gas could further increase the sustainability profile of the CNG fuel market for vehicles, thereby furthering the lower pollution advantage that CNG has above the liquid fossil fuels. Such incorporation of biomass based CNG requires development of corresponding control strategies for the energy efficient operation of the resulting infrastructure.
2. The focus of the current work is on the CNG fuelling station as a node in the gas delivery network. There exist other nodes within the gas delivery network such as the pressure boosting and pressure reduction stations that are also dependent on the electricity grid power and could benefit from similar optimal control strategies as proposed in this work.
3. The electricity use profile of other primary energy delivery networks could also consider similar pursuits as presented in this work, while considering their own unique configurations and complexities.
4. An exploration of possibilities of using demand response in primary energy delivery networks such as the gas delivery network similar to electricity demand response should be undertaken. Such programs, would be expected to have an effect on the electricity load profiles of the internal and peripheral energy-consuming nodes of the gas delivery network.

REFERENCES

[1] A. J. Krupnick, R. D. Rowe, and C. M. Lang, "Transportation and air pollution: the environmental damages," in *The Full Costs and Benefits of Transportation*. Springer, 1997, pp. 337–369.

[2] T. Lyons, J. Kenworthy, C. Moy, and F. Dos Santos, "An international urban air pollution model for the transportation sector," *Transportation Research Part D: Transport and Environment*, vol. 8, no. 3, pp. 159–167, 2003.

[3] R. Colvile, E. Hutchinson, J. Mindell, and R. Warren, "The transport sector as a source of air pollution," *Atmospheric Environment*, vol. 35, no. 9, pp. 1537–1565, 2001.

[4] P. Schmidt, W. Zittel, W. Weindorf, T. Rakasha, and D. Goericke, "Renewables in transport 2050–empowering a sustainable mobility future with zero emission fuels," in *16. Internationales Stuttgarter Symposium*. Springer, 2016, pp. 185–199.

[5] B. G. Pollet, I. Staffell, and J. L. Shang, "Current status of hybrid, battery and fuel cell electric vehicles: From electrochemistry to market prospects," *Electrochimica Acta*, vol. 84, pp. 235–249, 2012.

[6] S. J. Curran, R. M. Wagner, R. L. Graves, M. Keller, and J. B. Green Jr, "Well-to-wheel analysis of direct and indirect use of natural gas in passenger vehicles," *Energy*, vol. 75, pp. 194–203, 2014.

[7] S. Yeh, "An empirical analysis on the adoption of alternative fuel vehicles: the case of natural gas vehicles," *Energy Policy*, vol. 35, no. 11, pp. 5865–5875, 2007.

[8] M. Mikolajková-Alifov, F. Pettersson, M. Björklund-Sänkiaho, and H. Saxén, "A model of optimal gas supply to a set of distributed consumers," *Energies*, vol. 12, no. 3, p. 351, 2019.

[9] M. H. Albadi and E. El-Saadany, "A summary of demand response in electricity markets," *Electric Power Systems Research*, vol. 78, no. 11, pp. 1989–1996, 2008.

[10] K. Spees and L. B. Lave, "Demand response and electricity market efficiency," *The Electricity Journal*, vol. 20, no. 3, pp. 69–85, 2007.

[11] Q. Qdr, "Benefits of demand response in electricity markets and recommendations for achieving them," US Dept. Energy, Washington, DC, USA, Tech. Rep., 2006.

[12] G. Strbac, "Demand side management: Benefits and challenges," *Energy Policy*, vol. 36, no. 12, pp. 4419–4426, 2008.

[13] S. M. Amin, "For the good of the grid," *IEEE Power and Energy Magazine*, vol. 6, no. 6, pp. 48–59, 2008.

[14] R. Rankin and P. Rousseau, "Demand side management in South Africa at industrial residence water heating systems using in line water heating methodology," *Energy Conversion and Management*, vol. 49, no. 1, pp. 62–74, 2008.

[15] A. Olasoji, K. Akpeji, C. Gaunt, D. Oyedokun, K. Awodele, and K. Folly, "Economy-wide assessment of the impact of electricity supply disruption using hypothetical extraction," in *2018 IEEE PES/IAS PowerAfrica*. IEEE, 2018, pp. 607–612.

[16] A. Sebitosi, "Energy efficiency, security of supply and the environment in South Africa: Moving beyond the strategy documents," *Energy*, vol. 33, no. 11, pp. 1591–1596, 2008.

[17] R. Pelzer, E. Mathews, D. Le Roux, and M. Kleingeld, "A new approach to ensure successful implementation of sustainable demand side management (DSM) in South African mines," *Energy*, vol. 33, no. 8, pp. 1254–1263, 2008.

[18] N. N. Nahavandi and M. Farzaneh-Gord, "Numerical simulation of filling process of natural gas onboard vehicle cylinder," *Journal of the Brazilian Society of Mechanical Sciences and Engineering*, vol. 35, no. 3, pp. 247–256, 2013.

[19] F. Olmos and V. I. Manousiouthakis, "Gas tank fill-up in globally minimum time: Theory and application to hydrogen," *International Journal of Hydrogen Energy*, vol. 39, no. 23, pp. 12 138–12 157, 2014.

[20] M. A. Euritt, "Cost-effectiveness analysis of cng urban taxi operations." University of Texas at Austin. Center for Transportation Research, Tech. Rep., 1993.

[21] R. C. Elgin and C. L. Hagen, "Development and operation of a self-refueling compressed natural gas vehicle," *Applied Energy*, vol. 155, pp. 242–252, 2015.

[22] S. Ramoutar and C. Riverol, "A thermodynamic analysis of refueling a natural gas vehicle cylinder from a cascade reservoir using chilled natural gas," *Journal of Natural Gas Science and Engineering*, vol. 38, pp. 298–322, 2017.

[23] K. Kountz, C. Blazek, and W. Liss, "A new natural gas dispenser control system," in *International Gas Research Conference*, vol. 4. Government Institutes Inc, 1998, pp. 135–145.

[24] B. F. Price, "Apparatus and process for fast filling with natural gas," Dec. 6 1994, US Patent 5,370,159.

[25] R. E. Knowlton, "Natural gas storage and retrieval system," Feb. 21 1989, US Patent 4,805,674.

[26] A. M. Barajas, J. C. Buckingham, and S. Svedeman, "System for controlling the fill of compressed natural gas cylinders," Feb. 9 1999, US Patent 5,868,176.

[27] Y. Han, X. D. You, X. Zhang, H. Y. Wang, and C. Deng, "A novel design of the CNG dispenser electronic control system," in *Applied Mechanics and Materials*, vol. 448. Trans Tech Publ, 2014, pp. 3119–3122.

[28] M. Tsuchiya, H. Ogasa, H. Matsuura, H. Shimanuki, and I. Fujii, "Thermodynamic behavior of supply gas and influence on vehicle fuel fill line during CNG fast fill," SAE Technical Paper, Tech. Rep., 1996.

[29] M. Farzaneh-Gord, M. Deymi-Dashtebayaz, and H. R. Rahbari, "Studying effects of storage types on performance of CNG filling stations," *Journal of Natural Gas Science and Engineering*, vol. 3, no. 1, pp. 334–340, 2011.

[30] M. Saadat-Targhi, J. Khadem, and M. Farzaneh-Gord, "Thermodynamic analysis of a CNG refueling station considering the reciprocating compressor," *Journal of Natural Gas Science and Engineering*, vol. 29, pp. 453–461, 2016.

[31] S. Mokhatab and W. A. Poe, *Handbook of Natural Gas Transmission and Processing*. Gulf professional publishing, 2012.

[32] J. Xueqin, "Study of urban CNG station location arrangement and the size," *Public Utilities*, vol. 1, p. 005, 2007.

[33] H. J. Bang, S. Stockar, M. Muratori, and G. Rizzoni, "Modeling and analysis of a CNG residential refueling system," in *ASME 2014 Dynamic Systems and Control Conference*. American Society of Mechanical Engineers, 2014.

[34] K. J. Kountz, C. F. Blazek, and F. Christopher, "NGV fuelling station and dispenser control systems," Gas Research Institute, Chicago, Illinois, November, Tech. Rep., 1997.

[35] K. Kountz, "Modeling the fast fill process in natural gas vehicle storage cylinders," *American Chemical Society (1994)*, 1994. [Online]. Available: https://www.osti.gov/servlets/purl/10177364

[36] M. Farzaneh-Gord, "Compressed natural gas-single reservoir filling process," *International Gas Enginering and Management*, vol. 48, no. 6, pp. 16–18, 2008.

[37] G. Thomas, J. Goulding, and C. Munteam, "Measurement, approval and verification of CNG dispensers," National Weights and Measures Laboratory Report, Tech. Rep., 1999.

[38] M. Farzaneh-gord, S. Hashemi, and A. Farzaneh-kord, "Thermodynamics analysis of cascade reserviors filling process of natural gas vehicle cylinders," *World Applied Sciences*, vol. 5 (2), pp. 143–149, 2008.

[39] M. Deymi-Dashtebayaz, M. F. Gord, and H. R. Rahbari, "Studying transmission of fuel storage bank to NGV cylinder in CNG fast filling station," *Journal of the Brazilian Society of Mechanical Sciences and Engineering*, vol. 34, no. 4, pp. 429–435, 2012.

[40] S. H. Wellisz, "Regulation of natural gas pipeline companies: An economic analysis," *Journal of Political Economy*, vol. 71, no. 1, pp. 30–43, 1963.

[41] M. Frick, K. W. Axhausen, G. Carle, and A. Wokaun, "Optimization of the distribution of compressed natural gas (CNG) refueling stations: Swiss case studies," *Transportation Research Part D: Transport and Environment*, vol. 12, no. 1, pp. 10–22, 2007.

[42] M. Kuby, "The opposite of ubiquitous: How early adopters of fast-filling alt-fuel vehicles adapt to the sparsity of stations," *Journal of Transport Geography*, vol. 75, pp. 46–57, 2019.

[43] T. Franke and J. F. Krems, "Understanding charging behaviour of electric vehicle users," *Transportation Research Part F: Traffic Psychology and Behaviour*, vol. 21, pp. 75–89, 2013.

[44] K. S. Corts, "Building out alternative fuel retail infrastructure: Government fleet spillovers in e85," *Journal of Environmental Economics and Management*, vol. 59, no. 3, pp. 219–234, 2010.

[45] T. Gnann and P. Plötz, "A review of combined models for market diffusion of alternative fuel vehicles and their refueling infrastructure," *Renewable and Sustainable Energy Reviews*, vol. 47, pp. 783–793, 2015.

[46] M. J. Kuby, S. B. Kelley, and J. Schoenemann, "Spatial refueling patterns of alternative-fuel and gasoline vehicle drivers in Los Angeles," *Transportation Research Part D: Transport and Environment*, vol. 25, pp. 84–92, 2013.

[47] D. A. Hagos and E. O. Ahlgren, "Well-to-wheel assessment of natural gas vehicles and their fuel supply infrastructures–perspectives on gas in transport in Denmark," *Transportation Research Part D: Transport and Environment*, vol. 65, pp. 14–35, 2018.

[48] J. O. Jaber, "Future energy consumption and greenhouse gas emissions in Jordanian industries," *Applied Energy*, vol. 71, no. 1, pp. 15–30, 2002.

[49] F. Tong, P. Jaramillo, and I. M. Azevedo, "Comparison of life cycle greenhouse gases from natural gas pathways for light-duty vehicles," *Energy & Fuels*, vol. 29, no. 9, pp. 6008–6018, 2015.

[50] F. Tong, P. Jaramillo, and I. Azevedo, "Comparison of life cycle greenhouse gases from natural gas pathways for medium and heavy-duty vehicles," *Environmental Science & Technology*, vol. 49, no. 12, pp. 7123–7133, 2015.

[51] D. Karman, "Life-cycle analysis of GHG emissions for CNG and diesel buses in Beijing," in *2006 IEEE EIC Climate Change Conference*. IEEE, 2006, pp. 1–6.

[52] X. Ou, X. Zhang, and S. Chang, "Alternative fuel buses currently in use in China: life-cycle fossil energy use, GHG emissions and policy recommendations," *Energy Policy*, vol. 38, no. 1, pp. 406–418, 2010.

[53] A. Martinez-Mares and C. R. Fuerte-Esquivel, "A unified gas and power flow analysis in natural gas and electricity coupled networks," *IEEE Transactions on Power Systems*, vol. 27, no. 4, pp. 2156–2166, 2012.

[54] S. An, Q. Li, and T. W. Gedra, "Natural gas and electricity optimal power flow," in *2003 IEEE PES Transmission and Distribution Conference and Exposition (IEEE Cat. No. 03CH37495)*, vol. 1. IEEE, 2003, pp. 138–143.

[55] M. W. Shin, D. Shin, S. H. Choi, E. S. Yoon, and C. Han, "Optimization of the operation of boil-off gas compressors at a liquified natural gas gasification plant," *Industrial & Engineering Chemistry Research*, vol. 46, no. 20, pp. 6540–6545, 2007.

[56] M. A. Neseli, O. Ozgener, and L. Ozgener, "Energy and exergy analysis of electricity generation from natural gas pressure reducing stations," *Energy Conversion and Management*, vol. 93, pp. 109–120, 2015.

[57] A. Chebouba, F. Yalaoui, A. Smati, L. Amodeo, K. Younsi, and A. Tairi, "Optimization of natural gas pipeline transportation using ant colony optimization," *Computers & Operations Research*, vol. 36, no. 6, pp. 1916–1923, 2009.

[58] A. D. Woldeyohannes and M. A. A. Majid, "Simulation model for natural gas transmission pipeline network system," *Simulation Modelling Practice and Theory*, vol. 19, no. 1, pp. 196–212, 2011.

[59] J. Požívil, "Use of expansion turbines in natural gas pressure reduction stations," *Acta Montanistica Slovaca*, vol. 3, no. 9, pp. 258–260, 2004.

[60] M. Farzaneh-Gord and M. Deymi-Dashtebayaz, "Recoverable energy in natural gas pressure drop stations: a case study of the Khangiran gas refinery," *Energy Exploration & Exploitation*, vol. 26, no. 2, pp. 71–82, 2008.

[61] M. Farzaneh-Gord, S. Hashemi, and M. Sadi, "Energy destruction in Iran's natural gas pipe line network," *Energy Exploration & Exploitation*, vol. 25, no. 6, pp. 393–406, 2007.

[62] M. Elsobki and H. El-Salmawy, "Power generation using recovered energy from natural gas networks," in *Proceedings of the 17th International Conference on Electricity Distribution, Barcelona, Spain*, 2003, pp. 12–15.

[63] X. Xia and J. Zhang, "Energy efficiency and control systems–from a POET perspective," *IFAC Proceedings Volumes*, vol. 43, no. 1, pp. 255–260, 2010.

[64] K. C. Weston, "Energy conversion–the ebook," *University of Tulsa*, 2000.

[65] R. Saidur, S. Mekhilef, M. B. Ali, A. Safari, and H. A. Mohammed, "Applications of variable speed drive (VSD) in electrical motors energy savings," *Renewable and Sustainable Energy Reviews*, vol. 16, no. 1, pp. 543–550, 2012.

[66] X. Xia, J. Zhang, and W. Cass, "Energy management of commercial buildings-a case study from a poet perspective of energy efficiency," *Journal of Energy in Southern Africa*, vol. 23, no. 1, pp. 23–31, 2012.

[67] A. Antonopoulos, L. Ängquist, L. Harnefors, and H.-P. Nee, "Optimal selection of the average capacitor voltage for variable-speed drives with modular multilevel converters," *IEEE Transactions on Power Electronics*, vol. 30, no. 1, pp. 227–234, 2014.

[68] M. A. Oskouei and K. Awuah-Offei, "A method for data-driven evaluation of operator impact on energy efficiency of digging machines," *Energy Efficiency*, vol. 9, no. 1, pp. 129–140, 2016.

[69] M. F. Hordeski, *Dictionary of Energy Efficiency Technologies*. Fairmont Press, 2004.

[70] U. E. Ekpenyong, J. Zhang, and X. Xia, "Mathematical modelling for the social impact to energy efficiency savings," *Energy and Buildings*, vol. 84, pp. 344–351, 2014.

[71] K. Herter, P. McAuliffe, and A. Rosenfeld, "An exploratory analysis of California residential customer response to critical peak pricing of electricity," *Energy*, vol. 32, no. 1, pp. 25–34, 2007.

[72] D. Setlhaolo, X. Xia, and J. Zhang, "Optimal scheduling of household appliances for demand response," *Electric Power Systems Research*, vol. 116, pp. 24–28, 2014.

[73] Z. Wu, H. Tazvinga, and X. Xia, "Demand side management of photovoltaic-battery hybrid system," *Applied Energy*, vol. 148, pp. 294–304, 2015.

[74] M. H. Albadi and E. F. El-Saadany, "Demand response in electricity markets: An overview," in *2007 IEEE Power Engineering Society General Meeting*. IEEE, 2007, pp. 1–5.

[75] P. Jazayeri, A. Schellenberg, W. Rosehart, J. Doudna, S. Widergren, D. Lawrence, J. Mickey, and S. Jones, "A survey of load control programs for price and system stability," *IEEE Transactions on Power Systems*, vol. 20, no. 3, pp. 1504–1509, 2005.

[76] C. W. Gellings and J. H. Chamberlin, "Demand-side management: concepts and methods," 1987.

[77] S. Valero, M. Ortiz, C. Senabre, C. Alvarez, F. Franco, and A. Gabaldon, "Methods for customer and demand response policies selection in new electricity markets," *IET Generation, Transmission & Distribution*, vol. 1, no. 1, pp. 104–110, 2007.

[78] N. Wang, J. Zhang, and X. Xia, "Energy consumption of air conditioners at different temperature set points," *Energy and Buildings*, vol. 65, pp. 412–418, 2013.

[79] D. Setlhaolo and X. Xia, "Optimal scheduling of household appliances with a battery storage system and coordination," *Energy and Buildings*, vol. 94, pp. 61–70, 2015.

[80] W. Badenhorst, J. Zhang, and X. Xia, "Optimal hoist scheduling of a deep level mine twin rock winder system for demand side management," *Electric Power Systems Research*, vol. 81, no. 5, pp. 1088–1095, 2011.

[81] X. Zhuan and X. Xia, "Optimal operation scheduling of a pumping station with multiple pumps," *Applied Energy*, vol. 104, pp. 250–257, 2013.

[82] S. M. Sichilalu and X. Xia, "Optimal energy control of grid tied PV–diesel–battery hybrid system powering heat pump water heater," *Solar Energy*, vol. 115, pp. 243–254, 2015.

[83] N. I. Nwulu and X. Xia, "Implementing a model predictive control strategy on the dynamic economic emission dispatch problem with game theory based demand response programs," *Energy*, vol. 91, pp. 404–419, 2015.

[84] N. L. Newhouse and W. E. Liss, "Fast filling of NGV fuel containers," SAE Technical Paper, Tech. Rep., 1999. [Online]. Available: https://saemobilus.sae.org/content/1999-01-3739

[85] C. L. Su, J. L. Liu, D. L. Qiu, J. Y. Cai, and S. S. Li, "Intelligent compressed natural gas dispensers," *China Measurement & Testing Technology*, vol. 6, p. 041, 2008.

[86] H. H. Nguyen, V. Uraikul, C. W. Chan, and P. Tontiwachwuthikul, "A comparison of automation techniques for optimization of compressor scheduling," *Advances in Engineering Software*, vol. 39, no. 3, pp. 178–188, 2008.

[87] J. G. Calvert, "Glossary of atmospheric chemistry terms (recommendations 1990)," *Pure and Applied Chemistry*, vol. 62, no. 11, pp. 2167–2219, 1990.

[88] E. Heidaryan, J. Moghadasi, and M. Rahimi, "New correlations to predict natural gas viscosity and compressibility factor," *Journal of Petroleum Science and Engineering*, vol. 73, no. 1, pp. 67–72, 2010.

[89] A. Bahadori, S. Mokhatab, and B. F. Towler, "Rapidly estimating natural gas compressibility factor," *Journal of Natural Gas Chemistry*, vol. 16, no. 4, pp. 349–353, 2007.

[90] H. H. Nguyen and C. W. Chan, "Applications of artificial intelligence for optimization of compressor scheduling," *Engineering Applications of Artificial Intelligence*, vol. 19, no. 2, pp. 113–126, 2006.

[91] H. P. Bloch and J. J. Hoefner, *Reciprocating Compressors:: Operation and Maintenance*. Gulf Professional Publishing, 1996.

[92] E. Giacomelli, F. Bernardini, A. Pini, and H. Andree, "Application of gas turbines for large reciprocating compressor drive," in *ASME 1989 International Gas Turbine and Aeroengine Congress and Exposition*. American Society of Mechanical Engineers, 1989, pp. V004T10A006–V004T10A006.

[93] P. Walsh and J. Lamancusa, "A variable stiffness vibration absorber for minimization of transient vibrations," *Journal of Sound and Vibration*, vol. 158, no. 2, pp. 195–211, 1992.

[94] W. Booysen, M. Kleingeld, and J. Van Rensburg, "Optimising compressor control strategies for maximum energy savings," *ICUE, Cape Town*, pp. 10–12, 2009.

[95] C. K. Sun, V. Uraikul, C. W. Chan, and P. Tontiwachwuthikul, "An integrated expert system/operations research approach for the optimization of natural gas pipeline operations," *Engineering Applications of Artificial Intelligence*, vol. 13, no. 4, pp. 465–475, 2000.

[96] T. Mathaba, X. Xia, and J. Zhang, "Analysing the economic benefit of electricity price forecast in industrial load scheduling," *Electric Power Systems Research*, vol. 116, pp. 158–165, 2014.

[97] E. M. Wanjiru and X. Xia, "Energy-water optimization model incorporating rooftop water harvesting for lawn irrigation," *Applied Energy*, vol. 160, pp. 521–531, 2015.

[98] E. M. Wanjiru, L. Zhang, and X. Xia, "Model predictive control strategy of energy-water management in urban households," *Applied Energy*, vol. 179, pp. 821–831, 2016.

[99] A. M. Bagirov, A. Barton, H. Mala-Jetmarova, A. Al Nuaimat, S. Ahmed, N. Sultanova, and J. Yearwood, "An algorithm for minimization of pumping costs in water distribution systems using a novel approach to pump scheduling," *Mathematical and Computer Modelling*, vol. 57, no. 3, pp. 873–886, 2013.

[100] B. P. Numbi, J. Zhang, and X. Xia, "Optimal energy management for a jaw crushing process in deep mines," *Energy*, vol. 68, pp. 337–348, 2014.

[101] J. Currie, D. I. Wilson, N. Sahinidis, and J. Pinto, "OPTI: Lowering the barrier between open source optimizers and the industrial MATLAB user," *Foundations of Computer-Aided Process Operations*, vol. 24, p. 32, 2012.

[102] T. Faulwasser, M. Korda, C. N. Jones, and D. Bonvin, "On turnpike and dissipativity properties of continuous-time optimal control problems," *Automatica*, vol. 81, pp. 297–304, 2017.

[103] H. Zhang, F. Zhao, K. Fang, and J. W. Sutherland, "Energy-conscious flow shop scheduling under time-of-use electricity tariffs," *CIRP Annals-Manufacturing Technology*, vol. 63, no. 1, pp. 37–40, 2014.

[104] S. M. Baladi, J. A. Herriges, and T. J. Sweeney, "Residential response to voluntary time-of-use electricity rates," *Resource and Energy Economics*, vol. 20, no. 3, pp. 225–244, 1998.

[105] K. J. Kountz, W. E. Liss, and C. F. Blazek, "Automated process and system for dispensing compressed natural gas," Sep. 22 1998, uS Patent 5,810,058.

[106] R. Allan, R. Billinton, and M. De Oliveira, "Reliability evaluation of electrical systems with switching actions," in *Proceedings of the Institution of Electrical Engineers*, vol. 123, no. 4. IET, 1976, pp. 325–330.

[107] M. Bosman, "Availability analysis of a natural gas compressor plant," *Reliability engineering*, vol. 11, no. 1, pp. 13–26, 1985.

[108] H. M. He, W. S. Lin, and A. Z. Gu, "Preliminary technical study on L/CNG stations," *Natural Gas Industry*, vol. 27, no. 4, p. 126, 2007.

[109] H. X. Wang, M. He, L. Yang, N. Li, and Y. D. Wang, "Suggestions on relevant design codes for CNG filling stations in China," *Gas & Heat*, vol. 12, p. 027, 2009.

[110] H. He, H. Daume III, and J. M. Eisner, "Learning to search in branch and bound algorithms," in *Advances in Neural Information Processing Systems*, 2014, pp. 3293–3301.

[111] E. Shipley, "Study of natural gas vehicles (NGV) during the fast fill process." Master's thesis, West Virginia University, 2002.

[112] M. Farzaneh-Gord and M. Deymi-Dashtebayaz, "Optimizing natural gas fueling station reservoirs pressure based on ideal gas model," *Polish Journal of Chemical Technology*, vol. 15, no. 1, pp. 88–96, 2013.

[113] M. Schlüter, M. Gerdts, and J.-J. Rückmann, "A numerical study of MIDACO on 100 MINLP benchmarks," *Optimization*, vol. 61, no. 7, pp. 873–900, 2012.

[114] C. Cilliers, L. van der Zee, and M. Kleingeld, "Cost savings on mine dewatering pumps by reducing preparation-and comeback loads," in *Industrial and Commercial Use of Energy (ICUE), 2014 International Conference on the*. IEEE, 2014, pp. 1–8.

[115] C. Cilliers, "Cost savings on mine dewatering pumps by reducing preparation- and comeback loads," Master's thesis, North West University, Potchefstroom, 2014.

[116] A. van Tonder, M. Kleingeld, and J. Marais, "Investigating demand response potential in a mining group," in *Industrial and Commercial Use of Energy Conference (ICUE), 2013 Proceedings of the 10th*. IEEE, 2013, pp. 1–5.

[117] X. Xia and J. Zhang, "Operation efficiency optimisation modelling and application of model predictive control," *IEEE/CAA Journal of Automatica Sinica*, vol. 2, no. 2, pp. 166–172, 2015.

[118] K. Bhattacharya, M. H. Bollen, and J. E. Daalder, *Operation of Restructured Power Systems*. Springer Science & Business Media, 2012.

[119] R. Z. Ríos-Mercado and C. Borraz-Sánchez, "Optimization problems in natural gas transportation systems: A state-of-the-art review," *Applied Energy*, vol. 147, pp. 536–555, 2015.

[120] R. Kurz and S. Mokhatab, "Considerations on compressor station layout," *Pipeline & Gas Journal*, vol. 234, no. 9, p. 24, 2007.

[121] Y. Ginzburg, "Ang storage as a technological solution for the "chicken-and-egg" problem of ngv refueling infrastructure development," in *23rd World Gas Conference, Amsterdam*, 2006.

[122] X. Xia and L. Zhang, "Industrial energy systems in view of energy efficiency and operation control," *Annual Reviews in Control*, vol. 42, pp. 299–308, 2016.

[123] D. N. Luta and A. K. Raji, "Optimal sizing of hybrid fuel cell-supercapacitor storage system for off-grid renewable applications," *Energy*, vol. 166, pp. 530–540, 2019.

[124] V. Vongmanee and V. Monyakul, "A new concept of small-compressed air energy storage system integrated with induction generator," in *2008 IEEE International Conference on Sustainable Energy Technologies*. IEEE, 2008, pp. 866–871.

[125] A. Cortinovis, D. Pareschi, M. Mercangoez, and T. Besselmann, "Model predictive anti-surge control of centrifugal compressors with variable-speed drives," *IFAC Proceedings Volumes*, vol. 45, no. 8, pp. 251–256, 2012.

[126] R. Brealey, S. Myers, F. Allen, and P. Mohanty, *Principles of Corporate Finance, 11e*. McGraw-Hill Education, 1988.

[127] H. Tazvinga, "Energy optimisation and management of off-grid hybrid power supply systems," Ph.D. dissertation, University of Pretoria, 2015.

[128] L. Albright, *Energy Systems Engineering: Evaluation and Implementation*. McGraw-Hill Professional, 2012.